Proceedings of 3th Conference on Constructions in Desert Region

26-28/10/2023

Organized by AL-Juffra University

Funded by Ministry of Higher Education and Scientific Research-Libya

Contents

Numerical Analysis of the Flexural Behaviour of Masonry Walls Reinforced With FRP Under Out-Of-Plane Loading

*Abusaif Ishteewi[1], Manssuor Bin Miskeen[1], and Ahmed Alhodairi[2]

[1]Department of Architecture and Urban Planning Engineering, Faculty of Engineering, Wadi Alshatti University, Libya

[2]Department of Civil Engineering, Faculty of Engineering, Sebha University, Libya

*Email: abu.ishteewi@wau.edu.ly

Abstract In past earthquakes, unreinforced masonry structures (URM) performed poorly because masonry elements were unable to withstand the tensile forces generated by earthquakes. Several techniques have been proposed for strengthening existing masonry structures. Recent experiments have demonstrated the benefits of fibre reinforced polymers (FRPs) to Increase the efficiency of masonry wall performance. In this study, models of masonry walls reinforced with FRP strips are used to simulate the behaviour of out-of-plane loads applied to unreinforced masonry walls. The masonry material is modelled based on concrete damaged plasticity approaches, and the FRP strips are modelled based on their materials type Lamina. ABAQUS, model-based software, simulates the behaviour of unreinforced masonry walls strengthened with and without FRP on six previously tested walls. FE models can accurately represent the key features of the performance of un-strengthened and strengthened walls, according to a comparison between numerically obtained moment-deflection curves with experimentally available data. Analysing parametric models of validated masonry walls, certain parameters, including the reinforcement surface area ratio and type of reinforcement materials, have been assessed for their influence on the out-of-plane behaviour of the FRP-strengthened walls. As a result, the FRP laminates could significantly increase the wind and earthquake resistance of URM walls, as the FRP laminates provide greater out-of-plane deformation capability. Furthermore, with increasing FRP reinforcement surface area ratio, the FRP laminate becomes less effective for moment and deformation capacities.

Keywords: Earthquakes, URM, FRP, ABAQUS

1. Introduction

Most of the countries still use block masonry as a construction material due to its good heat insulation properties, high compressive strength, easy availability, soundness, durability, and it is relatively inexpensive. Masonry structures are made up of bricks and mortar that are orthotropic, inelastic, and no homogeneous and arranged in a particular manner [1]. Generally, buildings made of unreinforced masonry (URM) do not perform well in earthquakes and strong winds. Typically, URM buildings subjected to seismic forces and wind load experience two types of failure. Firstly, the lateral load-resisting systems of the building failed due to in-plane shear. Another failure mechanism occurs when seismic inertial forces or heavy wind cause out-of-plane bending [2]. Research has been conducted over the last 50 years into strengthening unreinforced masonry walls (URM) and improving their ability to resist bending and shear force under out-of-plane action. The use of steel bars was one of the first techniques to emerge for strengthening masonry walls [3]. However, fibre-reinforced polymers (FRP) are considered to be sustainable materials characterised by a high strength to weight ratio. It is effective at improving the performance of masonry walls FRP does have disadvantages; it is more expensive and has a lower fire resistance [3]. Masonry walls can however be reinforced with FRP to significantly improve their shear and flexural resistance as well as increase their ductility. Strengthening URM by using FRP strips is one of the proposed techniques for enhancing URM flexural performance under out-of-plane action. Several experimental studies were conducted using carbon, glass and aramid fibres in different configurations (horizontal, vertical and diagonal) at the external surface of the walls to investigate the effect of the FRP-reinforced on URM performance [4; 5; 6]. These studies included different ratios of FRP reinforcement and various types of masonry walls, such as clay bricks, stone and concrete blocks. The outcomes of these studies indicate the impact of using FRP strips to enhance bending load capacity, flexural strength and ductility behaviour of URM. The studies were extended to investigate the different types of failure modes, namely flexural or shear failure, and the main parameter effect on the type of failure. Further, experimental and numerical studies were conducted to develop and propose a design guideline to predict the ultimate flexural, shear and deformation capacity based on the reinforcement ratio and FRP configuration. This study was designed to suggest and validate a numerical model that can estimate the flexural behaviour and deflection of concrete block masonry walls reinforced with FRP strips. For this purpose, the finite element model was calibrated by means of a methodical process in order to evaluate the flexural and deformation performances. As a result, the validated model was used to investigate the impact of the FRP strips layout, FRP reinforced ratio, and the type of FRP on the load capacity, flexural capacity, and deformation of strengthened masonry walls under out-of-plane loading. The effect of these parameters on the gained bending capacity of masonry was evaluated and the uncertainty of the parameter used to simulate the walls is discussed.

2. Literature Review

Unreinforced masonry walls behaviour under out-of-plane action was analysed to investigate the bending behaviour. In addition, the techniques used to strengthen URM, namely using steel bars and FRP, to increase the flexural performance of masonry walls are also presented and discussed. Finally, previous research conducted on retrofitted and strengthened masonry walls to enhance the resistance of out-of-plane action due to earthquake or wind load were examined. URM building performs purely under out-of-plane action. In fact, because of the low stiffness and strength of masonry walls in out-of-plane directions, masonry structures are vulnerable since inertia forces are unrestrained due to the reduction of strength/mass ratio. Additionally, kinetic energy transmitted by an earthquake may result in overturning mechanisms [7]. Figure 1 shows examples of out-of-plane failure, namely failure of mortar joints, failure of bricks and flexural bending failure [8]. The use of hollow concrete blocks is widespread throughout the world and the main benefit of hollow concrete block masonry is a significant reduction in the weight of walls compared with solid masonry. Hollow concrete block masonry walls have a brittle failure mechanism in case of flexural bending under out-of-plane loading with a low ductility level.

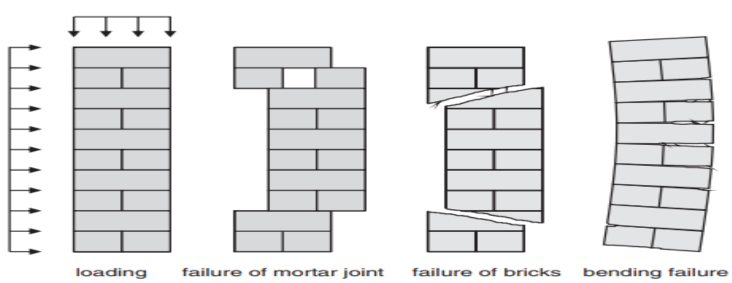

Figure.1 URM failure modes under out-of-plane loading (Lönhoff and Sadegh-Azar, 2018).

FRP is a high strength polymer containing long continuous fibres impregnated in a polymetric matrix, such as epoxy. The fibres provide stiffness and strength to the composite materials, while the matrix distributes the loads equally among the fibres. In civil engineering the common FRP composite reinforcement used to strengthen concrete structures are carbon fibre (CFRP), glass fibre (GFRP), basalt fibre (BFRP) and aramid fibre (AFRP). FRP composites are now implemented widely in construction. The FRP materials are identified and classified based on their mechanical properties. Flexural, shear, tensile strength, impact resistance, creep rupture and modulus of elasticity are the most common mechanical characteristics of FRP composites that are considered [9, 10]. FRP composites can be used in a variety of shapes to reinforce concrete, such as rebar, rod, tube, sheet, beam stirrup, plate, and textile and mesh fabric. Furthermore, masonry walls could be retrofitted and strengthened using most of the FRP composite shapes which have been mentioned (10). Several experimental studies have been conducted to investigate the behaviour of strengthened masonry walls under out-of-plane loading utilising various strengthening techniques with FRP composites. The most common finding is that FRP materials significantly increase the flexural capacity and ductility of strengthened masonry walls. [5] tested six full-scale hollow concrete block masonry walls, where five specimens were strengthened using GFRP sheets with different reinforcement ratios and stiffness and one URM wall was the control. The walls were subjected to uniform load of out-of-plane action until failure. The results of the study show that FRPs delays ultimate failure, in comparison with the URM control. Further, the FRP improved ductility capacity. Several types of failures were observed, and they were influenced by the FRP reinforcement layout and FRP reinforcement ratio. However, flexural failure due to FRP rupture occurred at the lowest FRP reinforcement ratio, where a failure due to debonding of the FRP laminate was observed at the higher FRP reinforcement ratio. Similarly, shear failure occurred at the highest reinforcement ratio. Research on the use of FRP to reinforce URM walls is extremely limited. Experimental studies should be improved to better understand how reinforced brick walls respond to lateral out-of-plane loads. However, these experiments are usually expensive, which means this procedure is not always the best choice. In this case, numerical analysis could be appropriate. Over the last two decades, a numerical approach has been used to estimate the behaviour of URM and

FRP reinforced masonry walls, and an analytical model was developed. Several numerical studies have been conducted to investigate the effect of out-of-plane loading on the FRP strengthening masonry walls, and some of the studies are outlined in this section. [11] Presented a finite element model that used layered shell elements to study the behaviour of masonry walls under out-of-plane loads. A masonry wall is analysed as a homogenised material with distinct directional properties calibrated from a wall's C-shape tested under application of pressure to its web. Validation of the layered shell model was done by using experiments reported in the literature that used out-of-plane datasets. In addition, the model was enhanced to accommodate reinforced masonry through a VUMAT subroutine suitable for the ABAQUS explicit algorithm. This model was used to analyse confined masonry as well as walls with high bond strength mortar joints. By extending the VUMAT algorithm to include shell elements in 3D, the in-plane behaviour of masonry walls can be simulated as well as out-of-plane behaviour. Study results revealed that the FE model successfully predicted out-of-plane behaviour for URM walls, and sensitivity analyses indicated that support conditions, aspect ratios, precompression, and opening had significant effects on wall ductility and strength. Alyavuz, Anil and [12] used a finite element model to model brick walls reinforced with CFRP strips to investigate the out-of-plane performance. ANSYS software is used to model six specimens, including one reference and five URM bricks walls reinforced with various configuration of CFRP strips. Multi-linear elastic material models were used to model brick and mortar masonry walls, while linear elastic material models were used to model CFRP strips. In the case of brick walls/CFRP strips interface, surface to surface contact elements from the ANSYS library are used. In this study, finite element simulations of load–displacement behaviour, damage distribution, and stress distribution between CFRP strips and brick walls were compared with experimental results, which were generally in agreement. In addition, a finite element analysis reliably predicted brick failure regions based on the distribution of shear stress. [6] Numerically simulated the behaviour of a URM and reinforced masonry wall with CFRP strips under out-of-plane action with the concrete damage plasticity (CDP) model. The masonry was modelled with a linear-elastic model, while the mortar joint was modelled with a continuum brick element. Consequently, a single block is formed. The FRP strips were modelled with reduced integration and high strain, allowing transverse shear deformation. The numerical model corresponded with the results of the experimental study, demonstrating that the overall flexural behaviour can be estimated using this model. The research also examined the properties of surface-to-surface contact for the FRP-masonry interface behaviour. This resulted in cohesive constitutive behaviour.

3. Modelling approach

Several modelling strategies using finite element modelling (FEM) were investigated to evaluate the behaviour of reinforced masonry walls with FRP under the impact of out-of-plane action. In this section, the FEM scheme developed is thus discussed, along with the performance of the simulated walls.

A. Modelling approach for unreinforced masonry walls

Masonry walls can be modelled using different types of model approach depending on the required accuracy and time of analysis. The main available models are the detailed micro-model, the simplified micro-model, and the macro-model, as shown in Figure 2 [13]. This study uses a simplified 3D micro-model to develop an analysis of reinforced masonry walls under out-of-plane loading. Masonry units are represented by continuum elements, whereas brick and mortar joints are represented by discontinuous elements. The numerical model was generated using the ABAQUS CAE user interface, which included all the parts, assembly, boundary conditions, meshing, applying loads, submitting jobs and examining the results. The block units were modelled using the solid element C3D8R of an eight-node linear brick element with reduced integration. The masonry unit defined by its elastic behaviour, based on specifying the Young's modulus and Poisson ratio. Nevertheless, A concrete damaged plasticity model (CDP) models the constitutive behaviour of concrete blocks based on continuous plasticity. It can be used to model brittle materials such as concrete masonry and other materials in any type of structure [14]. The CDP model deals with plastic behaviour, compressive behaviour, and tensile behaviour, in addition to incorporating the damage mechanism of concrete, which can thus be defined to increase the accuracy of the results as compared with other models. Joint interfaces were modelled using a zero-thickness of surface-based cohesive approach, defining hard contact behaviour between adjacent masonry surfaces using a contact pressure-overclosure relationship. The hard contact model assumes that surfaces transmit pressure when they are in contact, but that penetration and tensile stress transfer between surfaces are prevented. Therefore, this is consistent with the behaviour of contacting surfaces within masonry units [13]. The simplified micro-models presented in this study were generated in ABAQUS. The mesh generation of all models was conducted via global sizing, with dimensions of 100 mm for all block units. The steps adopted to conduct the numerical analysis then imposed either load or displacement on the model corresponding to the appropriate load control or displacement control. In both cases, actions were incrementally imposed. Thus, the models considered the large nonlinear displacement geometric impact. A general nonlinear static procedure was thus adopted, generating a Newton-Raphson algorithm solution which iteratively solved for equilibrium at each increment [13].

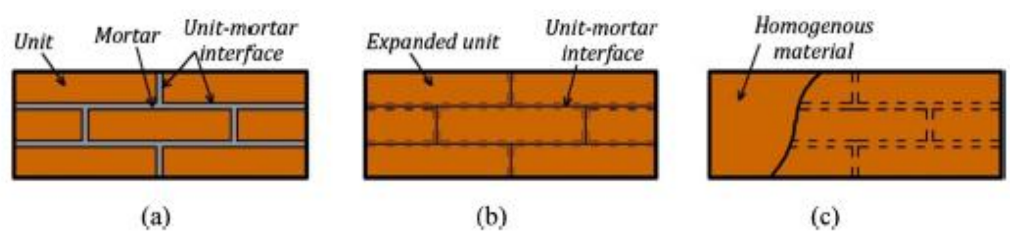

Figure 2 Modelling approaches for masonry walls: (a) detailed Micro-model; (b) simplified Micro-model; (c) Macro-model (Abdulla, Cunningham and Gillie, 2017)

B. Modelling approach for FRP strengthened masonry walls

The FRP sheets demonstrated linear elastic behaviour prior to brittle failure at stress levels equal to the ultimate rupture stress under tensile loading. The FRP sheet was thus modelled as a shell element of four nodes, with reduced integration (S4R) used to discretise the FRP sheets. The FRP sheets demonstrate linear elastic behaviour, and they were thus defined using the material type Lamina. The mesh was generated to provide an accurate solution with the shortest feasible analysis time, taking on a global size control of 50 mm. The FRP laminate is bonded to the external tension side of the masonry wall in order to distribute additional tensile stresses. In this way, the numerical model assumed full bonding between the FRP and the masonry wall, which prevented FRP failure modes, such as FRP debonding failures, from occurring. The orientation of the FRP was defined as a global coordinate system following the direction of the fibre.

C. Numerical simulation of unreinforced masonry walls

The elastic and inelastic behaviour of concrete blocks were both defined, the elastic behaviour directly by means of setting the Young's modulus of the concrete block equal to

30000 MPa and a Poisson ratio of 0.2, and the inelastic behaviour by means of the concrete damaged plasticity model (CDP) built into the ABAQUS software. The parameters required to define the plasticity model are the dilation angle (Ψ), the plastic potential eccentricity of concrete (ε), the ratio of compressive stress in the biaxial state to compressive stress in the uniaxial state (f_{b0}/f_{c0}), the shape factor of the yielding surface in the deviatoric plane (K), and a viscosity parameter. These values were obtained from the literature and calibrated with the experimental study. The recommended values of the yield shape surface K_c and eccentricity ε for the CDP model were 0.667 and 0.1, respectively, while the ratio of compressive stresses (f_{b0}/f_{c0}) was set to 1.16, as specified by the ABAQUS user manual. The values of the dilation angle Ψ and the viscosity parameter were set to 30 and 0.0001, respectively, identified from the literature and calibrated with the experimental study reported in [5]. The compressive behaviour of concrete in the CDP model was defined based on to stress-strain diagram for masonry concrete, as shown in Figure 3 [1]. Tensile behaviour was defined by the peak tensile strength for a masonry wall, giving a yield stress of 1.18 MPa and cracking strain equal to 0 [13].

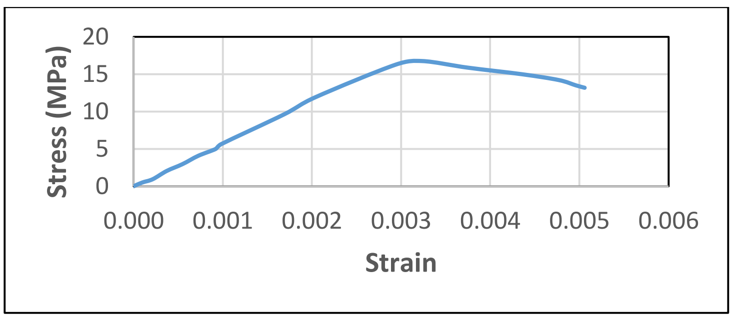

Figure 3. Compressive stress-strain curve for concrete block (Singh and Munjal, 2017)

The masonry wall was constructed using the same method as in the experimental study, with bonds created by using a full block of 200 X 400 X 200 mm and a half block of 200 X 200 X 200 mm to eliminate any effects of bond patterns. The wall was constructed with dimensions of 1600 X 1600 mm, with a width of one block (200 mm).

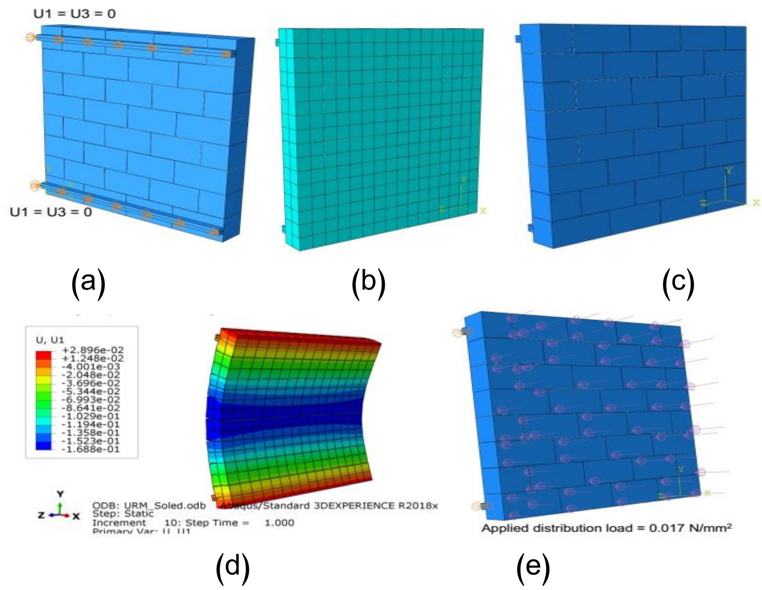

Figure 4: A typical URM wall (a) geometry, (b) finite element meshing, (c) boundary condition, (d) applied distribution load; (e) numerical deformation results

Two steel plates of 50 X 50 X 1600 mm were modelled to act as a support in the same direction as the bed joint and set at 100 mm distances from each edge of the wall to act as a roller supports to restrain vertical movement only during loading. The steel support was defined in terms of its elastic behaviour with a Young's modulus and a Poisson ratio of 190 GPa and 0.3, respectively. In addition, the plastic behaviour was defined with a yield stress of 210 GPa and a plastic strain equal to zero. Both steel plates were modelled as fully bonded to the masonry wall. The out-of-plane distribution load, which was modelled to simulate the pressure load from the airbag seen in the experimental test, was applied to all the specimens and the ultimate load applied for each specimen was calculated based on the ultimate moment results from the experimental study. The URM wall which acts as a control specimen, denoted as WC in the experimental study, was tested without any reinforcement with a maximum load of 0.017 N/mm^2: figure 4 illustrates the model geometry, finite element meshing, boundary condition, and applied loading for this URM wall.

D. Numerical simulation of GFRP strengthened masonry walls

The elastic behaviour of material type Lamina, available natively in the ABAQUS software, was used to simulate the GFRP strengthened masonry walls. The modulus of elasticity E1 in the hoop direction was specified as 16.9GPa based on the experimental study, with a thickness of 1.85mm, while E2, G12, G13 and G23 were defined with small values, specified as 7.5, 3.6, 3, and 3GPa, respectively, with a Poisson ratio of zero [15].

Four GFRP reinforced masonry walls with different layouts were thus modelled to validate the numerical model with the available data from the experimental study (5). The W1 specimen with horizontal and Vertical FRP strips developed in the experimental study was ignored, however, due to its similarity with specimen W4, which has only vertical FRP strips (that is, strips in a perpendicular direction to the bed joint). This is sufficient, as the test only considers one-way bending behaviour such that horizontal strips will not have a significant effect on the observed behaviour. Specimen W2 has two vertical single layer GFRP sheets with widths of 300 mm, in the same layout as W4, which has three GFRP sheets with widths of 150 mm. W3 has symmetric diagonal GFRP strips, while W5 has a vertical GFRP sheet bonded across the full surface of the wall. The ultimate load applied for each specimen is illustrated in Table 1.

The numerical modelling investigated the deflection behaviours for all specimens by observing the maximum deflection in the mid-span of the specimens. Furthermore, the masonry wall reinforced with GFRP sheets was shown to have enhanced bending moment capacity and deflection performance: Figure 5 illustrates the overall behaviour of reinforced masonry walls using GFRP strips.

Table 1. Applied load in the numerical analysis for each specimen

Wall identifier	Experimental Ultimate moment (KN.m)	Numerical load Applied calculated from maximum moment (N/mm^2)
WC	5.8	0.017
W2	40.6	0.118
W3	23.7	0.069
W4	38.3	0.112
W5	51.9	0.151

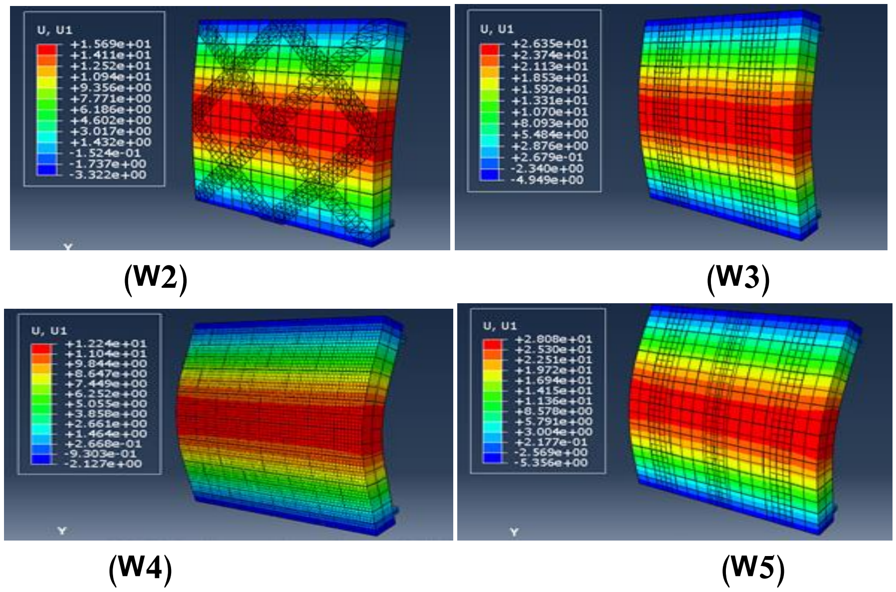

Figure 5. Numerical analysis results for GFRP sheet strengthened masonry walls

4. Validation of the numerical model approach

The numerical model results were validated using available data from the experimental test results discussed. The moment displacement relationships gathered from the numerical analysis for specimens WC, W2, W3, W4 and W5 were thus compared with the experimental results, as shown in figure 6. The URM control wall shows linear behaviour with sudden failure that is almost the same in both the experimental and numerical analysis cases; however, the numerical analysis offers a lower deflection value compared with the experimental study. The main reason for this is the uncertainties surrounding the parameters used to define the concrete block and joint interface; these details were not available from the experimental study and were thus taken from the literature, while the results suggest that more detailed calibration of each parameter is required to obtain more accurate result. Nevertheless, the numerical analysis for specimens W2 and W4 shows almost the same behaviours for the moment-deflection relationships between the numerical and experimental tests, although the maximum numerical deflection at mid-span is larger in the simulation than the experimental result, at 26.3 and 24.6mm, respectively for W2 and W4, while those in the experimental test were 20.8 mm for W2 and 20.2 mm for W4. These differences are likely to have arisen from the same parameter uncertainty noted previously.

The specimen W3, which is reinforced with symmetric diagonal GFRP, showed similar behaviours for the moment-deformation curve, with similar maximum deformations at mid span of 15.8 mm in the numerical analysis and around 17.6 mm in the experimental test. The specimen W5, reinforced with a GFRP covering across the full external wall surface, demonstrated high stiffness in the numerical analysis, with a lower deflection compared with the experimental result of 0.45 accuracy level. This significant high difference in the deflection relates to the difference in the frictional contact between the FRP and masonry walls, which is considered a specific node in the numerical model, while in the experimental test, friction applies across the full surface. The W5 specimen was thus omitted from the rest of the research, with only WC, W2, W3 and W4 having accuracy ratios of numerical deflection to experimental deflection between 0.89 and 1.3 considered.

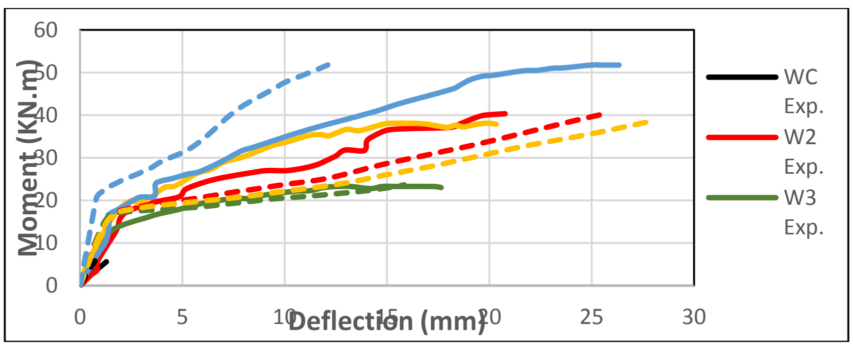

Figure 6. Compare of Moment-mid-span deflection behaviour for GFRP reinforced masonry wall in experimental and numerical study

The moment-FRP strain obtained from the numerical analysis was also compared with the experimental results, as shown in figure 7. The moment-FRP strain relationships generally demonstrated the same behaviours between the experimental and numerical analysis for specimens W2, W4 and W5, though this again differed in the diagonal FRP specimen.

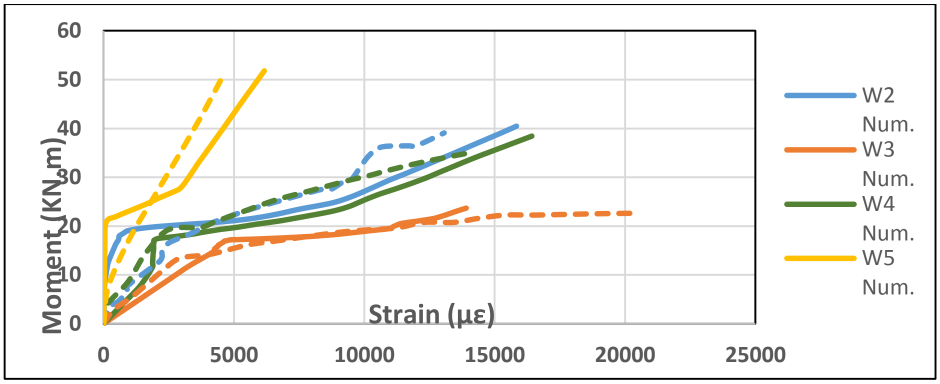

Figure 7. Compare of Moment-GFRP strain curve in the experimental and numerical study

5. The effect of FRP reinforcement ratio on the flexural behaviour of masonry walls

FRP reinforcement ratios were observed as having a clear impact on both the flexural performance of masonry walls and the ratio of increased flexural capacity when using GFRP and CFRP to strengthen masonry walls. The numerical analysis for the seven FRP reinforced masonry walls examined also illustrated various effects on the ductility performance of masonry walls. Figure 8 shows the effect of the FRP reinforcement surface area ratio on the bending moment capacity observed within the previous experimental study to investigate out-of-plane performance in strengthened masonry wall with GFRP by [5] and the numerical analysis of the use of both GFRP and CFRP on the validated model carried out in this study.

The figure 8 illustrates good agreement between the experimental and numerical analysis for walls strengthened with GFRP materials. However, based on numerical analysis, GFRP and CFRP strengthening of masonry walls has a significant influence on the gain in out-of-plane capacity, by up to 27.3% of FRP surface ratio. The flexural capacity also shows dramatic increases, growing from 302% to 562% in the numerical model using GFRP as FRP surface area increases from 18.8% to 27.3%, while in the numerical model with CFRP reinforcement, it improves from 302% to 703% as the surface area increases similarly. Nevertheless, the influence of these increases in the FRP surface area ratio are reduced at higher levels: as the FRP surface area ratio increases from 27.3% and 56.2%, the gained moment capacity increases from 562% and 722% using GFRP and from 703% and 958% using CFRP.

In terms of the influence of FRP materials on FRP reinforcement ratios and the gained moment capacity relationship, nether carbon nor glass FRP materials affect the gained moment capacity at surface area ratios of up to 18.8%. However, further increases in FRP surface area ratio result in a slight increase in gained flexural capacity for carbon strengthened masonry walls as compared with those using glass materials. Increases in carbon materials improve the moment capacity, by 25% at a 27.3% FRP surface area ratio and by up to 32% at a 56.2% FRP surface area ratio, as compared with using glass materials. This increase of moment capacity derived from using carbon materials to strengthen masonry walls is, however, not sufficiently significant to justify the high cost of CFRP in comparison with GFRP. Although using CFRP increases the gain in out-of-plane capacity more than GFRP, such increases are insignificant as compared with the overall improvement of moment capacity offered by URM. Moreover, the high cost of CFRP means that GFRP is a preferable option economically for use in strengthening masonry walls.

The FRP surface area ratio was considered only in vertical FRP strips, as diagonal FRP strips provide different performance with regard to bending capacity; even a high surface ratio of diagonal strips at 51.4% results in increases of moment capacity of 307 and 314% using GFRP and CFRP, respectively. This demonstrates that the vertical strips have a significant influence on improving flexural behaviour using less FRP than diagonal strips.

As illustrated in Figure 9, strengthening masonry walls with FRP offers significant improvement of the deflection for URM, which increases the ductility level for the relevant masonry. However, the FRP surface area ratios have less of an impact on deflection: where the FRP surface area ratio increases from 18.8% to 27.3%, the deflection changes from 9.7 to 22.7 mm for GFRP materials, and from 17.3 to 27.3 mm for CFRP materials. On increasing the FRP surface area ratio, the deflection thus remains mostly the same, being reduced only slightly when the FRP ratio rises over 40%; this applies to both types of FRP material. A high ratio of FRP materials, which will create high stiffness, will also impact on the ductility performance of the resulting masonry structure, affecting the failure mode of the masonry walls.

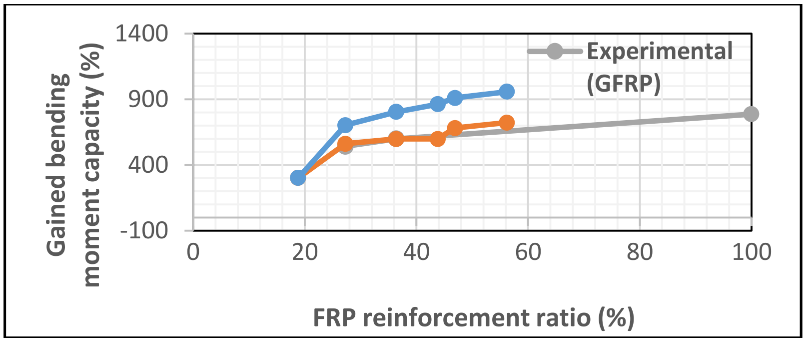

Figure 8. Effect of FRP surface area ratio on gained bending moment capacity

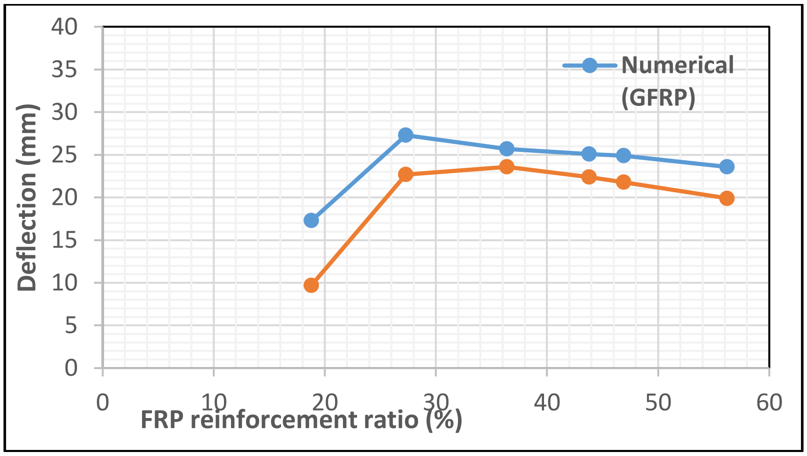

Figure 9. Effect of FRP surface area ratio on deflection

a. The effect of FRP reinforcement materials on the flexural behaviours of masonry walls

FRP material type is one of the parameters that affect the bending moment performance of masonry walls under out-of-plane loading. The differences in the mechanical properties for each type of FRP thus have significant impacts on strengthening masonry walls behaviour, with CFRP offering high stiffness at high cost, causing GFRP to be generally preferred as a cheaper material than CFRP. In this section, the effects on flexural performance of masonry walls of reinforcement with GFRP and CFRP materials is thus discussed, based on the validated numerical model.

Figures 10 and 11 show moment versus midspan deflection for all of the reinforced walls investigated. The curves show two distinct phases of response. During its first phase, the flexural response is almost linear, reaching a maximum of 1 to 2.5 mm midspan deflection. The tensile capacity of the mortar is reached during this phase, triggering crack initiation. When a joint is separated or the mortar-block is broken as a result of this, the load is then transferred to the next joint, and this process continues until the joint in the maximum moment region of the wall separates completely. The second phase of response involves reduced flexural stiffness due to joint separation. At this point, the flexural stiffness of the specimen is dependent on the percentage of FRP reinforcement. The moment–deflection curves thus show the influence of the FRP reinforcement and the type of FRP material used on masonry wall behaviours.

Focusing on figure 10, which offers a comparison between the experimental and numerical analysis of two type of FRP for three masonry walls, W2, W3 and W4, good agreement between the test types can be observed for all walls in terms of deflection, although the numerical analysis in walls W2 and W4 offers slightly higher values than those found experimentally. However, wall W3, strengthened using diagonal FRP strips gives almost the same behaviour, with the moment capacity improved by just over a half, at 23 KN.m, compared to walls W2 and W4, despite the FRP surface area ratio in W3 being much higher than in W2 and W4. Furthermore, the type of FRP reinforcement in masonry walls with diagonal configuration appears to have no effect on the flexural behaviour, as demonstrated in figure 10 (b). In the numerical analysis, walls W2 and W4 showed similar behaviours, and figure 10 (a) and (c) illustrate that the using CFRP to strengthen masonry walls increases the maximum moment capacity while decreasing deflection as compared with strengthening masonry walls using GFRP.

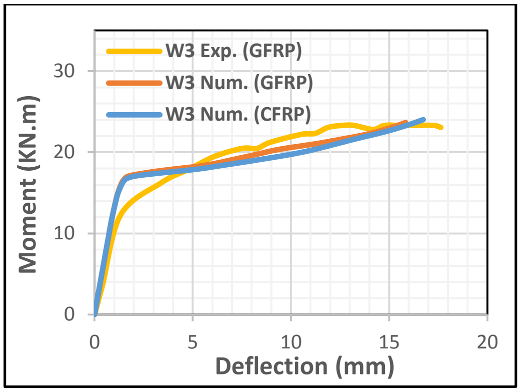

(a)

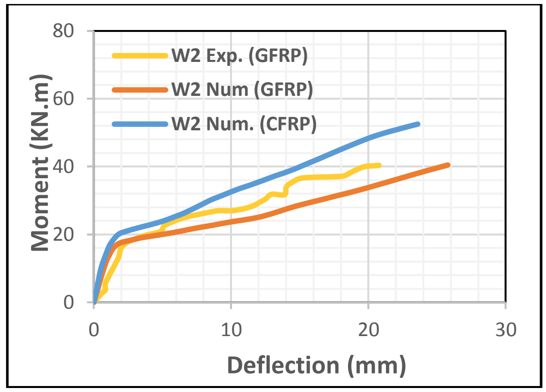

(b)

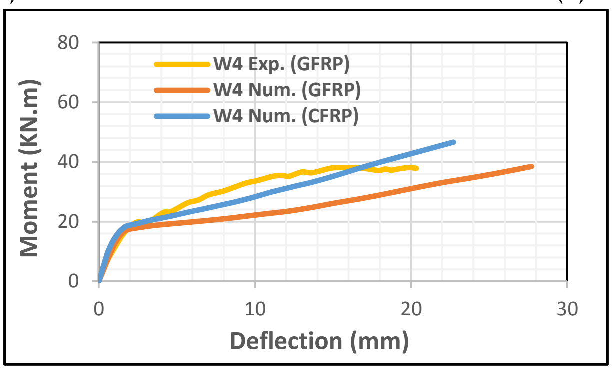

(c)

Figure 10. Moment deflection curves for walls (a) W2, with vertical strips, (b) W3, with diagonal strips, and (c) W4, with vertical strips

6. Conclusions

In this study numerical studies are conducted on the linear, nonlinear, and flexural behaviour of unreinforced and reinforced masonry walls subjected to out-of-plane loading. Experimental results and materials property data are obtained from [5, 16] tests in order to validate numerical models. A 3D model simulates unreinforced and FRP-reinforced walls using finite element (FE)-based software (ABAQUS) utilizing nonlinear materials defined by concrete damaged plasticity (CDP) behaviour to model block units. The mortar joint is simulated using a zero-thickness interface with cohesive behaviour, while FRP strips are modelled using linear material type Lamina. The experimental results and numerical simulation comparisons indicate that the model is able to reproduce the experimental behaviour accurately in terms of the ultimate moment, initial stiffness, and mid- span deflection of the FRP- reinforced masonry walls with vertical strips. The purpose of this study is to gain a better understanding of the effects of various parameters such as FRP reinforcement surface ratio and type of FRP materials on the out-of-plane performance of masonry walls reinforced with various FRP configurations. This study presents a detailed analysis of masonry walls that are reinforced with FRP to investigate a complex behaviour.

Based on the findings of this numerical study, we can draw the following conclusions:

- Externally bonded FRP composites can significantly increase the bending moment capacity of URMs under out-of-plane loads. Furthermore, the FRP laminates could substantially increase the out-of-plane deformation capability of URM walls, which indicates that FRP laminates could make an important contribution to enhancing wind and seismic resistance of masonry walls.
- Increasing in FRP reinforcement surface area ratio reduces the effectiveness of FRP laminate in terms of improving the moment and deformation capacity of URM walls.
- FRP diagonal strips have a smaller impact on the one-way moment capacity of masonry walls than vertical strips with the same reinforcement ratio.
- Using high strength FRP, such as CFRP strips, has less influence on improving flexural capacity. In addition, the high stiffness of FRP also reduces the deflection capacity of masonry walls as compared to FRP, which has a lower stiffness.

7. Recommendations of future research

A current research project evaluates the numerical behaviour of unreinforced and reinforced masonry walls using FRP. Despite the lack of test data for some material properties, the material parameters needed to validate the numerical model were gathered from the literature. Likewise, In the absence of a bond test that could provide the behaviour of the FRP/masonry interface, the FRP/masonry interface has been modelled as fully bonded. However, the bond test should be done to determine the real behaviour of FRP/masonry interface. A static out-of-plane loading model was formulated in this proposed numerical model. Therefore, future research should investigate the performance of FRP-strengthened masonry walls under both cyclic and dynamic loading, as well as under in-plane and out-of-plane loading. Further, a wide range of FRP and model configurations can be tested in order to evaluate the performance of the wall, including or not including openings made in the masonry walls. In this study, one-way bending moments were evaluated. Therefore, two-way flexural behaviour can be examined in the future, in addition to evaluating the influence of horizontal and diagonal FRP strips. Finally, as an extension of the current study and to incorporate the new modelling scheme for FRP reinforced masonry walls, a parametric study can be conducted to examine the influence of aspect ratio, openings (doors or windows), type of FRP, and applied vertical loads, etc.

REFERENCES

1. Singh, S. B. and Munjal, P. (2017) 'Bond strength and compressive stress-strain characteristics of brick masonry', Journal of Building Engineering, 9(June 2016), pp. 10-16. doi: 10.1016/j.jobe.2016.11.006.
2. Willis, C. R., Seracino, R. and Griffith, M. C. (2010) 'Out-of-plane strength of brick masonry retrofitted with horizontal NSM CFRP strips', Engineering Structures, 32(2), pp. 547-555. doi: 10.1016/j.engstruct.2009.10.015.
3. Galal, K. and Sasanian, N. (2010) 'Out-of-Plane Flexural Performance of GFRP-Reinforced Masonry Walls', Journal of Composites for Construction, 14(2), pp. 162-174. doi: 10.1061/(asce)cc.1943-5614.0000061.
4. Bui, T. T. and Limam, A. (2014) 'Out-of-plane behaviour of hollow concrete block masonry walls unstrengthened and strengthened with CFRP composite', Composites Part B: Engineering, 67, pp. 527-542. doi: 10.1016/j.compositesb.2014.08.006.
5. Elsanadedy, H. M. et al. (2016) 'Behavior and Design Aspects of FRP-Strengthened URM Walls under Out-of-Plane Loading', Journal of Composites for Construction, 20(6), p. 04016048. doi: 10.1061/(asce)cc.1943-5614.0000695.
6. Monaco, A. et al. (2017) 'Finite element analysis of the out-of-plane behavior of FRP strengthened masonry panels', Composites Part B: Engineering, 115, pp. 188-202. doi: 10.1016/j.compositesb.2016.10.016.
7. Ferreira, T. M., Costa, A. A. and Costa, A. (2015) 'Analysis of the Out-Of-Plane Seismic Behavior of Unreinforced Masonry: A Literature Review', International Journal of Architectural Heritage, 9(8), pp. 949–972. doi: 10.1080/15583058.2014.885996.
8. Lönhoff, M. and Sadegh-Azar, H. (2018) 'Seismic out-of-plane behavior of unreinforced masonry walls', Ce/Papers, 2(4), pp. 291-299. doi: 10.1002/cepa.844.
9. Mugahed Amran, Y. H. et al. (2018) 'Properties and applications of FRP in strengthening RC structures: A review', Structures, 16(September), pp. 208-238. doi: 10.1016/j.istruc.2018.09.008.
10. Shakir Abbood, I. et al. (2020) 'Properties evaluation of fiber reinforced polymers and their constituent materials used in structures - A review', Materials Today: Proceedings, 43, pp. 1003-1008. doi: 10.1016/j.matpr.2020.07.636.
11. Noor-e-khuda, S., Dhanasekar, M. and Thambiratnam, D. P. (2016) 'An explicit finite element modelling method for masonry walls under out-of-plane loading', Engineering Structures, 113, pp.

103–120. doi: 10.1016/j.engstruct.2016.01.026.

12. Alyavuz, B., Anil, Ö. and Bulut, N. (2016) 'Nonlinear finite element analysis of masonry wall strengthened with CFRP strips', Advanced Composite Materials, 3046, pp. 1-17. doi: 10.1080/09243046.2014.976735.
13. Abdulla, K. F., Cunningham, L. S. and Gillie, M. (2017) 'Simulating masonry wall behaviour using a simplified micro-model approach', Engineering Structures, 151, pp. 349–365. doi: 10.1016/j.engstruct.2017.08.021.
14. Halapi, M. and Murčinková, Z. (2016) 'Influence of the individual layers of laminate on the final static response', Procedia Engineering, pp. 143–148. doi: 10.1016/j.proeng.2016.06.648.
15. Munjal, P. and Singh, S. B. (2020) 'Out-of-plane response of ECC-strengthened masonry walls', Journal of Structural Integrity and Maintenance, 5(1), pp. 18-30. doi: 10.1080/24705314.2019.1692165.
16. Ahmed Alhodairi (2021). Numerical Analysis of the Flexural Behaviour of Masonry Walls Reinforced With FRP Under Out-Of-Plane Loading. Master Thesis, The University of Sheffield- Department of Civil and Structural Engineering

Effect of jute geotextile on bearing capacity of sand soil from Al-Qatroun, Libya

Fathia Alnaas
Department of Civil and Structural Engineering
OMAR ALMUKHTAR UNIVERSITY,
LIBYA
Email: fathia.alnaas@omu.edu.ly

Enas B. Altalhe
Department of Civil and Structural Engineering
OMAR ALMUKHTAR UNIVERSITY,
LIBYA
Email: enas.omer @omu.edu.ly

Samiha Abdelrahman
Department of Civil and Structural Engineering
OMAR ALMUKHTAR UNIVERSITY,
LIBYA
Email: samiha.abdelrahman@omu.edu.ly

Abstract

Recently there has been a strong demand for the use of jute geotextile for improving mechanical, in addition, and physical properties of cohesive less soil. The research aims to study the effect of applying jute geotextile on subsurface layer of sandy soil; additionally, this paper presents the results of laboratory load tests on model circular footings supported on reinforced sand beds. The experimental results showed that the most increase in ultimate bearing capacity (UBC) of footings on supported soil (by jute geotextile) is viewed as expanded by a variable of 2.02 when compared with soil without jute geotextile. Also to Verification of the experimental results of bearing capacity were compared with the theoretical bearing capacity that was determined by Meyerhof, Terzaghi, and Brinch. The experimental results are in good agreement with the Terzaghi equation by factor of 0.99, while Meyerhof equation and Brinch Hansen by a factor 0.89 and 0.91 respectively.

Keywords— jute geotextile, improved, bearing capacity, circular footing, sand soil

1. INTRODUCTION

Structural damage is usually caused by laying the structure's foundation on top of a loose layer of soil. Structural loads cannot withstand the loose soil layers. The result is subsidence and cracking of the structure, leading to collapse of the structure. Therefore, deep foundations are chosen when constructing structures in these loose soil layers. However, due to its enduring popularity, the design can be expensive to develop. Therefore, soil improvement is carried out to avoid the above problems. The most common method of soil amendment is the use of geosynthetics. These geosynthetics are used as constraints to build soil layers according to their thickness and strength (bearing capacity).

"Reinforced soil" refers to soil that has been strengthened by embedding reinforcing material in the form of strips, bars, sheets, or grids (meshes) within the soil mass. These materials oppose the pliable burdens that foster inside the supported soil mass when burden is applied to it. It is possible for an element with a low tensile strength to break or yield, rendering it useless. If the soil's tensile strength is sufficient but its extension under stress is high, the soil may exhibit significant movement or settlement because of the soil-reinforcement system's insufficient stiffness.

The initial investigation into the effect of soil reinforcement on increasing the bearing capacity of footings was carried out by Binquet and Lee [1, 2]. what's more, was then sought after by various others. Guido and others According to Akinmusuru and Akinbolade [3] and Akinmusuru, the bearing capacity of a single reinforced footing does not significantly increase with the number of reinforcement layers above 3. However, Das and Omar [5] and Boushehrian and Hataf [6] reported that a single reinforced footing was the best design (N=4).

One sort of ground improvement includes implanting metallic geosynthetics in the soil to upgrade its designing way of behaving. Reinforcement is one specific method for improving the shear, compression, hydraulic conductivity, and density mechanical properties of the soil. The ground improvement by giving help was furthermore before long in a long time ago. Utilizing the idea of soil support, the Babylonians built ziggurats multiple a long time back. A portion of the Great Wall of China is also constructed using reinforced soil. The soil building up strategy was used by the Dutch and Romans to support willow creature stows away and embankments. France's Henry Vidal [7] explored the essentials of built up soil development inside and out, exhibiting its everywhere application and fostering the levelheaded plan strategy. The researchers who carried out experimental studies to develop the subsequent modification to soil reinforcement are as follows: Abu-Farsakh et al. [8]; Chakraborty and Kumar [9]; for a built up soil structure, Abu El-Soud and Belal [10] proposed a bunch of plan boundaries.

Ranganathan [11] reported that the biodegradability of jute does not pose a problem for this end use once a road has been fully constructed and is in use. He also discussed the development and potential of JCT. According to Rao and Balan [12], the tensile strength of JGT embedded in soil would be negligible after three to four months. Rao and Vensiri [13] detailed that a dike developed over delicate earth involving JGT as a building up layer at its base performed well. He reasoned that the general operation of a supported bed is affected by the maturing of the soil, even though the JGT's rigidity decreased. Sahu and colleagues [14] examined the performance of Geojute reinforced in a soil bed under cyclic loading. They saw that overall show of black-top isn't obstructed even after complete biodegradation of Geojute. Jadhav and Damgir [15] utilized jute geotextile JGT to support soil and increment its bearing limit with progress.

The availability of land in urban areas is decreasing while the cost of land continues to rise in tandem with population growth. Subsequently, new offices can be added to lacking regions on account of metropolitan infill. Geotechnical engineers may encounter difficulties in this setting despite the possibility of weak foundation materials in undeveloped areas. It is fundamental to change the establishment soil or add a design fill to stay away from the significant expense of a profound establishment. In any case, the fundamental requirements of the concealed built-up soil have not been thoroughly investigated. Geojute support for expanding bearing limit has, no nether less, been the subject of not many investigations.

Accordingly, the reason for the ongoing review is to explore the improvement of the bearing limit of soil (sand) with support as normally happening geo jute.

2. OBJECTIVE OF PRESENT STUDY

The present investigation aims to:

a) To examine the bearing capacity of a model circular footing resting on a reinforced sand bed under vertical load.

b) To conclude the store settlement lead without geotextile and with geo-jute geotextile.

c) To see if the reinforced soil with geo-jute geotextiles has increased its bearing capacity.

3. EXPERIMENTAL PROCEDURE

3.1 The test tank

According to Kiran and Nagraj Bacha [16], the failure zone should have a maximum expansion along the sides that is 2.5 times the width of the footing, and the foundation should have a depth that is three times the width of the footing below the base of the footing. To avoid disfigurement, the test tank was constructed of inflexible steel with a thickness of 3 millimeters and contained roundabout stiffeners inside. The inside diameter of the cylindrical tank was 150 mm, and its height was 178 mm. 140 mm high was the sand in the tank. As displayed in Fig (1). During the exploratory work, the extreme breadth of the circular footing was 68 mm, and its thickness was 10 mm.

Fig. 1. Setup of Circular Footing

3.2 MODEL FOOTINGS

For the purposes of the experiments, a mild steel model footing with a diameter of 68 millimeters, a thickness of 22 millimeters, and a weight of 193.99 grams is used. A grove is cut into the center of the top face of the footing to place a rigid metallic ball that helps to apply a load between the footing and the bottom of the proving ring (Fig. 2). The footing is placed on the sand bed in such a way that it is rough, allowing for friction between the footing and the foundation soil when loads are applied.

Fig. 2. Circular Footing

3.3 Test Material

The sand was brought from Libya's Al-Qatroun and oven-dried for one day. Then, at that point, it was sieved in strainers having breadths of 4.75 mm and 0.075 mm. This study's sand was filtered through a 4.75-mm sieve but retained in a 0.075-mm sieve. Fig. 3 depicts the distribution of grain sizes. The attributes of the sand utilized in the examination were acquired through research facility tests, and the grain size conveyance is recorded in Fig.3 and table 1 separately.

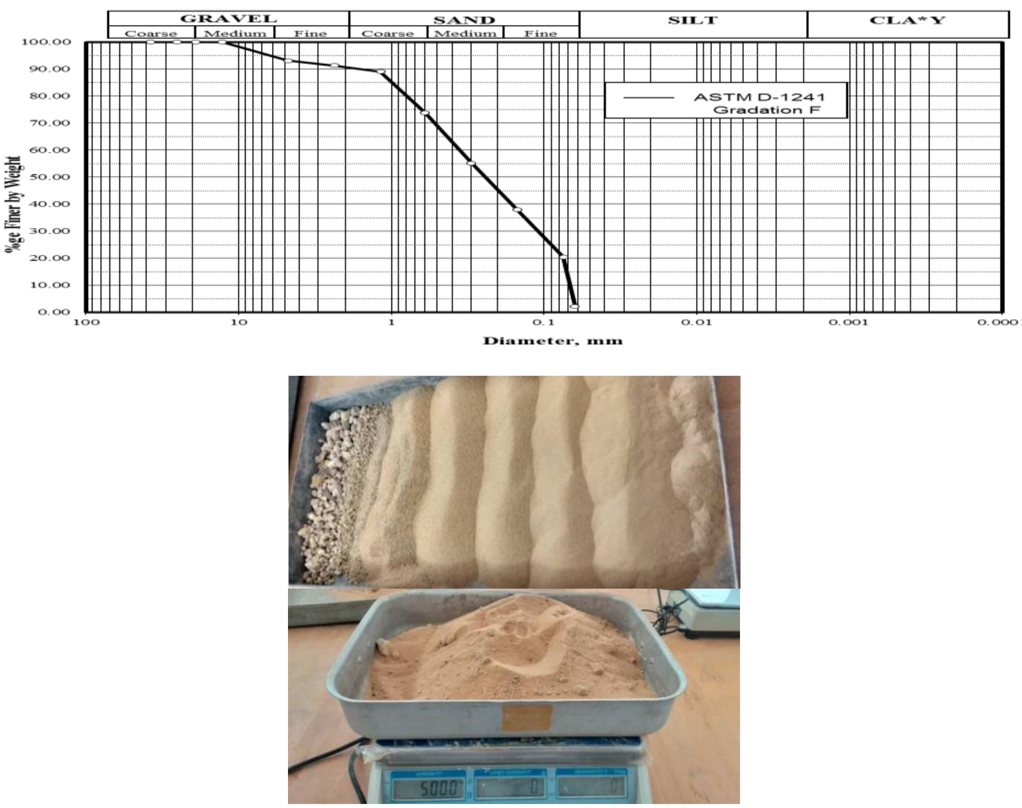

Fig. 3. The distribution of sand particle sizes

3.4 Geojute-geotextile

Geojute is the subject of this study (Fig. 4) functions as a geotextile. The jute gunny bags that are available in the local market are used to make this geojute. The geojute is cut to the required size from the jute gunny bags. The thickness of each strand of jute string utilized in the texture is roughly 1.0 mm, Elongation 3.5% and Modulus of Elasticity 20.4 kg/cm2.

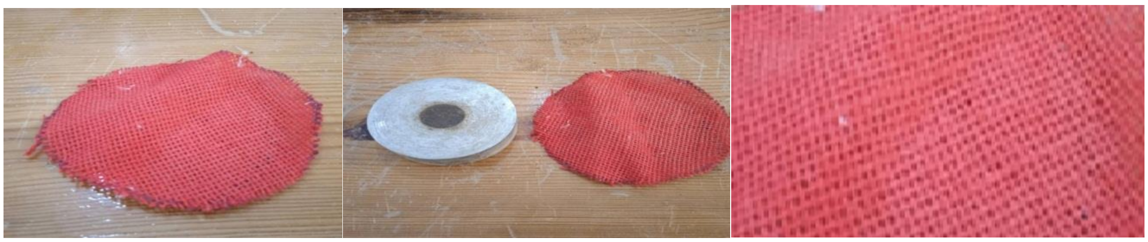

Fig. 4. Geo-jute geotextile

Table. 1. Geotechnical Property of Sand

Properties	Value/ Description
Physical properties	
Moisture Content (W)	67%
Water adsorption	1.98 %
Specific gravity	2.536
Permeability(cm/sec)	.117
Bulk Unit Weight (g/cm^3)	1.843
Relative Density(D_r)	26%
Residual effective angle of internal friction (φ')	19
Maximum dry unit weight (g/cm$^{3)}$	2.004
Minimum dry unit weight (g/cm^3)	1.74
Grain size distribution and classification	
D10(mm)	0.068
D30(mm)	0.12
D60(mm)	0.359
Uniformity coefficient (Cu)	5.28
Curvature Coefficient (Cc)	0.59 (the soil is gap-graded soil
USCS	Loose Sand

There are three categories for the failure mechanism: failure due to punching, general, and local shear. Likewise, it was accounted for that the idea of the failure in the soil for a definitive burden relies upon the compressibility of the soil and the proportion between the depth of the foundation and the footing width [17]. The punching shear was the failure mechanism, as depicted in Figure (5), which is in line with the results of [17].

Fig. 5. Failure shape of the footing with a 68mm diameter

Additionally, the footing was not bulging; consequently, the results were unaffected by the dimension of the model. The results of the test showed that there was a good amount of repeatability, which increased confidence in the preparation of the sand sample and the performance of the equipment. Subsequently, it was feasible to deduce that the exploratory information upheld the hypothetical expectation and could be utilized to assess the upsides of utilizing roundabout balance on geo-jute supported soil.

4. RESULTS AND DISCUSSION

4.1 Verification of experimental result

Terzaghi [18] extended earlier equations to account for the weight of soil and the bearing capacity effect of soil above the foundation base. Terzaghi's equation has many assumptions: 1) The soil is semi-infinite, homogeneous and isotropic; 2) The problem is two-dimensional; 3) Thebase of the footing is rough; 4) Mohr-Coloumb criteria; 5) The ground surface is horizontal; 6) The failure is caused by general shear; 7) The overburden pressure at foundation level is equal to a surcharge load (γD_f, whereγ is the effective unit weight of soil, and D_f is the depth of foundation less than the width B of the foundation). Terzaghi's equation is:

$$q_u = 1.3CN_c + \gamma D_f N_q + 0.3B\gamma N_\gamma \quad (1)$$

Meyerhof [19] proposed a general bearing capacity equation that takes into account the shape and inclination of the load because Terzaghi's method only works with circular footing. The general form of equation suggested by Meyerhof for bearing capacity is

$$q_u = CN_c S_c d_c i_c + \gamma D_f N_q S_q d_q i_q + 0.5B\gamma N_\gamma S_\gamma d_\gamma i_\gamma \quad (2)$$

Meyerhof's equation [20] was extended by Hansen [17]. The equations used by two researchers to calculate the values of Nc and Nq were distinct from those used to calculate the values of N_γ.

$$N_\gamma=(N_q-1)\tan(1.4\Phi)\,\text{(Meyerhof)} \tag{3}$$

$$N_\gamma=1.5(N_q-1)\tan\Phi \quad \text{(Hansen)} \tag{4}$$

As a result, the shape and N_γ factors are the primary contributors to variation in results. Table 2 provides a summary of the outcomes of the three methods.

Table 4 Comparison of different methods in bearing capacitycalculation

Method	Nc	Nγ	qu/(kN·m−2)
TERZAGHI	16.56	3.07	272.4
MEYERHOF	13.93	2.4	246.29
BRINCH HANSEN	13.93	2.48	249.4
Our study	—	—	≈ 275

The ultimate load (q_u) for each test was considered. The load corresponding to *S/B*= 5% can be taken as the given (Fig 6).

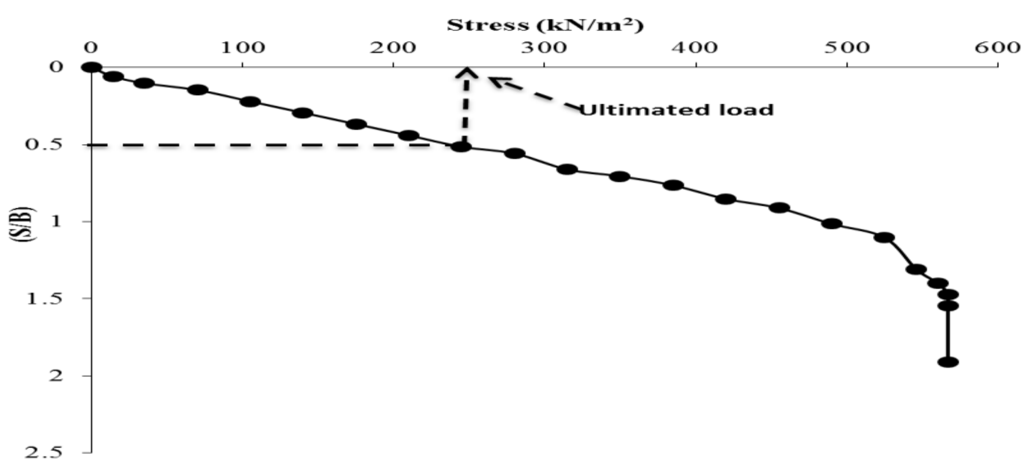

Fig.6. Bearing capacity calculation

The theoretical bearing capacity determined by Meyerhof, Terzaghi, and Brinch Hansen and the measurements of our study are compared in Figure 7. The experimental results are in good agreement with the Terzaghi equation, Since the load corresponding to S/B= 5% value is (0.99). on the other hand, the Meyerhof equation and Brinch Hansen measurements underestimate the bearing capacity determined by the experimental results. the overestimated factor was determined by The method used to predict the ultimate bearing capacity. the over prediction rate is (0.89) for the Meyerhof equation and (0.91) for the Brinch Hansen equation.

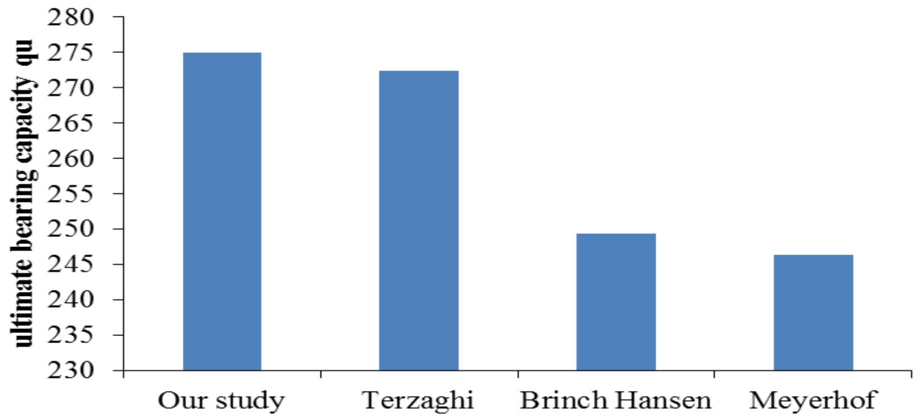

Fig.7. Comparisons between the theoretical bearing capacity and the Experimental value.

4.2 Effect of reinforcement on Bearing Capacity Ratio(BCR)

Load- settlement characteristics were obtained from various tests. The tests were conducted till failure and corresponding load and settlement were recorded. The terms Bearing Capacity Ratio (BCR) and Settlement Reduction Factor (SRF) are used for convenience to interpret the test data. The tests were conducted for four different values of H such as 0.25cm, 0.5cm, 0.75 and 1.0cm.

$$BCR = \frac{q_r}{q_0} \tag{5}$$

$$SRF = (\frac{S}{B})_r / (\frac{S}{B})_0 \tag{6}$$

The load-settlement behavior of footings on reinforced sand at various depths of geo-jute geotextile reinforcement i.e. 0.25cm to 1.0cm is compared with that of unreinforced sand. The results are reported in Figs. 8.

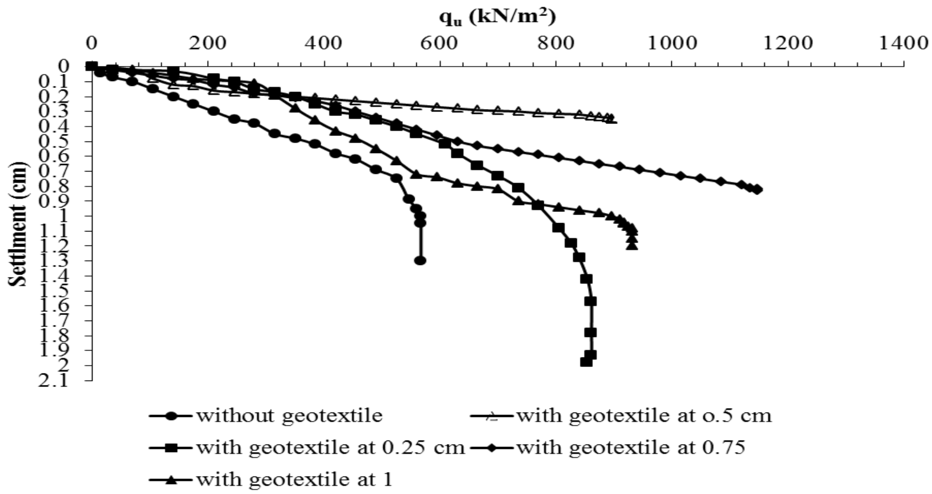

Fig.8. Variation of load-settlement of circular footing on reinforced sand.

4.3 Effect of depth of reinforcement on Bearing Capacity Ratio(BCR)

Figure 9 depicts the relationship between the bearing capacity ratio and the reinforcement depth. The most effective reinforcement zone is found between the depths of 0.25cm and 0.75cm, where the bearing capacity ratio of reinforced soil increases until it reaches the depth of 0.5 and gradually decreases until it reaches the depth of 1.0cm. As a result, the best depth was found to be 0.5cm. Geo-jute geotextile increases the UBC by a factor of 1.50 and 2.02 at the optimal reinforcement depth. The increase and decrease of bearing capacity ratio with respect to increase of depth may be due to the stress distribution theory. When a load is act on the foundation depth, the load is distributed within the influence zone of 1.0cm depth. The load intensity is high at the mid height of the influence zone i.e., 1.0cm. But in the present study, the load intensity is high within the zone of 0.25cm to 0.75cm and obtained maximum value at 0.75 by the application of reinforcement.

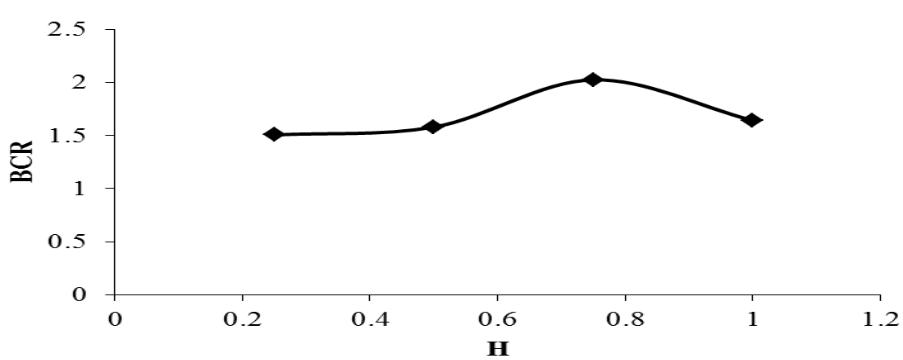

Fig. 9. The variation of BCR with H.

4.4 Effect of reinforcement on settlement

Settlement was also studied in relation to the effect of reinforcement. SRF decreases with increasing H values for all reinforcements when H = 0.5 is observed. SRF values, on the other hand, increase with increasing at H = 0.75, and at H=1.0, SRF values for all reinforcements are at their lowest. The variation of SRF with H values are depicted in Figure 10. This result can be explained by the fact that an increase in the depth of the geo-jute geotextile reinforcement layer greatly increases the bearing capacity of the unreinforced footing compared with that of the reinforced footing. The critical embedment depth-to-failure depth ratio H is approximately 0.5. On the two sides of the critical H ratio, the efficiency of the reinforcement seems to decrease significantly (as indicated by the reduction in settlement values). When H = 1.0, the performance of the reinforced sand becomes minimal. When the restraining force exerted by the reinforcement is imposed on soil elements, a re-orientation of the strain characteristics associated with the restraint of the minor principal strain of the soil elements occurs near the reinforcement [22]. A part of the reinforced zone with relatively large reinforcement force behaves like a part of a rigid footing and transfers a major part of the footing load to the deep zone. This load transfer mechanism seems to reach the optimum when the reinforcement embedment depth-to-failure depth ratio H is approximately 0.5. At large embedment depths, the contribution to the load transfer mechanism caused by the presence of the reinforcement reduces significantly.

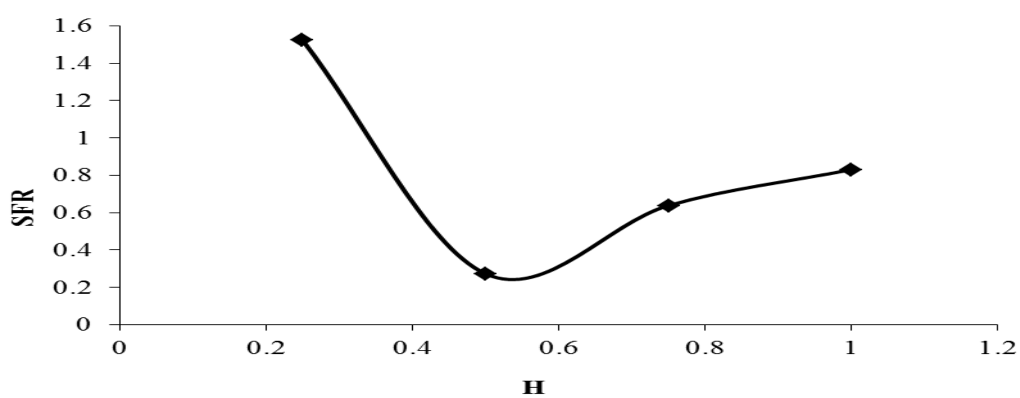

Fig. 10. The variation of SFR with H/B ratios.

5. CONCLUSION

The final bearing capacity of a circular footing supported by a single layer of geo-jute (for reinforcement) beneath a 68 mm circular footing in a sand bed subjected to a vertical centric load was determined through laboratory model tests. Loose sand has been the subject of tests.

1. The maximum gain in ultimate bearing capacity is observed when the reinforcementis placed at a depth of 0.75cm.
2. The most effective zone of reinforcement lies between depths of 0.25cm to 0.75cm.
3. At a distance of 0.75 centimeters from the failure depth, the soil's bearing capacity doubles.
4. The experimental results are in good agreement with the Terzaghi equation, as the load corresponding to S/B= 5% value is (0.99).
5. Meyerhof equation and Brinch Hansen overestimated the ultimate bearing capacity of experimental results. The overestimated factor depended upon the method used for predicting the ultimate bearing capacity. In Meyerhof equation the over pridicting rate (0.89), in Brinch Hansen is (0.91).
6. BCR also increased by a factor of 1.50 to 2.02.

References

[1] J. Binquet and K. L. Lee, "Bearing Capacity Tests on Reinforced Earth Slabs," Journal of the Geotechnical Engineering Division, vol. 101, no. 12, pp. 1241–1255, Dec. 1975.

[2] J. Binquet and K. L. Lee, "Bearing Capacity Analysis of Reinforced Earth Slabs," Journal of the Geotechnical Engineering Division, vol. 101, no. 12, pp. 1257–1276, Dec. 1975.

[3] J. O. Akinmusuru and J. A. Akinbolade, "Stability of Loaded Footings on Reinforced Soil," Journal of the Geotechnical Engineering Division, vol. 107, no. 6, pp. 819–827, Jun. 1981.

[4] V. A. Guido, G. L. Biesiadecki, and M. J. Sullivan, "Bearing capacity of a geotextile-reinforced foundation," presented at the International conference on soil mechanics and foundation engineering 11, San Francisco, CA, USA, 1985, pp. 1777–1780.

[5] Das, B. M., and Omar, M. T. “The effect of foundation width on model tests for the bearing capacity of sand with geogrid reinforcement”, Jour. of Geotech. andGeolog. Eng., 12 (2), (1994) 133-141.

[6] J. H. Boushehrian and N. Hataf, "Experimental and numerical investigation of the bearing capacity of model circular and ring footings on reinforced sand," Geotextiles and Geomembranes, vol. 21, no. 4, Aug. 2003, pp. 241–256.

[7] Vidal H (1966) La terre Armée. Annales de l’Institut Technique de Batiment et de Travaux Publics No.223, France.

[8] M. Abu-Farsakh, Q. Chen, and R. Sharma, "An experimental evaluation of the behavior of footings on geosynthetic-reinforced sand," Soils and Foundations, vol. 53, no. 2, pp. 335–348, Apr. 2013.

[9] M. Chakraborty and J. Kumar, "Bearing capacity of circular foundations reinforced with geogrid sheets," Soils and Foundations, vol. 54, no. 4, pp. 820–832, Aug. 2014.

[10] S. Abu El-Soud and A. M. Belal, "Bearing capacity of rigid shallow footing on geogrid-reinforced fine sand—experimental modeling," Arabian Journal of Geosciences, vol. 11, no. 11, May 2018, Art. no. 247.

[11] Ranganathan SR Development and potential of jute geotextiles. Geotextiles Geomembr 13(6–7) (1994) 421–434

[12] Rao GV, Balan K Durability of Jute Fabric. In: International seminar and technomeet on “environmental geo-technology with geosynthetics”, New Delhi (1996)

[13] Rao PJ, Bindumadhava, Vensiri M Construction of highway embankment on soft marine soil using jute geo-textiles. In: National seminar on “application of jute geotextile & innovative jute products”, New Delhi (2003)

[14] Sahu R. B, Hazra H. K, Som N. "A laboratory study on geojute Reinforced soil bed under cyclic loading" published in National Jute Board (Jute Manufactures Development Council) (2006)

[15] Jadhav SP, Damgir RM Use of jute geo textile for strengthening of sub grade of road work. Government Col-lege of Engineering Aurangabad, Maharashtra(2011)

[16] Kiran and Nagraj Bacha" An Experimental Study on Behaviour of Bearing Capacity and Settlement of Circular and Square Footing Resting on Reinforced Sand Bed Stratified with Lateritic Soil" International Journal of Engineering Research & Technology (IJERT) Vol. 4 Issue 06, June-2015- ISSN: 2278-0181.

[17] Vesic A.S., Bearing Capacity of Shallow Foundations, Foundation Engineering Handbook, Winterkorn and Fang, 1975.

[18] Terzaghi. K. Theoretical soil mechanics [M]. New York: Wiley & Sons, 1943.

[19] Meyerhof, G.G." The ultimate bearing capacity of foundations on slopes" Proc. 4th Int. Conf. on Soil Mechanics and Foundation Engineering, Vol. 1, 1957.pp 384-386

[20] Meyerhof, G. G. “Some Recent Research on the Bearing Capacity of Foundations.” Canadian Geotechnical Journal 1 (1): 1963. 16–26.

[21] Hansen, J. B. "A revised and extended formula for bearing capacity ". Copenhagen: Danish Geotechnical Institute Bui, 1970, 28: 5−11.

[22] Tatsuoka.F, and Yamauchi. H "A reinforcing method for steep clay slopes using a non-woven geotextile" Geotextiles and Geomembranes, Vol. 4,1986, Pages 241-268

List of notations

B, L: width and length of footing
C: Cohesion of soil
Cu : Uniformity coefficient
D_{10} : Effective diameter
D_{60}: 60% of the soils particular are finer than this size.
D_{30} : 30% of the soil particular are finer than this size.
D_f: the depth of footing
γ: the effective unit weight of soil
H: Thickness of geo-jute layer of surface of failure
$K_p = \tan^2(45+\phi/2)$, passive pressure coefficient.
$(S/B)_o$: Settlement ratio for unreinforced soil and at failure
q_o: Average contact pressure of footing for unreinforced soil at failure
q_{ult}: the ultimate load per unit length of footing;
q: Average contact pressure for reinforced soil at failure
$(S/B)_r$: Settlement ratio for reinforced soil and at failure
d_c, d_γ and d_q: the depth factors;
S_c, S_q and S_γ: the shape factors;
i_c, i_q and i_γ : the load inclination factors.
N_c, N_q and N_γ: the bearing capacity factors. They are functions of the angle of friction, Φ.
Φ :the angle of internal friction` of the soil

A review: Concrete From Construction Solid Waste

By Dr. Hana Abd Alftah Aljewifi*

(*): Associated Professor at Civil Engineering Department, Laboratory of building materials, University of Omar AL Mukhtar,Albyda, El Beida, Libya

Email: ***hana.aljewifi@omu.edu.ly***

Abstract _ Every year, a significant amount of construction trash is produced as a result of the modernisation of cities and the growth of human civilization. These building wastes may produce 4 billion tons of garbage annually, and the volume is rising. Since very little of these building wastes are recycled and the majority are immediately disposed of or landfilled, environmental contamination is becoming a severe problem.

It has been a popular issue for scholars in many nations and areas of the world to figure out how to utilize this portion of recycled materials to efficiently transform trash into treasure.

Some researchers have looked at the idea of performance loss in items made from recycled materials. When recycled aggregate is prepared as recycled concrete, the mortar adhesion rate of the secondary recycled aggregate recovered from the recycled concrete can be more than twice that of the primary recycled aggregate. They found that the mortar attached to the recycled aggregate is the main factor affecting the performance degradation of the aggregate. Numerous studies have revealed that recycled concrete's mechanical qualities can still satisfy design specifications.

The author of this work will focus on the microstructural at the Scanning Electron Microscopic (SEM) of a few selected studies in order to investigate the relationship between the concrete and recycled aggregate. SEM was used to evaluate the contact bond between concrete and waste materials such waste paper, waste glass, crushed glass sand, various industrial solid wastes, and PVC waste powder. The interfacial transition zone (ITZ) is still to be a contentious topic. Additional ideas include microstructural research on rubber concrete or the use of used auto tires in concrete. Concrete with modified asphalt and crumb rubber is another. The results contradict claims made in the literature about the weak connection between tire rubber particles and the matrix of cement paste. Scanning Electron Microscopy (SEM) tests showed a denser microstructure of recycled aggregate concrete depends on percentage of replacement, corroborating the general finding that the microstructure characteristics of concrete rely on a range of percentages of waste materials.

Keywords: Waste Materials, Concrete, Interfacial transition zone, Scanning Electron Microscopic, Microstructure.

1. Introduction

The sustainable benefits of solid waste usage in concrete include the possibility of reducing solid waste and greenhouse gas emission and preservation of raw materials. This current study examines the effect of recycled solid waste as aggregate, glass and rubber as a partial and complete substitute for natural aggregate or sand in producing eco-friendly concrete. The solid waste were divided to physical (arises from construction content all materials as: sand, steel, paper…etc.); and non physical which occurs during la construction process and doesn't add any value to construction [1]. Recycled concrete aggregate (RCA) leads to a possible solution to the environmental problem caused by concrete waste, and reduce the negative environmental impact of the aggregate extraction from natural resources [2]. Additionally, adding glass or crumb rubber to concrete characteristics has many benefits. This paper presents a comprehensive review on the use of RCA, glass powder and crumb rubber in concrete, based on the experimental data available in the published researches. The most important physical, and mechanical, properties of these wastes are discussed in this paper. However, more emphasis has been given to discuss the effects of recycled waste on the fresh and hardened properties, and durability of concrete.

2. Problem statement

Because the concrete primarily depend on mixing ratios, resistance types, and environmental conditions for the introduction of solid waste as basic materials from one country to another, it is now difficult to count them because there are no standards from the current research in the introduction of various waste types.

3. Objective

An investigation of how solid waste concrete affects the advent of reality and utility in a contemporary building. And study of these works from a theoretical perspective, and their assessment.

4. Waste solid types

4.1. Waste of recycle coarse aggregate

According to Awoyera et al., 2022 [3], the RCA's quality would be ascribed to the need for water, which distinguishes it from the NCA in terms of unit weight, absorbency, mechanical strength, and chemical durability. The performance of the obtained datum indicates that the water requirement of the RCA varies and declines as the quality of the RCA stack improves. The straight relationship between the RCA stack's water needs and its physical, mechanical, and chemical qualities determines how RCA concrete is designed to be mixed.

Simple-crushed coarse aggregate (SCRCA) and simple-crushed fine aggregate (SCRFA) were produced by simply crushing building solid refuse in order to address the issues of a large quantity of waste generated during construction and a lack of natural material (coarse and fine aggregates). To acquire particle-shaping coarse aggregate (PSRCA) and particle-shaping fine aggregate (PSRFA) using this methodology, SCRCA and SCRFA were subjected to particle-shaping, and the recovered powder (RP) generated during the particle-shaping process was assembled.

4.1.1. Influence RCA on mechanical performance

Several academics have studied the performance of concrete mixed with recycled aggregate to assure the performance of recycled concrete products, see **Table 1,2**.

Table 1 : Comparison of mechanical properties between RCA and NA.

Ref	Compressive strength RCA	Remarks
[4]	0 to 24% lower than that of NCA for coarse RCA only. 15-40% lower than that of NCA for coarse and fin RCA.	Concrete containing coarse and/or fine RCA can be produced with adequate levels of compressive and -flexural strength for paving and other applications, sometimes even with

		100% replacement of virgin aggregate with RCA
[5] [6] [7] [8]	decreased up to 25% depending upon the quality of RCA	
[9]	The higher air content normally found in the concrete mixes containing RCA may also lead to lower strength values.	RCA concrete may have the similar and sometimes higher compressive strength than NCA concrete if the RCA is derived from a source of old concrete, which was originally produced with a lower water to cement ratio than the new concrete.
[10] [11]	high-performance concrete: 20 to 30% reduction in compressive strength	Due to the use of RCA
[6] [12] [13]	Self compacting concrete of NCA and RCA: the difference in compressive strength at the same age was not significant.	The fine RCA can also affect the compressive strength of concrete.
[14] [15]	Remplacement N.A in Concret , Mortar.	The mortar attached to the recycled aggregate is the main factor affecting the performance degradation of the aggregate. The mortar adhesion rate of the secondary recycled aggregate recovered from the recycled concrete can be **more than twice** that of the primary recycled aggregate.
[16]	RS, recycled self-compacting concrete, 25, 50; 75 and 100 ratio	the use of RFA instead of RS had little effect on the performance of recycled self-compacting concrete.
[17]	Concrete a gradient of 7%, 14%, 21%, and 28% using RCA rather than NCA	The mechanical properties of recycled concrete could still meet the design requirements.
[18]	Recycled concrete: SFRFA by using steel fiber	a significant performance improvement compared with the concrete prepared with RFA.
[19]	Recycled concrete: RS; Different %	RFA substitution rate was 60%, the strength of recycled concrete reached its peak.
[20]	Dry-mixed masonry mortar contain: RP ; SCRFA; PSRFA ; river sand (RS); the ratio 0, 10, 20, and 30; 100; 100 and 100 respectively. C/S ratio is 1:4.	The replacement rate of RP is less than 20%, it has little effect on the properties of products..
[21]	The strength was lower at the age of 28 days, the NCA concrete gained strength gradually	
[22]	Compressive strength decreases when NA is replaced by RCA. Total concrete porosity increases when NA are replaced by RCA.However, mechanical strength further decreases ~11% with incorporation of silica fume (SF) (either 5 or 10%). This suggests that removing the effect of RC, performance reduction attributable to SF is only around 4%.	Overall, mechanical performance decreases with increasing content of coarse RCA and increases with concrete age (because of hydration progress), including for reference mixes. the higher strength decrease in non-structural concrete appears to be due to failure at the ITZ and to crack propagation through the cement paste itself

Table 2 : Comparison of mechanical properties between RCA and NA.

Ref	Flexural strength RCA	Remarks
[4]	The flexural strength of RCA concrete is typically 0 to 10% lower than that of NCA concrete	
[21]	the 3-day flexural strength of RCA concrete was higher than that of NCA concrete.	The strength was lower at the age of 28 days, the NCA concrete gained strength gradually and had a higher flexural strength than RCA concrete at later age.
[23] [24]	RCA did not produce any significant negative impact on the flexural strength of concrete. Nevertheless, the RCA concrete with adequate flexural strength can be produced for different applications, sometimes even with 100% replacement of NCA	

4.1.2. RCA durability

Concrete's durability refers to its ability to resist insensitive service conditions such as abrasion, chemical assault, and weathering. If the mixture proportioning is done correctly and good quality is maintained during construction, RCA concrete may be exceptionally durable even when the RCA is made from concrete that has durability, [2].

4.1.3. RCA Microstrucutre

The SEM microstructure of RCA concrete was porous, and, the ITZ of RCA was composed of micro cracks, and fissures, which relatively weakened the surrounding hardened mortar matrix, [22], [25]. The ability to withstand compressive strength, the crush resistance of aggregate, is determined by aggregate crushing value [26]. Recycled aggregate has a relatively higher value due to weak interfacial transition zone (ITZ) and adhered mortar, which is not observed in natural aggregate. High value indicates the weakness of aggregate. The carbonation treatment such as carbonated recycled concrete aggregates (CRCA) improved the original ITZ together with the adherent mortar in the RCA, see **Figure 1**. Thus ITZ with hydration products $CaCO_3$, which improved its microhardness [27].

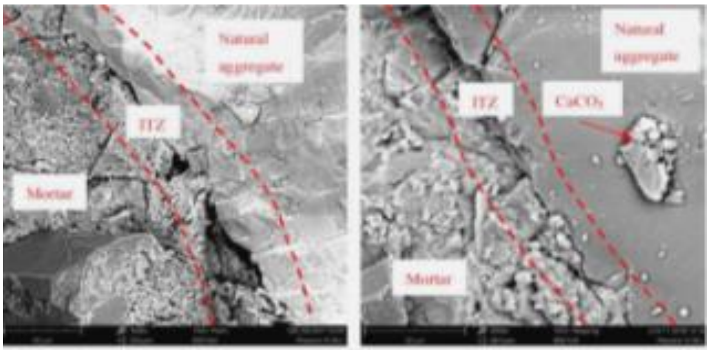

Figure 1: SEM images: ITZ in RCA before (left) and after (right) treatment [27].

The basic and mechanical properties and microstructure of hydration products of dry-mixed mortar were analyzed, and the maximum substitution rate of RP was determined.

The performance of recycled concrete prepared with PSRCA and PSRFA is also very close to that of products prepared with NCA and RS. The failure morphology of PSRCA and RSRFA concrete is also similar to that of NCA and RS concrete. D. Pedro, 2019 et al.,[22] have demonstrated that higher concrete porosity contributes to decreased compressive strength, since distance between hydration products prevents them from forming strong bonds. On the other hand, the use of higher quality coarse RCA probably favored the creation of stronger matrix/aggregate bond as shown in **Figure 2**, and fracture takes place mainly throughout NA.

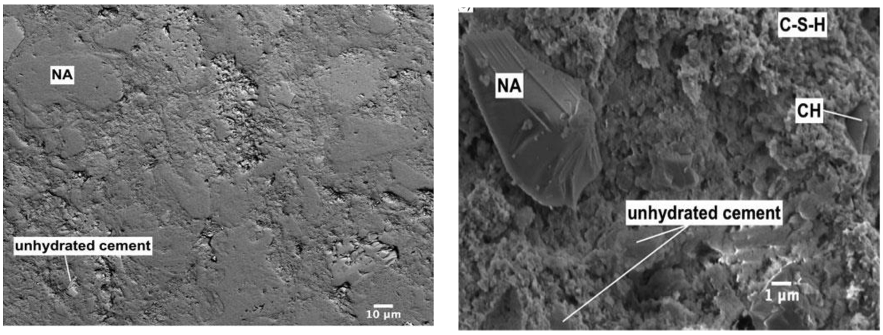

Figure 2: BSE image: dense matrix and strong ITZ bond (left). SE image: dense matrix and scarcity of ettringite, CH (right) [22].

The mixes produced by replacing all NA with coarse and fine present more heterogeneous cement matrix and with the presence of SF, showing agglomerates poorly bonded to the remaining structure.

4.2. Waste glass as partial

4.2.1. Classification of waste glass

The physical properties of the crushed waste glass (WG), sand and gravel aggregate materials. The particle size gradation for the glass sand, natural sand and gravel aggregate were carried out using sieve analysis, **Tables 3 and 4** are showed the properties and composition of WG.

Table 3 : Chemical composition and physical properties of waste glass [28].

Reference	Composition										Fineness moduluss	Specific gravity	Water absorption (%)	Density (kg/m^3)
	SiO_2	Al_2O_3	Fe2O3	CaO	MgO	SO_3	K_2O	No_2O	TiO_2	Cr_2O_3				
[28] [29]	64.31	19.98	6.25	10.61	0.63	0.25	0.74	12.52	0.61	0.02	2.99	2.5	0.4	1680

Table 4 : Composition of manufactured glass waste by weight.

Ref.	Fin waste glass by weight to substitute sand in the concrete (%)	Cement (%)	Natural sand (4.75 mm) (%)	Natural granite (19 mm) (%)	Concrete type	W/C	Remarks
[28] [29]	0 25 50 75 100	100 100 100 100 100	100 75 50 25 0	100 100 100 100 100	OC	0.5	However, concrete containing 25% and 50% waste glass contents showed significant enhancement in strength, but it is recommended that the optimum glass content should be 25% for the production of sustainable eco-concrete. Light gray glass, In USA [29]
[30]	White (WG):25-50-75-100 Green (GG): 25-50-75-100 Brown (BG): 25-50-75-100	100 100 100	Natural sand: 1. non-reactive aggregate 2. Glass Cullet (GC) the reactive aggregate for ASR		Mortar bars (25x25x285)	0.47	1. The increment in GC content reduces resistance against ASR due to the reactive silica content 2. The glass color also has an effect on ASR resistance. 3. GG aggregate shows the best performance for 25% glass content regarding ASR resistance.

[31] [32]	8mm glass cullet of different colours: clear (i.e. uncoloured): 50% ,100% green and amber: 50% or 100%	100	0.3 mm quartz, sand		70 x 70 x 280 mm mortar, C/S 1:3 with fly ash	The water content of each mortar was set to achieve the same consistence (125 ± 10 mm).	The use of clear, green and amber glass cullet, 100% of replacement, slightly compromised the mechanical performance of mortars, in particular flexural strength, due to the bad grain size distribution of the glass. A considerable expansion due to ASR was detected by using clear glass cullet.

Usage of FA or Li_2CO_3 (Lithium carbonate), increases resistance against ASR; 20% FA or 2% Li_2CO_3 provide enough ASR resistance for 25% GC replacement ratio in all glass colors. Furthermore, it can be concluded that usage of more than 20% FA or 2% Li_2CO_3 is required.

4.2.2. Influence waste glass on mechanical performance

Waste glass has influence on mechanical properties of concrete with limit percentage as indicated in **Table 5**.

Table 5 : Mechanical properties of waste glass concrete**.**

Ref.	Mechanical tests						Code	Remarks
	N. Specimens	Slump test	Treatment ages (days)	Compressive strength (MPa)	Flexural test	Expansion test (%)		
[28]	60	√	3 7 28 90	20			In USA ASTM C136 (2014)	The workability and the mechanical strength of the concrete produced decreased withincreasing waste glass content.
[30]			3 9 14 21			< 0.20 < 0.10 < 0.10 < 0.10	ASTM C 1260	The expansion increases with an increase in amount of glass. However, usages of these admixtures reduce expansions occurring because of ASR.
[31]	3 (50% by weight of quartz sand); (clear GC, green and amber mix) 3 (100 % by weight of sand); (clear GC, green and amber mix glass powder 50% by weight of quartz sand (mix GP-50%, added to the mortar mixtures).	125 ± 10 mm W/C ratio is 60-65% higher in order to reach the same fresh mortar workability (due to the greater water absorption of glass powder with respect to quartz sand).	3 28 180	GC (50%) (30-40 MPa) GC (100%) (25-30 MPa) GP-50% (25-40 MPa) in the case of glass powder used together with fly ash replacing cement.	GC (50%) (6 MPa) GC (100%) (4-5 MPa) GP-50% (5-6 MPa) According to ASTM C 1260, expansion larger than 0.2% at 14 days is considere d potentially deleteriou.		EN 1015-3	Loss of resistance could be the presence of widespread cracking in 1.The specimens made of 100% clear waste glass that was detected by visual inspection. 2. color is less evident than in clear cullet mixtures

4.2.3. Waste Glass Microstrucutre

The microstructural examination of selected samples was conducted to analyze the bond between the concrete aggregate and cement paste at the microscopic level. The bonding between the aggregate and binder is considered fundamental for better transfer of stresses between the binder and aggregates especially at the interfacial zone, which influences the concrete strength [33]. As well as developed aggregate–cement paste interface, and the hydration product having a structure with no pores and cracks. The SEM view of concrete containing 25% FWG shows compact microstructure like the control; however, very few voids can be seen but no cracks. But the SEM micrograph for the 100% FWG clearly shows a microstructure with many pores, which may be as a result of the angular grain shape and smooth surface of the waste glass sand particles resulting in poor bond formation especially at the interfacial zone.

According to [33] [34], they mentioned that the concrete strength at the interfacial zone is significantly influenced by factors like the surface roughness of the aggregate, using inert micro-fillers and chemical reaction between the cement paste and aggregate, see **figure 3.** The SEM result also shows a non homogeneous concrete paste owing to the glassy texture of the glass particles surface. This explains the low results recorded for both the compressive and tensile strengths at 28 days especially at higher replacement dosages of glass sand. The green, brown color glass would be the least reactive in ASR due to its high content of Cr_2O_3, [35]. The different alkali resistance of colored glasses is attributed to the manufacturing process more than to the chemical content, which differs only slightly, [36]. The ASR expansion in glass concrete due to the expansion of concrete caused ASR expansion, and Na^+ and Ca^{2+} are firstly dissolved from glass, when the OH in pore solution attacks the glass surface, then the silicate network depolymerizes, [37]. The reaction occurs to form ASR gel of C–N–S–H, as shown in Eq (1):

$$Ca^{2+} + Na^{+} + [SiO(OH)_3] \rightarrow C\text{-}N\text{-}S\text{-}H \qquad (1)$$

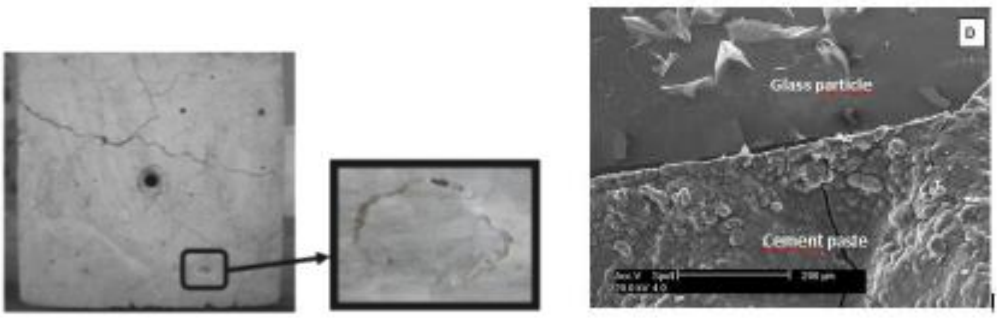

Figure 3: Pictures of a specimen with 100% uncolored glass cullet (left), SEM (right) [31].

4.3. Crumb rubber waste

The use of tire rubber particles as aggregate in concrete showed promising results in producing a new type of concrete that has relatively enhanced energy absorption and fracture criteria compared with normal concrete. The crumb rubber (CR), which is the recycled rubber from tires, has become a common additive in hot mix asphalt mixture due to its improvement of the mechanical performances of asphalt mixtures, see **Table 6**. Incorporating tire rubber particles in the concrete matrix as replacement of coarse or fine aggregate resulted in a decrease in the fresh concrete slump and unit weight and an increase in air content. While the compressive strength of the rubber concrete was significantly reduced as the tire rubber particles replacement level increases, significant enhancements in the impact resistance and fracture toughness of concrete were observed, [38].

Table 6 : Comparison of various treatment methods of rubber waste on concrete.

Treatment method	Mechanism	Advantage	Disadvantage
Pre-treating with NaOH [39]	Remove zinc stearate from rubber particle surface, make rubber surface hydrophilic.	High efficiency, widely used and synergy with other methods.	The compressive strength isn't improved, even slightly reduced.
Pre-treating with Potassium Permanganate (KMnO4) [40]	Oxidize rubber surface to make the surface hydrophilic.	High efficiency, cheap, and alternative chlorinated oxidizer.	Complicated operation and time consuming.
Pre-coating with limestone powder (LP) [41]	Make the rubber surface hydrophilic and rough.	Cheap and easy access to raw materials.	The void content and water absorption increase.
Pre-coating with cement [42]	Make rubber hydrophilic and strengthen the elastic modulus.	High efficiency and easy access to raw materials.	Excessive cement coating isn't of conductive to the increase of density.
Pre-treating with mortar [43]	Facilitate the bonding between rubber and cement., mortar more rough than cement paste	Increasing compressive strength and flexural strength	Control the workability values.

4.3.1. Classification of Rubber Particles

Main waste from automobile and truck tyres are rubber. The rubber composition of the tyre is shown in **Table 7** and **Figure 4**.

Table 7: Classification of the rubber particles according to [43].

Name	Particle size range	Replacement type
Shredded tyre	100-230 mm in width, 300-460 mm in length.	Coarse aggregate
Chipped tyre	13-76 mm.	Coarse aggregate
Fiber rubber	2-5 mm in width, 10-22 mm in length.	Fine aggregate
Crumb rubber	0.425-4.75 mm.	Fine aggregate or cement
Granulated crumb rubber	0.5 – 9.5 mm	Coarse aggregate or fine aggregate
Rubber powder/ rubber ash	≤ 0.425 mm	Cement

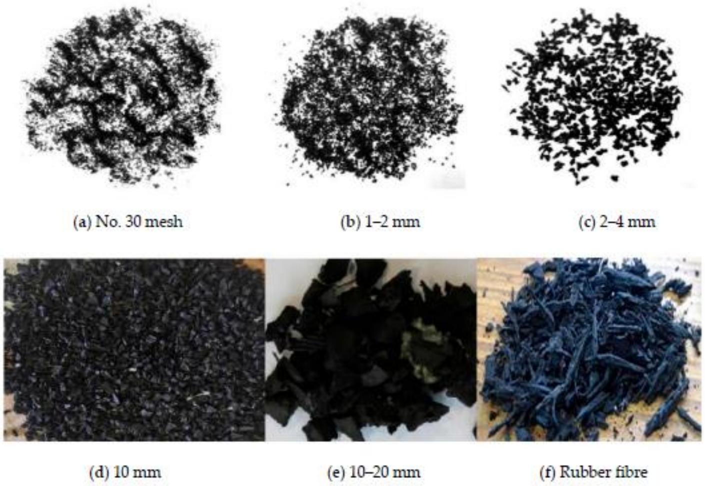

Figure 4: Various sizes of tire particles, according to [38].

4.3.2. Waste crumb rubber durability

L. Yang et al., 2022 [38] Discuss and analyze the influence of solid waste replacement rates, replacement patterns, particle size and treatment methods. Results show that an increase in rubber content can improve the chloride penetration resistance, acid and sulphate attack resistance, freeze–thaw resistance, and alkali–silica reaction damage resistance of concrete, and the content of 5–20% has a significant improvement effect. Rubber replacing fine aggregate is the best scheme for durability, followed by cement and coarse aggregate. In addition, the recommended rubber particle size is 0–3 mm. However, the rubber particle has adverse effects on abrasion resistance, impermeability, water absorption resistance and carbonation resistance. The pre-treatment of rubber or the additions of supplementary cementitious materials are effective and viable ways of improving the durability of RC. Further research is needed on the long-term durability of RC, as well as on ductility, energy absorption, and thermal and corrosion resistance.

4.3.3. Waste crumb rubber microstructure

Chipped and crumbed tire rubber particles were used to replace coarse and fine aggregate with different volume replacement levels. By using the Environmental Scanning Electron Microscope (ESEM), the results showed that crumb rubber is well dispersed in the asphalt mixture when the conditioning time is increased. The extensive micro cracking in the tire particle vicinity and indentations in the cement matrix at locations where tire particles were pulled out. These indentations actually play a role on enhancing the bond strength between the tire particles and the cement paste, and existing internal tension cracking in a tire rubber particle matrix itself. And the stress transfer between the two phase composites exists and the tire rubber particles experienced tensile strains prior to failure [38] [44]. In the rubberized concrete, it is obvious that no interface bonding between cement paste and rubber tire has been maintained, see **Figure 5, 6**. Without an interface bonding, stress transfer between fibers and cement paste is possible owing to a mechanical interlocking [45].

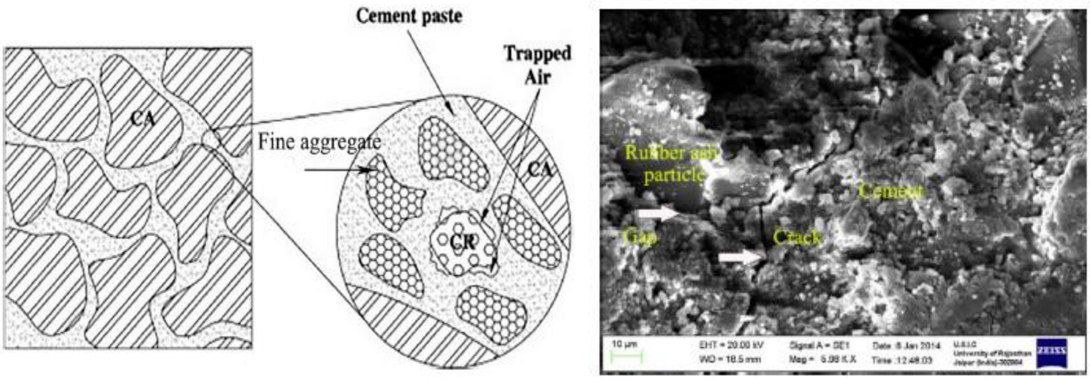

Figure 5: Microstructure of CR concrete (left); microstructure of RC containing 20% rubber ash (right) [38].

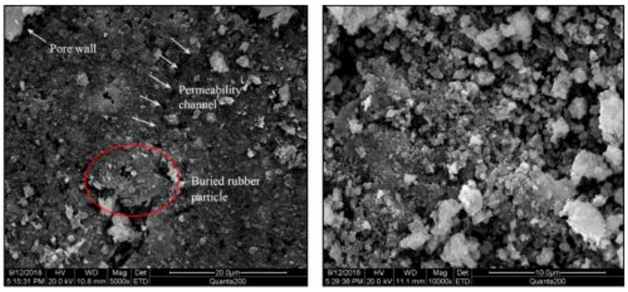

(a) Specimen with 2% CE contient. (b) Specimen with 4% CE contient.
Figure 6: SEM of foamed concrete incorporated with RC, [38].

5. Review of the authors' main views

Water requirement and its effect on the properties of RCA are very necessary at the stage of mixing design of RCA concrete as the RCA properties affect the target properties of RCA concrete before its implementation in-situ. The lower coarse to fine aggregate ratio leads to a higher quantity of mortar attached to coarse RCA particles, and thus results in a reduction in the strength of RCA concrete [According to Tavakoli and Soroushian (1996)], [46] [47].

The compressive strength was lower than that of conventional concrete when the coarse aggregate is replaced by 100% RCA. It recommended no more than 50% of replacement, [47]. The workability and the mechanical strength of the concrete produced decreased with increasing waste glass content. It is recommended that the optimum glass content should be 25% for the production of sustainable eco-concrete [28], since, concrete containing 25% and 50% waste glass contents showed significant enhancement in strength. In general, all the mixtures with 100% glass cullet, are less resistant in bending with 50% replacement, due to the grain size distribution of aggregate particles, which is close to that optimized according to the suggestions of [48], only if 50% sand is replaced by glass cullet; while is too poor of fine particles if only glass cullet is used. Also in the case of flexural strength, the use of glass powder confirmed its evident pozzolanic effect, [31]. Rubberized concrete shows ductile behavior and a plastic failure mode. The choice of the optimal replacement ratio of the tire rubber particles can yield concretes with desirable strength and fracture toughness criteria for different applications [44]. The rubberized concrete has to confirm certain requirements for mechanical properties; these values are considerably decreased with the addition of waste tire pieces [49]. Moreover, the extensive microcracking observed at the particle vicinity supports the hypothesis that the soft aggregate-like behavior of the tire particles generates tensile strains at the tire rubber particle surface which thereafter results in microcracking in the cement paste vicinity. Microstructural investigation of the rubber concrete supported the view that the major reduction of strength might be attributed to the behavior of the tire rubber particles as a soft aggregate rather than to the reduction of bond between the tire particles and the cement paste.

6. Conclusions and Recommendation

Researchers have developed a more ecologically friendly form of concrete that uses solid waste in place of cement, sand, or coarse aggregate. Additionally, the authors assert that recycled concrete may be an ideal replacement for non-structural purposes. They have shown that it is possible to use any readily available material as trash as long as it is taken into consideration while adding it to concrete. Any ingredient added to concrete will not result in the same behavior as plain concrete. These studies' findings in the areas of chemistry, physics, and mechanics enable us to use solid waste to either eliminate or reduce garbage from landfills. Future researchers frequently get recommendations for alternative test protocols or ambient circumstances because to the lack of standardized durability test methodologies.

7. Reference

[1] A. Ebraik, Z.Hatush, A. AlBarkous. " Waste materials recycled in construction projects" المؤتمر الوطني التاسع لمواد البناء والهندسة الانشائية , 29-30 November, Tripoli, Libya,(2022), 319-330.
[2] M. D. Safiuddina, U.J. Alengaramb, M. M. Rahmanb, M. Abdus Salamb, and M .Z. Jumaatb, "Use recycled concrete aggregate in concrete: A review", Journal of Civil Engineering and Management , (2013), 1 – 35.
[3] P.O. Awoyera, C. Thomas and M. S. Kirgiz. "The structural integrity of recycled aggregate concrete produced with fillers and pozzolans".book, ISBN 978-0-12-824105-9 (2022), 445-467.
[4] ACPA. 2009. "Properties of concrete containing RCA". Cited on 2 may (2011) Available from internet: http://www.pavement.com/Downloads/TS/EB043P/TS043.5P.pdf.
[5] K. Rahal. "Mechanical properties of concrete with recycled coarse aggregate". Building and Environment, (2007), 42(1): 407- 415.
[6] A Ajdukiewicz, A. Kliszczewicz; "Influence of recycled aggregates on mechanical properties of HS/HPC". Cement and Concrete Composites, 24(2), (2002), 269-279.
[7] T.C. Hansen. "Recycling of Demolished Concrete and Masonry". Oxfordshire, (1992),UK.
[8] L. Evangelista, J. de Brito. "Mechanical behaviour of concrete made with fine recycled concrete aggregates ", Cement and Concrete Composites, 29(5), (2007), 397-401.
[9] K.W. Anderson, J.S. Uhlmeyer, M. Russell. "Use of recycled concrete aggregate in PCCP: Literature Search", WSDOT Research Report WA-RD 726.1,(2009), Washington State Department of Transportation (WSDOT), Olympia, Washington, USA, 37 p.
[10] C.L. Hwang, J.J. Liu, L.S. Lee, F.Y. Lin. "Densified mixture design algorithm and early properties of high-performance concrete", Journal of the Chinese Institute of Civil and Hydraulic Engineering; 8(2), (1996), 217-219.
[11] L.S. Li, C.L. Hwang. "A quality assurance system of SCC in Taiwan". In Proceedings of the First North American Conference on the Design and Use of Consolidating Concrete, Chicago, USA, (2002), 275-280.
[12] K.K. Sagoe-Crentsil, T. Brown, A.H. Taylor. "Performance of concrete made with commercially produced coarse recycled concrete aggregate". Cement and Concrete Research, (2001), 31(5): 707−712.

[13] Z.J. Grdic, G. Toplicic-Curcic, I.M. Despotovic, N.S. Risti. “Properties of self compacting concrete prepared with coarse recycled concrete aggregate”. Construction and Building Materials, (2010), 24(7): 1129−1133.
[14] C. Thomas, J. de Brito, A. Cimentada, J. Sainz-Aja. “ Macro- and micro-properties of multi-recycled aggregate concrete”. J. Clean. Prod. 245, (2020), 118843.
[15] R. Wang, N. Yu, Y. Li. “Methods for improving the microstructure of recycled concrete aggregate: A review”. Constr. Build. Mater. (2020), 242, 118164.
[16] R.Y. Hassan, G.A. Faroun, S.K. Mohammed.” Mechanical properties of concrete made with coarse and fine recycled aggregates”. Mater. Today Proc. 2021.
[17] M. C. Shah, K.K, Gupta, A. Nainwal, A. Negi, V. Kumar. “Investigation of mechanical properties of concrete with natural aggregates partially replaced by recycled coarse aggregate (RCA)”. Mater. Today Proc. (2021).
[18] D. Gao, F. Wang. “Effects of recycled fine aggregate and steel fiber on compressive and splitting tensile properties of concrete” J. Build. Eng. 44, (2021), 102631.
[19] M. Kaarthik, D. Maruthachalam. “A sustainable approach of characteristic strength of concrete using recycled fine aggregate”. Mater. Today Proc. 2020.
[20] H. Zhenwen. “Concrete from Construction Solid Waste” . Construction & Building Technology, 2021. Retrieved from https://encyclopedia.pub/13828
[21] P.C. Yong, D.C.L Teo. “Utilisation of recycled aggregate as coarse aggregate in concrete”. UNIMAS E-Journal of Civil Engineering. 1(1), (2009), 1-6.
[22] D. Pedro, M. Guedes, J. Brito, L. Evangelista, “Microstructural Features of Recycled Aggregate Concrete: From Non-Structural to High-Performance Concrete, Microscopy and Microanalysis”. 25, (2019), 601–616.
[23] M.D. Safiuddina, U.J. Alengaramb, M. M. Rahmanb, M. Abdus Salamb, and M .Z. Jumaatb, , F. F. Jaafarb, H. Binti Saadb “Properties of High-Workability Concrete with Recycled Concrete Aggregate” Materials Research. 14(2), (2011), 248-255.
[24] ACI Committee 555R. (2001). “Removal and Reuse of Hardened Concrete”.
[25] A, Afizah, E.R. Mohd., A.Salina, A. Abdul Ghapar , Dayang Siti: H.A. Engineering “Behavior of Concrete with Recycled Aggregate”, MATEC Web of Conference 87 , 01002 (2017), ENCON 2016.
[26] S.A. Memon, Z. Bekzhanova and A. Murzakarimova.” A Review of improvement of interfacial transition zone and adherent mortar in recycled concrete aggregate”. Buildings 2022, 12, 1600. , available on: https://doi.org/10.3390/buildings12101600.
[27] Y. Li, S. Zhang, R. Wang, Y. Zhao, C. Men. “Effects of carbonation treatment on the crushing characteristics of recycled coarse aggregates”. Constr. Build. Mater. j. 201, (2019), 408–420. [CrossRef].
[28] O. M. Olofinnade, A. N. Ede, J. M. Ndambuki, B. U. Ngene, I. I. Akinwumi & O. Ofuyatan. “Strength and microstructure of eco-concrete produced using waste glass as partial and complete replacement for sand”. Cogent Engineering (2018), 5: 1483860. Available on: https://doi.org/10.1080/23311916.2018.1483860.
[29] ASTM C136. “Standard test method for sieve analysis of fine and coarse aggregates”. West Conshohocken, PA: American Society for Testing and Materials International. (2014). doi:10.1520/C0136_C0136M-14.
[30] İ. B. Topçu A.R. Boğa, T. Bilir. “Alkali-silica reactions of mortars produced by using waste glass as fine aggregate and admixtures such as fly ash and Li2CO3”. Waste Management j, 28(5), (2008),878-84.
[31] V. Corinaldesi, A. Nardinocchi. “ Influence of recycled glass addition on mortar properties”. Proc. of the Second Intl. Conf. on Advances In Civil, Structural and Mechanical Engineering- CSM 2014.
[32] EN 1015-3. “Methods of test for mortar for masonry”. Determination of consistence of fresh mortar (by flow table). (1999).
[33] S. Mindess, F. J. Young, D. Darwin, (2003). “Concrete (2nd ed.)”. New Jersey: Prentice Hall.
[34] J. P. Ollivier, J. C. Maso, B. Bourdette. “Interfacial transition zone in concrete”. Journal of Advance Cement Based Material, 2, (1995), 30–38. doi:10.1016/1065- 7355(95)90037-3.
[35] A. Saccani, M.C. Bignozzi. “ASR expansion behavior of recycled glass fine aggregates in concrete”. Cement and Concrete Research, 40(4), (2010), 531–536.
[36] R.K. Dhir, T.D. Dyer, M.C. Tang . “Alkali–silica reaction in concrete containing glass”. Materials and Structures, 42(10), (2009), 1451–1462.
[37] C. Shi. “Corrosion of glasses and expansion mechanism of concrete containing waste glasses as aggregates”. Journal of Materials in Civil Engineering, 21(10), (2009), 529–34.
[38] L. Yang, C. Jiaqi, W. Ruijun, Z. Yu, and T. Xiaogen. “A Review of the durability-related features of waste tyre rubber as a partial substitute for natural aggregate in concrete”. Buildings j, 12, (2022), https://doi.org/10.3390/buildings12111975.
[39] N. Segre, Joekes, I. “Use of tire rubber particles as addition to cement paste”. Cem. Concr. Res. 30, (2000), 1421–1425.
[40] L. He, Y. Ma, Q. Liu, Y. Mu. “Surface modification of crumb rubber and its influence on the mechanical properties of rubber cement concrete”. Constr. Build. Mater. 120, (2016), 403–407.
[41] O. Onuaguluchi. “Effects of surface pre-coating and silica fume on crumb rubber-cement matrix interface and cement mortar properties”. J. Clean. Prod., 104, (2015),339–345.
[42] S. Guo, Q. Dai, R. Si, X. Sun, C. Lu. “ Evaluation of properties and performance of rubber-modified concrete for recycling of waste scrap tire”. J. Clean. Prod, 148, (2017), 681–689.
[43] A.M.N El Kogha, E. A. Elmusrati, M. F. Najjar, and A.T.Abdurrahman.”Effect of crumbed rubber treatment on rubberized concrete properties” المؤتمر الوطني التاسع لمواد البناء والهندسة الانشائية , 29-30 November, Tripoli, Libya,(2022), 101-108.

[44] M. M. Reda Taha, M. ASCE1, A. S. El-Dieb, M. A. Abd El-Wahab, and M. E. Abdel-Hameed. “Mechanical, Fracture, and Microstructural Investigations of Rubber Concrete”. JOURNAL OF MATERIALS IN CIVIL ENGINEERING (2008), 640 -649.
[45] M. Emiroglu, M. Halidun Kelestemur, S. Yilihz. “An investigation on ITZ microstrucutre of the concrete containing waste vehicle tire”. Uluslar Arasl Kmlma Konferansl Uildiriler Kitahl 7~, 9 KaslJn 2007 ProoceerJings of 8th Inlernatlonal Fracture Conftrcncc 7 - 9 Novemher 2007 Isianbul/Turkey.
[46] M. Tavakoli, and P. Soroushian. “Drying shrinkage behavior of recycled aggregate concrete”. Concrete International, 18(11), (1996), 58–61.
[47] Md. Siddikur Rahman, Md. Bellal Hossain, R. Ruksana. “Strength Behaviour of Recycled Concrete with Partial Replacement of Conventional Aggregate”. International Journal of Environment, 2(2), (2012), 80–86.
[48] Bolomey, J. “Revue Matèr Constr Trav Publ”, Edition C. (1947).
[49] E. Mehmet, M.K. Halidun, S. Yildiz,. “An investigation on ITZ microstructure of the concrete containing waste vehicle tire”. In Proceedings of the 8th International Fracture Conference, Istanbul, Turkey, 7–9 November (2007), 454–459.

Review of Solid Waste's Effects on the Properties of Asphalt Mixtures

Foad Mohamed Elkut

Department of Civil Engineering, Faculty of Engineering, Elmergib University, Al-komes, Libya

Foad.elkut@yahoo.com

Abstract

Rapid population growth coupled with an increase in the consumption rate has led to a poor state of solid waste management that depends on burying or burning waste for disposal at alarming rates in Libya, despite the dominance of recyclable materials in the composition of these wastes. Within the framework of efforts to stimulate the use of sustainable development towards integrating solid waste as renewable materials, paving the way for a sustainable future for the manufacture of asphalt mixtures and an environmentally friendly and cost-effective alternative Therefore, the use of solid waste, whether as coarse or fine aggregate or as fillers in the form of powder, ash, or fibre, as an additive is considered one of the intelligent solutions for sustainable development in road paving. This systematic review aims to provide insights into the potential for incorporating solid residues into asphalt mixtures based on the pioneering efforts of researchers over the past decade. The results indicated that the incorporation of several types of solid residues improved the penetration index, which led to a decrease in the sensitivity to temperature and significantly increased the viscosity, which could improve the engineering properties of the binder in addition to being effective in enhancing the hardness, rutting resistance, and moisture sensitivity of the modified asphalt mixtures compared to reference mixes. We also recommend developing regulations and specifications for regular recycling of waste and by-products as an incentive to reduce demand for natural resources and preserve the environment in Libya.

Keywords: Sustainable Development, Penetration Index, Viscosity, Waste Incorporation, Environment.

Introduction

The amendment of producing asphalt mixes with waste materials serves as an avenue to limit the enormous volume of waste produced from various sources. This also reduces the consumption of naturally mined materials, therefore minimising the carbon footprint and the pavement industry's impact on the environment [1]. The overall objective of the manuscript is to review the recycling of waste materials generated from various sources, such as household, agricultural, and industrial, to minimise natural resource exploitation, lower energy demand, and enhance overall pavement performance. In recent decades, many pavement engineers and researchers have focused on modifying asphalt using waste materials. Accelerated urbanisation and civilization have generated enormous amounts of waste, leading to significant disposal issues and negatively impacting the environment. Asphalt pavement industries have converted solid waste materials from landfills into binders or mixtures as mineral filler, aggregate, or fibre asphalt modifiers [2]. Transportation infrastructure plays a crucial role in this context, as any new construction or rehabilitation consumes considerable natural materials. Most paved road networks consist of asphalt pavements whose maintenance and further expansion depend upon the continual and frequent availability of natural resources like aggregates and asphalt binders. Various additives and modifiers have been used to improve the performance of conventional bitumen under different loading and temperature conditions generated from various sources, such as (a) Agricultural waste like biomass wastes; (b) Industrial wastes such as fly ash, slag, and cellulose waste; (c) Domestic wastes such as incinerator residue, polymers, chemical modifiers, antistripping agents, waste glass, and scrap rubber; (d) mining wastes such as coal mine refuse; and (e) construction and demolition wastes such as recycled fine concrete aggregates and brick dust, as shown in Table 1 [3]. According to Global Waste Generation Statistics and Facts (2020), the amount of municipal solid waste (MSW) is foreseen to escalate by 70% to 3.4 billion metric tons in 2050 as a result of urbanisation, modernization, and population growth [4]. Fig. 1a demonstrates that the areas of East Asia and the Pacific and Europe and Central Asia generate the most waste, which consists of 43% of the world waste generated, while regions of the Middle East and North Africa generate the least waste, about 129 million tons, as shown in Fig. 1b [5].

Table 1. Wastes production quantity and highest contribution country [3]

Source	Waste produced	Production	Country with highest contribution
Household waste	Food waste	931 MT (61%—household, 26%—food service, 13%—food retails)	China (91.6 MT)
	Plastic	367 MT	United States (105 kg per capita)
	Waste cooking oil (WCO)	10 MT	United States (5.5 MT)
	Glass waste	129 MT	–
	Electronic waste	53.6 MT	China (10 MMT)
Agricultural waste	Rice husk ash (RHA)	7.4 MMT	Indonesia (76 MT)
	Sugarcane bagasse ash (SCBA)	390 MT	Brazil (181 MMT)
	Palm oil fuel ash (POFA)	–	Malaysia (19.15 MT)
	Groundnut shell ash (GSA)	44.12 MT	China
Industrial waste	Ceramic waste	22 BT	–
	Coal fly ash (CFA)	1143 MT	China (600 MT)
	Steel slag (SS)	190–280 MT	China (100 MT)
	Bauxite residue/red mud	300 MT	–
	Crumb rubber modified binder (CRMB)	1–1.8 BT	Kuwait (42 MT)

Note: MT = million tonnes; MMT = million metric tonnes; BT = billion tonnes.

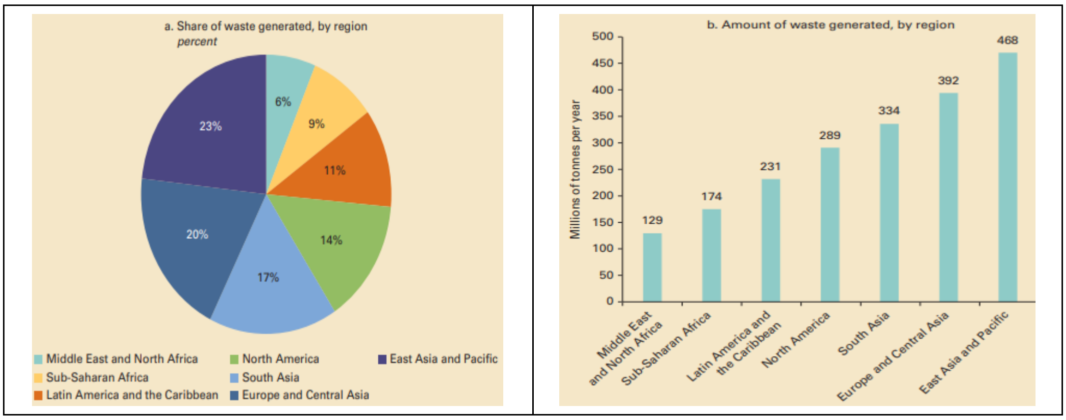

Figure 1. Waste Generation by Region [5].

The circular economy represents an alternative to the linear economic model of "take, make, consume, and dispose of" that still prevails. It aims to maintain the usefulness of products, components, and materials for as long as possible while preserving their value. The principal phases of a circular economy model are presented in Fig. 2. Each of these phases offers different opportunities to decrease costs and dependence on natural resources, boost new business models, and reduce the production of waste and emissions for the environment [6].

Figure 2. The main phases of a circular economy model [6].

The emergence of the asphalt pavement industry had been revolving around conventional Hot Mix Asphalt (HMA), which involved the mixing of natural mineral aggregates as a structural skeleton and asphalt binder while applying high discharge temperature requirements to provide driving comfort, stability, durability, and water resistance, which consume a high amount of fossil fuels and contribute to greenhouse gas emissions [7]. Given escalating sustainability concerns and the need for cleaner production, the asphalt technologies that contribute to temperature and harmful emission reduction as compared to HMA, namely Warm Mix Asphalt (WMA) and Cold Mix Asphalt (CMA), are developed to ensure the sustainability of the asphalt pavement industry [8]. Furthermore, Stone Matrix Asphalt (SMA) and porous asphalt mixtures justify the applicability of solid waste in diversified fields of asphalt pavement for specific usability.

As presented in Table 2, the origin and type of solid waste play a significant role in predetermining the options before incorporating solid waste into asphalt binder and asphalt mixture, respectively.

Table 2. Options to Incorporate of Wastes Materials into Asphalt Binder [3].

Industry	Solid waste classification		Options to incorporate solid waste into the asphalt binder			*Usage (%)
	Origin	Type	Powder	Ash	Fibre	
Plastic	Computer	Electronic	✓	–	–	5.0
	Petrochemical	Polyethylene	✓	–	–	4.0
	Packaging		✓	–	–	4.0
	Milk packaging		✓	–	–	4.0
Rubber	End of life tyre	Crumb rubber	✓	–	–	10.0
			✓	–	–	50.0
			✓	–	–	18.0
			✓	–	–	15.0
			✓			20.0
Coal	Power plant	Fly ash	–	✓	–	15.0
Agriculture	Straw producer	Straw composite	–	–	✓	0.5

Note: * Usage % is the percentage of solid waste incorporated by weight of asphalt binder in the references.

As such, the option selection process for solid waste can be simplified by mimicking the conventional asphalt mixture composition, whereby solid waste resembles fine and coarse aggregates or mineral fillers in the form of powder, ash, and fibre. To fully harness its potential, solid waste resembling coarse aggregate should be further crushed into finer aggregate or even ground to be used as mineral filler in powder form. In addition, solid waste on asphalt pavement can be classified into two main categories: wet-processed and dry-processed. In the wet process, solid waste is added directly into the asphalt binder at high temperatures, where mechanical mixing is required to achieve a homogeneous waste-modified binder blend. The mixing temperature and mixing time depend on the nature of the solid waste source and asphalt binder. In the dry process, solid waste is added directly to the asphalt mixture, either as a replacement for a portion of the aggregates or as a replacement for the aggregates themselves [9]. Waste production is increasing significantly in Libya due to the increasing population and rapid urbanisation. Currently, recycling waste processes are very limited, resulting in all of it being disposed of in landfills, automatically affecting human health and the living environment. There are major gaps concerning differences in waste production in Libya, including different construction materials and systems, standards, practises, and economic considerations [10]. The results of the studies showed that the average quantities generated (0.3–1.0) at the rate of 0.64 kg per person per day, the percentage of organic materials was 36.3%, and 32.5% of recyclable solid waste such as glass, paper, plastic, and metal, and these percentages are close to those of other studies in African and Arab countries [11].

A simple solution and the most practical way to recycle is to utilise it in the construction of flexible pavements. The highways in Libya show distress during the initial period of service due to heavy vehicular loading and severely high temperatures in the summer. There are many types of local waste materials that can be successfully used as mineral fillers in hot asphalt concrete mixtures instead of ordinary Portland cement and limestone powder. The reason behind the utilisation of conventional bitumen 60/70, which does not satisfy the performance requirements at high temperatures, is because of the required high-performance grade (PG) in hot and arid climates [12]. Several recent studies have suggested that using reclaim, reuse, recycling, and fillers of waste in place of virgin materials in optimum proportion would lead to the production of sustainable asphalt mixes with satisfactory engineering performance in an environmentally friendly and cost-effective manner [13].

Asphalt modifications

Various overlapping options from respective industries are proven to be tricky prior to pondering upon the available options and, more so, the usage percentage of solid waste. Hence, it is imperative for researchers to have comprehensive guidelines for addressing the incorporation options of solid waste into asphalt binder and asphalt mixture, respectively, as shown in Fig. 3. The main prerequisite property tests are grade, flakesiness, and elongation (%), Size (mm), and Water absorption (%), with options focusing on aggregates and fillers, namely powder, ash, or fibre [14]. Even though there are various prerequisite properties to be tested before incorporating solid waste into asphalt mixtures, the justification for these tests is to address the main engineering limitations while empowering solid waste application as an alternative to solid waste management and sustaining an eco-oriented pavement industry.

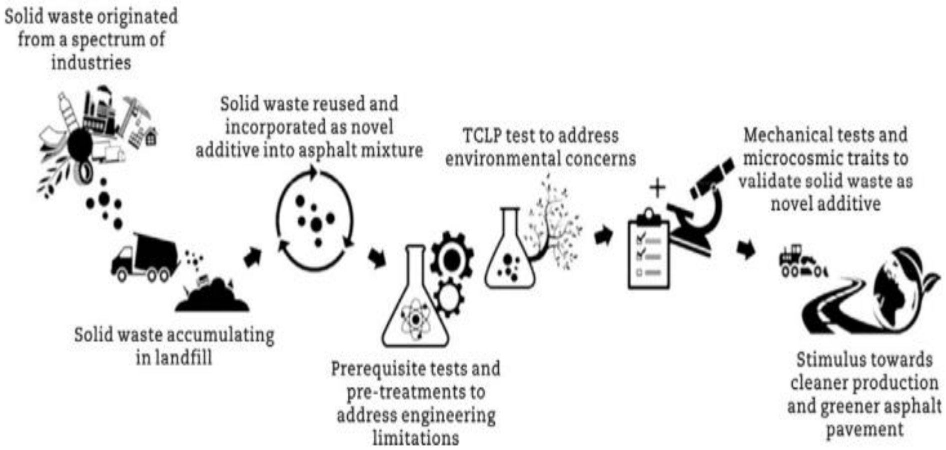

Figure 3. The main phases of incorporation of solid waste into the asphalt binder [3].

The dynamic properties and durability of conventional asphalt, however, are deficient in resisting pavement distress. Hence, the task of current asphalt researchers and engineers is to look for different kinds of waste that can be modified into asphalt. The agriculture sector is one of the primary waste-producing industries and generates large amounts of biomass. The processing of agricultural products (milling, oil extraction) also creates substantial byproducts that become waste when left unutilized. Many biomass wastes with high fuel values, such as rice husk, palm oil ash, sugarcane bagasse, and waste wood, can be recycled as fuel for electricity generation. Studies have suggested that ashes produced after controlled burning of agricultural biomass could be readily utilised in asphalt technology, as shown in Fig. 4.

Figure 4. Solid waste from the agriculture industry.

Extensive programmes of investigations have been carried out to evaluate the suitability of many types of mineral fillers to substitute the costly common fillers used, such as ordinary Portland cement and limestone powder; meanwhile, there are many types of local waste materials (recycle) that can be used successfully as a mineral filler in hot asphalt concrete mixtures, such as waste of glass, ceramic, bricks, biomass ash, coal fly ash, electric arc furnace dust, glass powder, marble dust, and other similar byproducts from various processes, when added to their optimum proportion, have displayed promising results in various aspects of asphalt mix performances. Mineral fillers play a dual role in asphalt mixtures: first, they act as a part of the mineral aggregate by filling the voids between the coarser particles in the mixtures and thereby strengthening the asphalt mixture; second, when mixed with asphalt, fillers form mastic, a high-consistency binder or matrix that cements lager binder particles together; most likely, a major portion of the filler remains suspended in the binder while a smaller portion becomes part of the load-bearing framework [15]. The type and amount of filler used in hot asphalt mixtures would affect the properties of the mixes. The use of industrial and by-product wastes as replacements for mineral fillers in asphalt mixtures to enhance the properties and performance of asphalt concrete pavements by reducing the binder's inherent temperature susceptibility. Despite being used in limited concentration, the inclusion of filler in asphalt mixes has significant influences on the properties of mixes, such as (i) filler satisfying the aggregate gradation specification and influencing the strength and volumetric requirements of the mix [16]. (ii) filler extends the bitumen to increase the bitumen volume in the mixture and reduce the optimum bitumen content and material cost of the mix [17]; (iii) filler stiffens the bitumen to improve the mechanical properties of the mixture and not only influences the ability of mixes to resist permanent deformation at high temperatures but also cracking resistance at low temperatures and fatigue life at intermediate temperatures [18]; (iv) influence ‘‘bond" in the aggregate–bitumen system, which further effects moisture sensitivity of mix [19]; (v) fillers also influence the ageing process of asphalt mixes by either catalysing oxidation or by hindering the diffusion of oxygen in mastic [20]; (vii) influence the thermal performance of asphalt mixes [21]; (vii) influence the constructability of mix by influencing its mixing and compaction temperature [22]. All these effects are ultimately linked to the physical and chemical characteristics of the chosen filler, its interaction with bitumen, and its volumetric concentration in the mix. According to Larsen et al., the bitumen modification provides binders with (i) a sufficient increase in consistency at the highest temperature in pavements to prevent plastic deformation, (ii) an increase in flexibility and elasticity of binders at low temperatures to avoid crack deformations and loss of chippings, (iii) an improvement of adhesion to the bitumen into aggregates, (iv) improved homogeneity, high thermal stability, and ageing resistance, which helps reduce the hardening and initial ageing of the binders during mixing and construction [23]. Hence, the choice of suitable filler is a primary concern among field engineers. The term reinforced pavements refer to the use of one or more reinforcing layers within the pavement structure. Another application of pavement reinforcement is the use of reinforcement elements in asphalt overlays to provide adequate tensile strength to the asphalt layer and to prevent failures of the pavement such as reflection cracking [24]. Among the many kinds of research, Various forms of waste plastic are used as modifiers for the bitumen, as shown in Fig. 5 [25]. The waste plastics contain various polymers, such as Thermoplastic polymers and crumb rubber.

Figure 5. Various forms of waste plastics used as modifiers [25].

It proved effective in improving some of the bitumen's specifications, such as the hardness at high temperatures, crack resistance at low temperatures, and moisture–induced damage [26]. In different studies, the binder was replaced by polyethylene plastics, tire rubber, coal fly ash, and straw composite fibres to improve the performance of asphalt mixtures against rutting and fatigue [27]. Additionally, the use of different types of construction and demolition waste as recycled materials, including recycled concrete aggregates (RCA), recycled masonry aggregates (RMA), mixed recycled aggregates (MRA), and reclaimed asphalt pavement (RAP), in the base layers of transportation infrastructure can be seen as a viable alternative to natural aggregates without significant compromise on infrastructure performance and represents social, economic, and environmental benefits [6]. Microcosmic traits, namely surface morphology, mineralogical composition, and chemical composition, by innovative utilisation of SEM, XRD, and XRF, respectively, are to fortify the mechanistic performance. Several research efforts have been established to reiterate fibre influence on tensile strength and resilience modulus of SMA incorporating coconut, sisal, cellulose, and polyester fibres to demonstrate the good mechanical performance of tensile strength and modulus resilience, thus preventing asphalt binder from draining [28]. Several techniques exist for the production of WMA. The three generally accepted are those using (i) organic additives; (ii) chemical additives; and (iii) foaming techniques [29]. Organic additives are usually waxing and fatty amides, which can reduce the viscosity of the binder above the melting point of the binder. Common waxes used in the production of WMA are Sasobit and Asphaltan B. On the other hand, chemical additives are usually emulsifiers and surfactants that do not reduce the binder viscosity but improve the coating of aggregates by reducing the surface energy of the aggregate/binder interface and/or the inner friction. Products such as Rediset and Evotherm are often used [30]. In order to improve the moisture resistance of asphalt mixtures, the use of antistrip agents (ASA) is the most common method of improving the moisture susceptibility of asphalt mixes. The primary goal of an antistrip additive is to eliminate the moisture sensitivity of the HMA mixture by improving the bond between the asphalt binder and the aggregate. Typical antistrip agents used today are fatty amines and fatty amidoamines. It should be noted that an effective additive must improve both the unconditioned and moisture conditioned properties in order to ensure good long−term performance, nanomaterials (Zycosoil), lime, and SBS were used in different studies [31]. Nanomaterials were found to be very effective in making the asphalt mixture less susceptible to moisture damage, and the rheological properties of bitumen are enhanced because of the very high surface area to volume ratio of nanoparticles [32].

On the other hand, the use of recycled asphalt materials in the foundation and auxiliary layers can reduce global warming by 20%, energy consumption by 16%, water consumption by 11%, and hazardous waste generation by 11%. In Green design, 40% of global primary energy consumption and CO_2 emissions are related to material production [33]. Research and development into the ability of roads and roadside infrastructure to harness solar energy to power roadside lighting and adjacent buildings is currently being undertaken by businesses, academic institutions, and research agencies around the world. Projects related to pavements include solar collector systems embedded into the pavement layers or solar collector panels placed over, or next to, the road, as shown in Fig. 6. [34].

(a) (b)

Figure 6. Solar Energy (a) Solar Roadways, (b) SolaRoad bicycle path

Conclusions

The staggering accretion of solid waste requires a global effort to strive for efficient waste management and outsourcing ecological treatments. The asphalt pavement industry consumes a gigantic scale of natural resources while contributing to thermal and greenhouse emissions and is viewed as a high-potential alternative for the application of solid waste as an asphalt modifier and waste reduction. In efforts to urge cleaner and greener asphalt production, a growing trend towards the usage of solid waste as a renewable material is paving the way for a sustainable future for the asphalt pavement industry. The concise options of incorporating solid waste into asphalt mixtures, coupled with proven performance, are a green and cost-effective alternative to mitigate various pavement distresses. Different options as coarse or fine aggregates and as fillers in powder, ash, or fibre form stimulate further research interest in incorporating a diversified range of solid waste into the asphalt binder and asphalt mixture. Solid waste as a secondary raw material enables industries to reduce landfill disposal and diversify profitable ventures while cultivating impactful economic and sustainable ecological benefits. Moreover, in most cases, using solid wastes improves the engineering characteristics of asphalt, such as resistance against rutting, ageing resistance, water damage resistance, stiffness, flow value, and indirect tensile strength. Inducing sustainable novel additives that enhance service and bonding characteristics in asphalt mixtures will significantly reduce the cost of future asphalt mixture production and maintenance.

Recommendations

In order to increase the commercial viability of solid waste and pave the way for the creation of environmentally friendly and green asphalt pavement, it is my recommendation that the supply and demand factors of solid waste be taken advantage of. This will result in significant cost savings, effective waste management alternatives, and new profitable ventures. I also recommend developing regulations and specifications for regular recycling of waste and by-products for road construction as an incentive to reduce demand for natural resources and preserve the environment in Libya.

References

[1]. Choudhary, Jayvant, Brind Kumar, and Ankit Gupta. "Utilization of solid waste materials as alternative fillers in asphalt mixes: A review." *Construction and building Materials* 234 (2020): 117271.

[2]. Wong, Tracy Leh Xin, Mohd Rosli Mohd Hasan, and Leo Choe Peng. "Recent development, utilization, treatment and performance of solid wastes additives in asphaltic concrete worldwide: A review." Journal of Traffic and Transportation Engineering (English Edition) (2022).

[3]. Hasan, M. R. M., Chew, J. W., Jamshidi, A., Yang, X., and Hamzah, M. O. "Review of sustainability, pretreatment, and engineering considerations of asphalt modifiers from the industrial solid wastes." Journal of Traffic and Transportation Engineering, 6(3), (2019): 209-244.

[4]. Cayumil, Romina, et al. "An overview on solid waste generation and management: Current status in chile." Sustainability 13.21 (2021): 11644.

[5]. Kaza, Silpa, et al. "What a waste 2.0: a global snapshot of solid waste management to 2050." World Bank Publications, (2018).

[6]. Pereira, P. M., and Vieira, C. S. A. "Literature Review on the Use of Recycled Construction and Demolition Materials in Unbound Pavement Applications." *Sustainability*, *14*(21), (2022):13918.

[7]. Kowalski, K. J., Król, J., Radziszewski, P., and Wayman, M. "Eco-friendly materials for a new concept of asphalt pavement." *Transportation Research Procedia*, *14*, (2016):3582-3591.

[8]. Hasan, Mohd Rosli Mohd, Shu Wei Goh, and Zhanping You. "Comparative study on the properties of WMA mixture using foamed admixture and free water system." *Construction and Building Materials* 48, (2013): 45-50.

[9]. You, L., Long, Z., You, Z., Ge, D., and Diab. "A. Review of recycling waste plastics in asphalt paving materials." *Journal of Traffic and Transportation Engineering*. (2022).

[10]. Ali, A. "Development of a framework for sustainable construction waste management." A case study of three major Libyan cities. *The (PhD) thesis, Wolverhampton university*, (2018).

[11]. Moftah, W. A., Marković, D., and Moftah, O. A. "Characterization of household solid waste and management in Tripoli City-Libya". *Open Journal of Ecology*, *6*(07), (2016):435.

[12]. Khedr, S., and Saudy, M. "Development of superpave regional implementation framework in developing countries with hot and arid climates: Egyptian case study." *Case Studies in Construction Materials*, *18*, (2023): e01772.

[13]. Xu, F., Zhao, Y., and Li, K. "Using waste plastics as asphalt modifier: A review." Materials, 15(1), (2022): 110.

[14]. AL-Saffar, N. A. "The Effect of Filler Type and Content on Hot Asphalt Concrete Mixtures Properties." Al-Rafadain Engineering Journal, 21(6), (2013).

[15]. Singh, S., Khairandish, M. I., Razahi, M. M., and Kumar. "Preference Index of Sustainable Natural Fibers in Stone Matrix Asphalt Mixture Using Waste Marble." *Materials*, *15*(8), (2022): 2729.

[16]. Zulkati, A., Diew, W. Y., and Delai, D. S. "Effects of fillers on properties of asphalt-concrete mixture." *Journal of transportation engineering*, *138*(7), (2012): 902-910.

[17]. Choudhary, J., Kumar, B., and Gupta, A. "Laboratory evaluation on recycling waste industrial glass powder as mineral filler in hot mix asphalt." In *Proceedings of the Civil Engineering Conference—Innovation for Sustainability, Hamirpur, India*, (2016): pp. 9-10.

[18]. Wang, H., Al-Qadi, I. L., Faheem, A. F., Bahia, H. U., and Reinke, G. H. "Effect of mineral filler characteristics on asphalt mastic and mixture rutting potential." *Transportation Research Record, 2208(1),* (2011): *33-39.*

[19]. Modarres, A., and Alinia Bengar, P."Investigating the indirect tensile stiffness, toughness and fatigue life of hot mix asphalt containing copper slag powder." *International Journal of Pavement Engineering, 20(8),* (2019): *977-985.*

[20]. Recasens, R. M., Martínez, A., Jiménez, F. P., and Bianchetto, H. "Effect of filler on the aging potential of asphalt mixtures." *Transportation Research Record,* 1901(1), (2005):10-17.

[21]. Chen, M. Z., Lin, J. T., Wu, S. P., and Liu, C. H. "Utilization of recycled brick powder as alternative filler in asphalt mixture." *Construction and Building Materials*, *25*(4), (2011): 1532-1536.

[22]. Matos, P., Micaelo, R., Duarte, C., and Quaresma, L. "Influence of bitumen and filler on the selection of appropriate mixing and compaction temperatures." *International Journal of Pavement Research and Technology, 7(4),* (2014): *237-246.*

[23]. Sidikova, T., Barxanadjyan, A., Hakimov, R., Sabirova, D., and Mirsaatov, R. "The impact that crushed rubber can have on the quality of bitumen and asphalt concrete." In IOP *Conference Series: Materials Science and Engineering*, Vol. 883, No. 1, (2020):12198.

[24]. Mashaan, N. S., Ali, A. H., Karim, M. R., and Abdelaziz, M. "A review on using crumb rubber in reinforcement of asphalt pavement " *The Scientific World Journal*, (2023).

[25]. Choudhary, J., Kumar, B., and Gupta, A. "Utilization of waste glass powder and glass composite fillers in asphalt pavements." *Advances in Civil Engineering*, (2021):1-17.

[26]. Oda, S., Fernandes Jr, J. L., and Ildefonso, J. S. "Analysis of use of natural fibers and asphalt rubber binder in discontinuous asphalt mixtures." *Construction and Building Materials*, *26*(1), (2012): 13-20.

[27]. Nejad, F. M., Azarhoosh, A. R., Hamedi, G. H., and Azarhoosh, M. J. "Influence of using nonmaterial to reduce the moisture susceptibility of hot mix asphalt." *Construction and Building Materials*, *31*, (2012): 384-388.

[28]. Chen, Z., Wu, S., Xiao, Y., Zhao, M., and Xie, J. "Feasibility study of BOF slag containing honeycomb particles in asphalt mixture." *Construction and Building Materials*, *124*, (2016):550-557.

[29]. Hamzah, M. O., Golchin, B., Jamshidi, A., and Chailleux, E. "Evaluation of Rediset for use in warm-mix asphalt: A review of the literatures." *International Journal of Pavement Engineering*, *16* (9), (2015): 809-831.

[30]. Caputo, P., Abe, A. A., Loise, V., Porto, M., and Oliviero Rossi, C. "The role of additives in warm mix asphalt technology: An insight into their mechanisms of improving an emerging technology." *Nanomaterials*, *10* (6), (2020):1202.

[31]. Nejad, F. M., Azarhoosh, A. R., Hamedi, G. H., and Azarhoosh, M. J. "Influence of using nonmaterial to reduce the moisture susceptibility of hot mix asphalt." *Construction and Building Materials*, *31*, (2012):384-388.

[32]. Yang, J., and Tighe, S. "A review of advances of nanotechnology in asphalt mixtures." *Procedia-Social and Behavioral Sciences*, *96*, (2013):1269-1276.

[33]. Jamshidi, A., Hamzah, M. O., and Shahadan, Z. "Selection of reclaimed asphalt pavement sources and contents for asphalt mix production based on asphalt binder rheological properties, fuel requirements and greenhouse gas emissions." *Journal of Cleaner Production*, *23* (1), (2012): 20-27.

[34]. Sharp, K., Ralston, K., Bogumil, K., Asadi, H., and Latter, L. "Review of future pavement technologies." *Port Melbourne, VIC, Australia: Australian Road Research Board*, (2017).

DESIGN AND PROPERTIES OF CRUMB RUBBER AGGREGATES ADDITIVE IN HOT MIXTURE ASPHALT CONCRETE

Abdallh, A.A. Lhwaint*
Department of Mining Engineering/Faculty of Natural Resources /Aljufra University. Libya
*cross-bonding author:Abdallhlhwaint@gmail.com

Mohammed A. Al Madani**
Department of Materials & Corrosion Eng./Engineering Faculty /Sebha University / Libya
**Cross-bonding author: Moh.ibrahim@sebhau.edu.ly

A.A.Lashlem***
Department of Mining Engineering/Faculty of Natural Resources /Aljufra University. Libya
***Cross-bonding author: a.b.lashlem@gmail.com

ABSTRACT

This research aims to establish the design and properties of crumb rubber aggregates additive in hot mixture asphalt concrete. Rubber crumb is rubber waste which is processed through mechanical grinding or tire milling into small splinters. The objective of this research is to have high durability of flexible pavement with different percentages of crumb rubber. The experiment was done respectively through several phases as follows: preparation, quality examination of materials such as aggregate and asphalt, mixed-planning, and specimen testing implementation with Marshall Test. Properties of crumb rubber-like type stability and flow of durability can affect the different stability and flexibility of pavement. The data collected from the laboratory experiments were presented in different forms like tables, charts, diagrams, etc. The results from the crumb rubber asphalt mixture show that there is an increase in the amount of crumb rubber in a mixture of hot mix concrete asphalt. This mixture can increase the Marshall stability by 2.5 % crumb rubber higher than the other mixtures with crumb rubber.

Keywords: Tire wastes, HMA, Marshall test, stability, Flow, MQ and VMA.

1-Introduction

Roadways are an important part of the infrastructure for transportation in many countries. Road construction engineers should take into account both the safety requirements of Vehicle drivers and the economic considerations of road construction. In general, to achieve safe and economical road design road designers have to implement the safety and economy into three basic requirements for designing good roads, which are: environmental factors, traffic flow conditions, and pavement mixtures quality (Peralta, 2009).

A properly designed road will endure to the end of the road designed life without so much maintenance. However, due to certain distress such as fatigue failure, rutting, and other pavement deteriorations, the pavement performance will be greatly affected by time, the pavement characteristics change with time, and this may lead to pavement cracking (Mahrez, 1999). The discomforts on the pavement surface generally are more associated with the properties of pavement binder and pavement mixture, in which an asphaltic binder of the flexible pavement is the most common in causing poor pavement performance. Rutting, fatigue cracking, and water-related damages are among the main distress that causes the pavement surface to fail permanently.

The purpose of this analysis is to realize the feasibility of using crumb rubber as an additive in modified hot mix asphalt with some contrast to improve the quality of asphalt and learn the properties of crumb rubber asphalt. Comparing the two types of properties of the hot mix asphalt (without and with crumb rubber). Comparing the two types of the hot mix asphalt materials (without and with crumb rubber) to the Marshall properties (stability, flow, Marshall Quotient (MQ), Void in Total Mix (VITM), Void Filled with Asphalt (VFWA), and air void for optimum asphalt contact (Mashaan, 2013).

2 Materials and properties

The primary materials used in this analysis are: coarse aggregate asphalt AC 60/70, fine aggregate, and CR All the key properties of the materials used were tested for further research; multiple experiments were carried out to determine their properties in compliance with the AASHTO, and Bina Marga 2014, Britsh standard conditions referred to as standard AASHTO and Bina Marga specifications (Bina Marga, 2014) .

.2.1. Asphalt

Asphalt Properties Test AC 60/70 produced by CO. PERTAMINA. The table presents the results of properties test asphalt AC 60/70, Table.1 shows some properties of the bitumen 60/70. This test was conducted according to (Bina Marga, 2010) presents the properties test results for each form of 60/70 asphalt.

Table.1 Result of properties test of asphalt 60/70

No	Characteristics	Result	Specification (Bina Marga |2014)
1	The Specific gravity of asphalt	1.035	Min.1
2	Penetration (mm)	64.3	60-79
3	Ductility (cm)	142	Min. 100
4	Flashpoint and fire point (^{O}C)	328 -399	Min. 200
5	Softening point (^{O}C)	52.5	48 - 58
6	Asphalt solubility in TCE (tri chlore enthelyn)/CCL	99.115	MIN.99

.2.2. Aggregate

The mixture used as the ingredients for the hot mix asphalt. The analysis as a Table is based on the properties testing of coarse aggregate and fine aggregate**.**

1. **A.Properties of Aggregates.**

At the preliminary stage, the aggregate was sieved following Indonesian standards and separated on the selected aggregate gradation according to the size of sieves. The total weight needed for aggregates was 1200 grams. Table.2 and Figure.1 show the aggregate gradation specification for HMAand the gradation used in this study.

Based on Figure.1, it can be concluded that the selected aggregate gradation used in this study can meet Bina Marga's graduation requirement. (2014). Similar to hot mix asphalt, aggregate products need to be tested to determine whether the requirements are met by their properties. In this analysis, many aggregate properties have been evaluated, specific gravity, abrasion, flakiness and elongation indices, and so on, to ensure that the aggregates used in asphalt mixtures can be used.

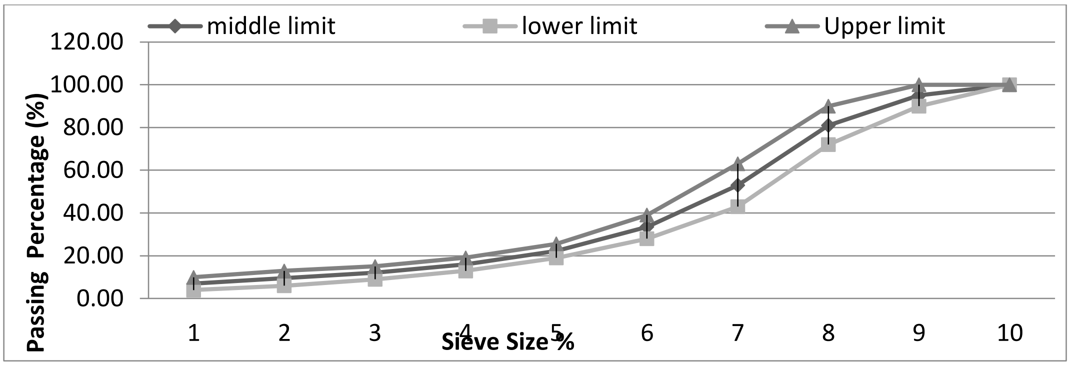

Figure.1 Gradation limit for Hot Mix Asphalt Concrete

Table.2 Properties of coarse aggregate

No	Properties	Result	Specification (Bina Marga2014)
1	The Bulk specific gravity of coarse aggregate ^{O}C	2.64	≥ 2.5
2	SSD specific gravity of coarse aggregate ^{O}C	2.67	≥ 2.5
3	Apparent specific gravity of coarse aggregate ^{O}C	2.714	≥ 2.5
4	Water absorption of coarse aggregate ^{O}C	1.02	≤ 3
5	Abrasion ^{O}C	24.08	≤ 40
6	Adhesiveness ^{O}C	92.15	≥ 95

Table.3 Properties of fine aggregate

No	Properties	Result from Fine aggregate	Specification (Bina Marga 2014)
1	The Bulk specific gravity of fine aggregate ^{O}C	2.52	≥ 2.5
2	SSD specific gravity of fine aggregate ^{O}C	2.59	≥ 2.5
3	Apparent specific gravity of fine aggregate ^{O}C	2.723	≥ 2.5
4	Water absorption of fine aggregate ^{O}C	2.94	≤ 3

.3 Marshall Properties Test Results.

Aggregates are inert granular materials such as sand, gravel, or crushed stone that, along with water and Portland cement, are an essential ingredient in concrete. Aggregate is used in this study consist of course and fine aggregates, coarse aggregate is characterized as the aggregate that exceeds the sieve size of 4.75 mm. Where fine aggregate is the aggregate, whose size is less than 4.75 mm, for example, sand is used as a fine aggregate in the preparation of HMA. Fine aggregates generally consist of natural sand or crushed stone with most particles passing through a 3/8-inch sieve.

The test is conducted to have the optimum results of the hot mix asphalt with crumb rubber. The tests here were performed for various types of mix with CR composition of 0% (without CR), 2.5%, 4.5%, 6.5%, and 8.5% CR. In every CR content, the results from Marshall Stability tests are presented. The test results include the following Marshall Properties, which are: Marshall Stability (in Kg), Flow (in mm), Void (containing air) in Mix, VIM (in %), Marshall Quotient, MQ (in Kg/mm), (Total) Void in Mineral Aggregates, VMA (in %), and Void Filled with Asphalt, VFWA (in %).

For the gradation of aggregates used in this study, the following specification is used to determine the optimum bitumen content to be used in the field (Bina Marga, Indonesia, 2017):

- Marshall Stability, minimum value = 800 Kg.
- Marshall Flow, minimum value = 3 mm to maximum value = 5 mm.
- MQ, minimum value =250 Kg/mm to maximum value = 350 Kg/mm.
- VIM, minimum value = 3.5% to maximum value = 6%.
- VMA, minimum value = 15%, no maximum value.
- VFWA, minimum value = 65%, no maximum value.

The above specification will determine the optimum asphalt content to be prescribed for the actual design AC mixture in the field.

.3.1. Mixture without Crumb Rubber Content (0% CR)

Summary of the results of complete Marshall Tests for hot AC mixture with 0% CR can be given in Table.4, while the Stability correlations are given in Figure 5.2

Table.4 Results of Marshall Properties of Hot Mix Asphaltic Concrete without crumb rubber (0% CR)*

AC (%)	Stablity (Kg)	Flow (mm)	VIM (%)	Mq (kg/mm)	VMA (%)	VFWA (%)
5.0	1685.49	4.45	1.06	378.76	9.24	52.67
5.5	1813.50	4.90	7.67	370.10	17.28	55.63
6.0	1621.48	4.92	5.22	329.57	17.01	66.43
6.5	1173.44	4.97	4.99	236.10	16.95	70.58
7.0	803.63	5.73	1.05	140.25	16.57	93.64

The minimum value of VMA ,in this case, is 16%, which primarily depends on the maximum diameter of the aggregate used in the mixtures. In this study, the maximum diameter of the aggregate is 1 inch (= 2.5 cm).

In Figure 2 by plotting only the asphalt contents that are meeting the specification of each Marshall parameters. The range of asphalt contents that are meeting all the parameters are those between 5.9 % - 6.30 %, and this narrow percentage of the range is the number of asphalt contents to be specified for application of AC mixture with 0% CR.

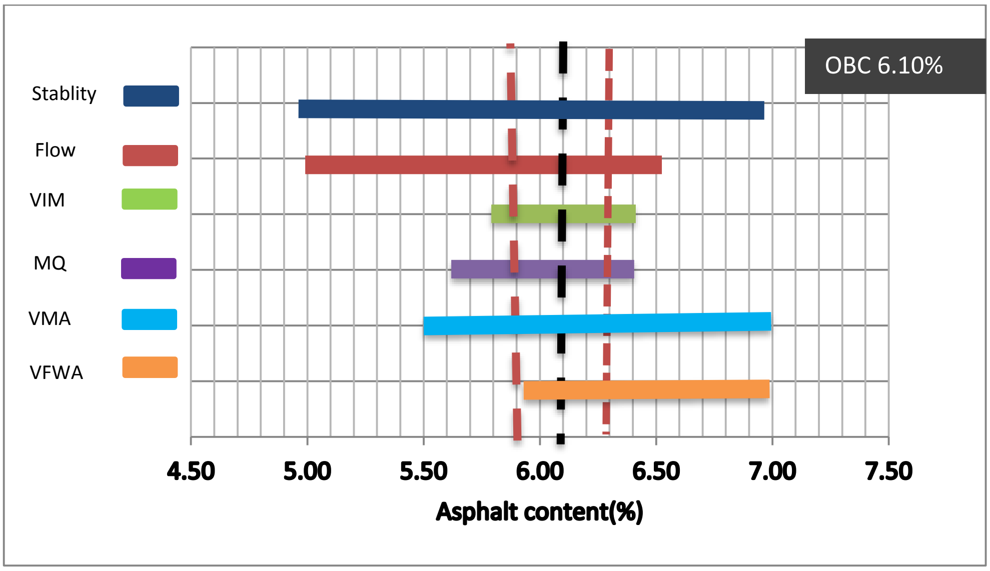

Figure 2. Summary of Optimum Bitument Content, OBM, for Marshall Properties for AC mixtures with 0% CR. (CR = crumb rubber).

.3.2. Mixtures with Crumb Rubber Content of 2.5%.

The results of the complete Marshall Test for hot AC mixture with 2.5% CR can be given in Table.5, while the Stability correlation is given in Figure 3 The percentage of crumb rubber here is a percentage of weight. Therefore, for each hot mix specimen with a total weight of 1200 grams, the 2.5% CR represents the weight of a 30-gram crumb rubber.

Table.5. Results of Marshall Properties of Hot Mix AC with 2.5% CR*

Table 5. Hot Mix Asphalt Concrete of crumb rubber at 2.5 %

AC (%)	Stability (kg)	Flow (mm)	VIM (%)	Mq (kg/mm)	VMA (%)	VFWA (%)
5.0	576.05	3.00	4.34	192.02	15.23	66.53
5.5	917.42	3.15	4.94	291.24	15.84	68.80
6.0	1322.79	3.80	4.83	348.10	16.78	71.22
6.5	960.09	4.20	3.15	228.59	17.95	82.43
7.0	853.41	4.90	2.07	174.17	18.05	88.52

Marshall Properties test are analyzed in Table 5 were obtained the following observations that the OBC when added 2.5% crumb rubber is 6.20% bitumen, which is shown in Figure 3.

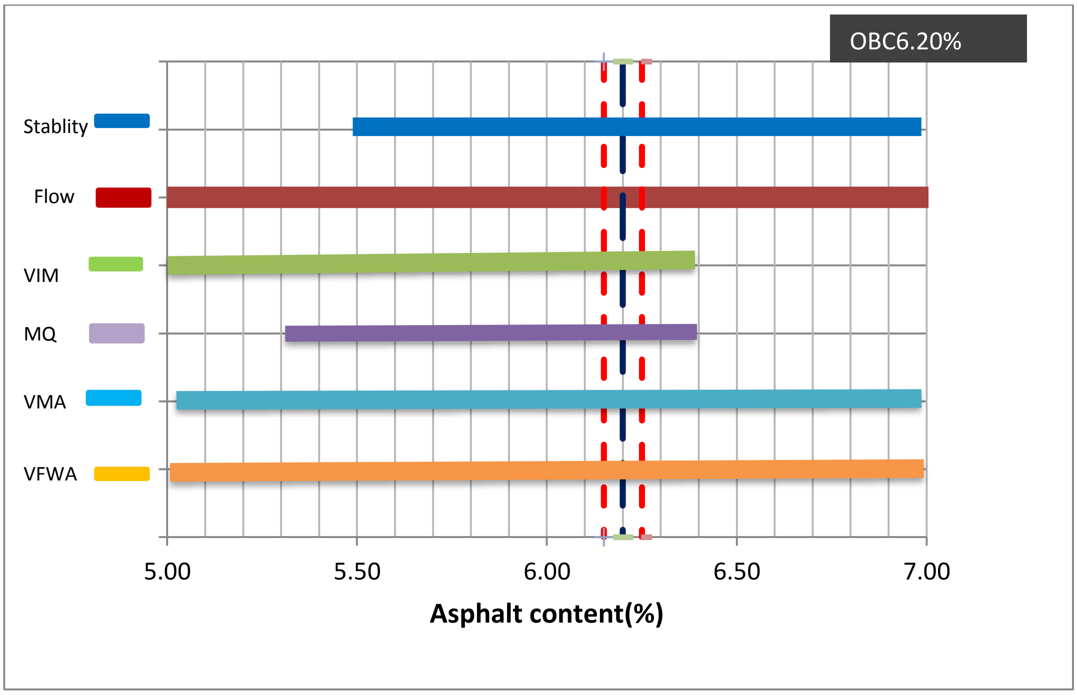

Figure 3 Summary of Optimum Bitumen Content, OBM, for Marshall Properties for AC mixtures with 2.5% CR. (CR = crumb rubber).

.3.3. Mixtures with Crumb Rubber Content of 4.5%.

The results of the complete Marshall Test for hot AC mixture with 4.5% CR can be given in Table 5.6 and the Stability correlations are given in Figure 5.16. The percentage of crumb rubber here is by weight. Therefore, for each hot mix specimen with a total weight of 1200 grams, the 4.5% CR represents the weight of 54-gram crumb rubber.

Table.6. Results of Marshall Properties of Hot Mix AC with 4.5% CR*

AC(%)	Stability (Kg)	Flow (mm)	VIM (%)	Mq (Kg/mm)	VMA (%)	VFWA (%)
5.0	426.71	3.10	4.30	137.65	13.20	67.42
5.5	533.38	3.20	3.48	166.68	13.52	74.30
6.0	746.73	3.35	4.63	222.91	24.45	73.18
6.5	1066.76	3.40	5.36	313.75	21.64	67.14
7.0	917.42	3.45	7.60	265.92	22.22	65.78

The data can be summarized in Figure 4 by plotting only the asphalt contents that are meeting the specification of each Marshall parameters. The range of asphalt contents meeting all the parameters is those between 6.1 % - 6.40%. with the OBC = 6.25%. This is the asphalt content specified for application of AC mixture with 4.5% CR

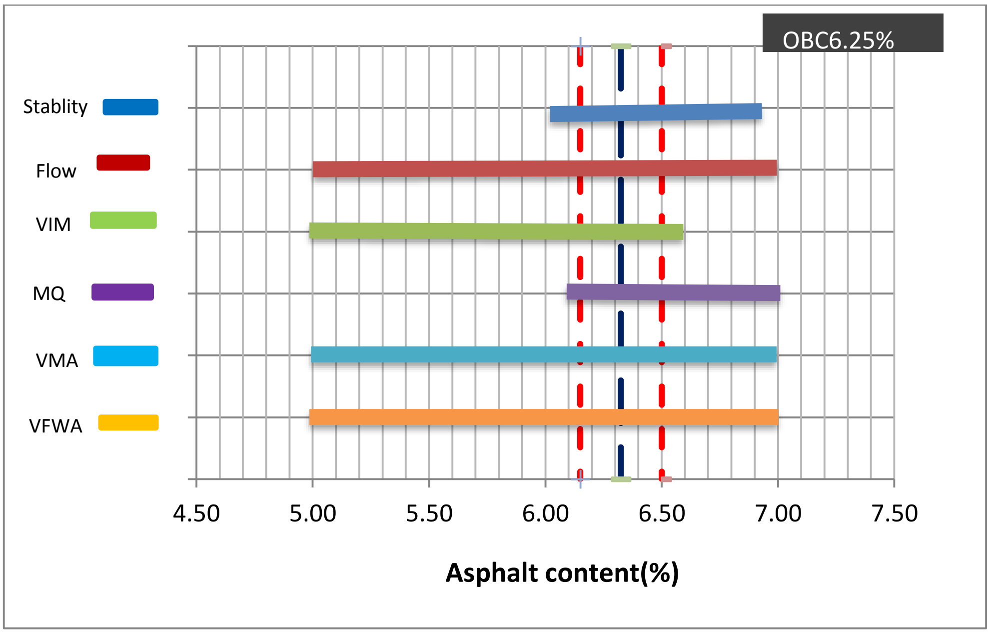

Figure 4 Summary of Optimum Bitumen Content, OBM, for Marshall Properties for AC mixtures with 4.5% CR. (CR = crumb rubber).

.3.4. Mixtures with Crumb Rubber Content of 6.5%.

The results of the complete Marshall Test for hot AC mixture with 6.5% CR can be given in Table.7. and the Stability correlations are given in Figure 5.23. The percentage of crumb rubber here is by weight. Therefore, for each hot mix specimen with a total weight of 1200 grams, the 6.5% CR represents the weight of 78-gram crumb rubber.

Table.7. Results of Marshall Properties of Hot Mix AC with 6.5% CR*

AC(%)	Stability (Kg)	Flow (mm)	VIM (%)	MQ (kg/mm)	VMA (%)	VFWA (%)
5.0	1280.12	3.20	5.23	400.04	14.04	62.77
5.5	1429.46	3.45	5.03	414.34	14.91	66.29
6.0	1280.12	3.66	5.42	349.76	16.31	66.74
6.5	960.09	3.70	5.77	259.48	17.63	67.29
7.0	746.73	3.80	3.66	196.51	18.82	80.54

.

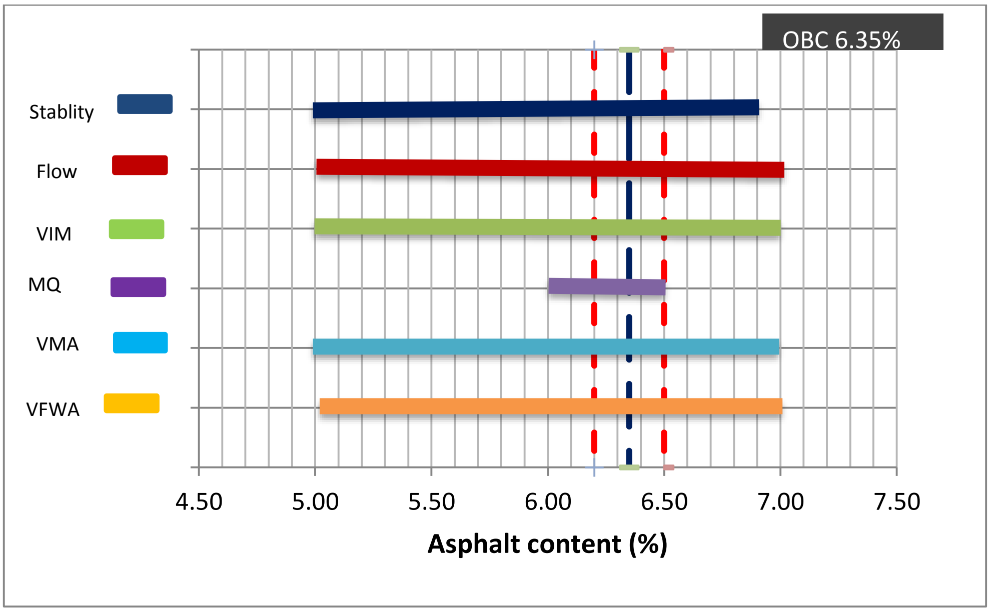

Figure 5. Summary of Optimum Bitumen Content, OBM, for Marshall Properties for AC mixtures with 6.5% CR. (CR = crumb rubber).

.3.5. Mixtures with Crumb Rubber Content of 8.5%.

The results of the complete Marshall Test for hot AC mixture with 8.5% CR can be given in Table 8. and the Stability correlations are given in. The percentage of crumb rubber here is by weight. Therefore, for each hot mix specimen with a total weight of 1200 grams, the 8.5% CR represents the weight of 102-gram crumb rubber.

Table 8. Results of Marshall Properties of Hot Mix AC with 8.5% CR*.

Asphalt Content (%)	Stability Kg	Flow mm	VFWA (%)	VMA (%)	MQ (kg/mm)	VIM (%)
5.0	810.74	3.35	34.97	11.84	242.01	14.74
5.5	1216.11	3.70	48.14	11.46	328.68	11.05
6.0	597.39	3.90	42.58	9.77	153.18	11.60
6.5	469.38	4.10	52.31	10.10	114.48	12.42
7.0	256.02	4.20	50.06	11.02	60.96	14.27

.4. Analysis of the Marshall Properties for Different CR content.

The analysis here is performed by comparing the results of the Marshall Properties in Section 5.3.1 to 5.3.5. to find the best CR content based on for the following rationales:

1. Marshall Stability

Marshall Stability represents the strength of the AC mixture against compressive and shear stresses caused by the repetition of vehicle tire passing, especially for heavy truck tires. The higher Stability means the stronger the AC mixture against damages due to heavy truck traffic.

2. Flow

The flow values represent the resistance of asphaltic pavement against permanent deformation under the repetitive load of heavy truck traffic. The higher flow means the pavement is more vulnerable to rutting, while lower flow means the pavement is more rigid and less vulnerable to permanent deformation or rutting. However, the flow values are limited to certain upper and lower limits (in this case is 5% and 3%, respectively). Too high value of flow means softer asphaltic pavement that is more easily to undergo permanent deformation; yet, too low value of flow means the pavement is too brittle. Therefore, the better AC mixtures are those with lower flow, providing that the values are still within the corridor of the specified upper and lower limits.

3. Marshall Quotient (MQ)

Marshall Quotient (MQ), also represents the strength of asphaltic mixture against tire-induced stresses, especially heavy truck traffic. The higher MQ also means the stronger pavement against tire stresses. Yet, the MQ values are restricted to certain upper and lower limits (in this case is 350 Kg/mm and 250 Kg/mm, respectively). Too high MQ also means the pavement is too rigid and too brittle, so that it may be more prone to cracking. Whereas, too low MQ means the pavement is more easily to undergo permanent deformation under repetitive loading of heavy truck traffic. Therefore, MQ is the reflection of the toughness and resilience of the mixture against stress and deformation. Because MQ = Stability/flow, the same Stability of specimen tested but with the lower flow will yield higher MQ. This means, even if the Stability values are the same, the AC pavement with higher MQ will have more resistance to deformation after subjected to repetitive loading than those with lower MQ. Therefore, higher MQ values mean better AC mixtures, providing that the values are still within the corridors of the specified upper and lower limits.

4. VIM

VIM represents the amount of air still remains inside the AC mixture after the mixture is compacted to become pavement. The amount, in this case, is limited to 3.5% to 6%. The lower limit, 3.5%. is the minimum air still needed inside the mix so that bleeding will not occur in the pavement after the pavement is subjected to many years of repetitive heavy truck traffic. Repetition of truck traffic will cause the pavement will become further densified, so that when no more enough void of air remaining inside the pavement, bitumen binder will be forced to flow outside to the surface of the pavement and to cause bleeding. Bleeding is not permitted in the asphaltic pavement because it may cause the pavement more slippery and hazardous to the traffic. On the opposite side, the higher limit of VIM, 6%, is the limit for the pavement not to become too porous so that water may enter the pavement and dwell inside the pavement. This condition has been known to cause the pavement to deteriorate and crumble more easily so that the pavement is more likely to be damaged prematurely. Therefore, the better quality of AC mixtures are those with VIM values closer to the average value of the specification, which is $(3.5 + 6)/2 = 4.75\%$.

To find the better quality of the AC mixtures with different content of CR, each of the results of the Marshall Properties should be given scores. The score is 1 for the best one, 2 for the second one, 3 for the third, etc. The scores are finally accumulated by just simple addition and the CR content with the least value is chosen as the best AC mixtures for all the Marshall properties describes above.

It should be noted here that the VMA and the VFWA are not included in the qualitative analysis, because the VMA and VFWA are only for the initial condition for the aggregates and gradation; they are not related to the asphalt content or CR content. Therefore, as long as the

VMA and VFWA specifications are already met according to the specification, the other Marshall properties should be used as the determining factors.

Table..9 Comparison of Marshall tests of HMA with CR and without CR

	%Crumb Rubber content in mix			
	%CR	2.5%CR	4.5%CR	6.5%CR
(OBC)	6.10	6.20	6.25	6.35
Stability (kg)	1621.48	1322.79	1066.76	1280.12
Flow (mm)	4.92	3.80	3.40	3.66
Marshall Quotient (kg/mm)	329.56	377.94	313.75	349.76
VIM (%)	5.22	4.83	5.36	5.42
VMA (%)	17.01	16.78	21.64	16.31
VFWA (%)	66.43	71.22	67.14	66.54

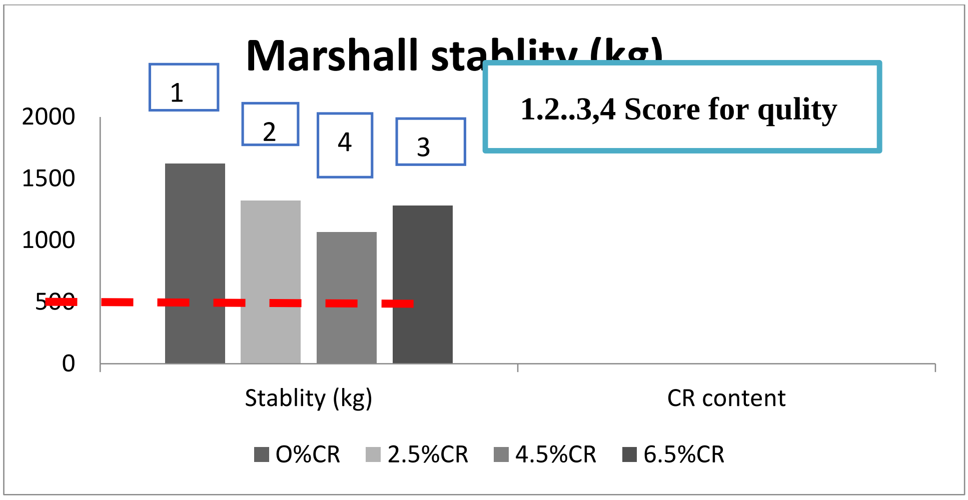

Figure 6. Comparison of cases Stability test for HMA with and without CR

5.4.1 The Marshall Stability

When comparing the test results for Stability in Table.9 and Figure 6 optimal stability. The results in stability tests respectively without CR at AC 6.0% was 1621.48 kg, with 2,5% CR at AC 6% was 1322.79kg, with 4.5%CR at AC 6.0% was 1066.76kg, with 6.5%CR at AC6 % was 1280.12kg.

Factor since extensive crumb rubber application reduces the coarse aggregate point of contact within the mixture. The use of crumb rubber can result in higher density or more porous bitumen. Consequently, the mixture becomes more flaccid to lead to a drop in the stability value. The resilience of aggregates reduces as the crumb rubber content increases (Mashaan et al. 2013). Increasing crumb rubber has been found to reduce HMA stability, with a higher percentage of crumb rubber yielding the lowest stability value.

Table. 10 Comparison of Flow (mm) of Hot Mix Asphalt Concrete with CR and

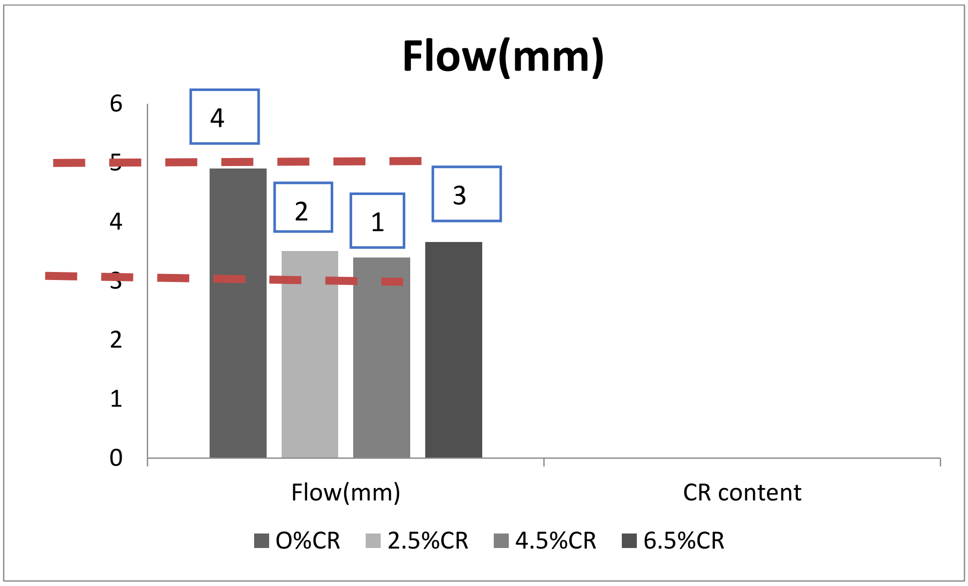

Figure .7 Comparison of cases flow test for HMA with and without CR

5.4.2 The Marshall Flow

Comparing the outcome of the Flows check-in Table 7 Figure 5.37, the hot mix asphalt concrete flow test volume improved as the CR quality rose from 5% to 7%. Higher flow values can be associated with increased air void (more compaction required) by using more CR in the mixture, resulting in a more versatile mix. Therefore, it can be inferred that the lower amount of crumb rubber increases the flow but the higher volume of asphalt reduces the flow. The mixtures are more stable with the inclusion of asphalt content; while the resistance to deformation decreases, it can result in a high flow value (Mashaan et al. 2013). It has been stated that applying crumb rubber additive to asphalt concrete increases the mixture flow before maximum crumb rubber content is obtained. Crumb rubber with additional content is good at higher temperatures with high flow. while very low permeability and more rigidity in small flow. Asphalt content with additional crumb rubber can lead to high flow value, This means that good against rutting, and permeability.

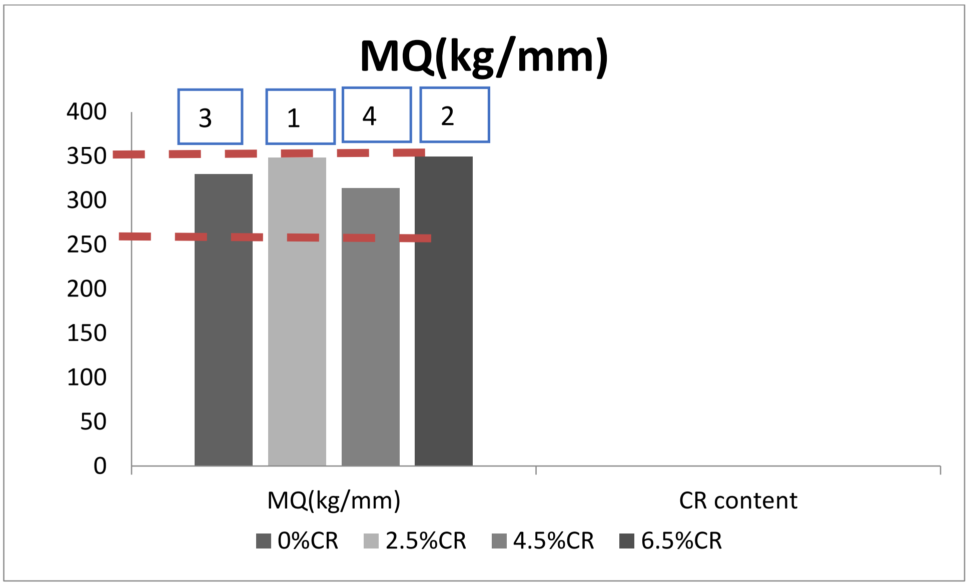

Figure. 8 Comparison of cases of MQ test for HMA with and without CR

5.4.3 Marshall Quotient (MQ)

The MQ test results evaluated in Figure 8 show that HMA without crumb rubber, 2.5%, 4.5%, and 6.5% CR have maximum MQ values of 303.01, 348.10, 313.75, and 349.76 kg/mm, accordingly at AC 6%. Therefore, it can be inferred that MQ can improve by increasing the percentage of crumb rubber content. This is because voids have space within the compacted mix to transfer the HMA. The combination of asphalt construction and rubberized HMA mixtures is a trade-off in high binder quality to boost long-term longevity and efficiency. Moreover, enough space in place can prevent rutting, instability, flushing, and bleeding. The details can be seen in Table.9 the MQ.

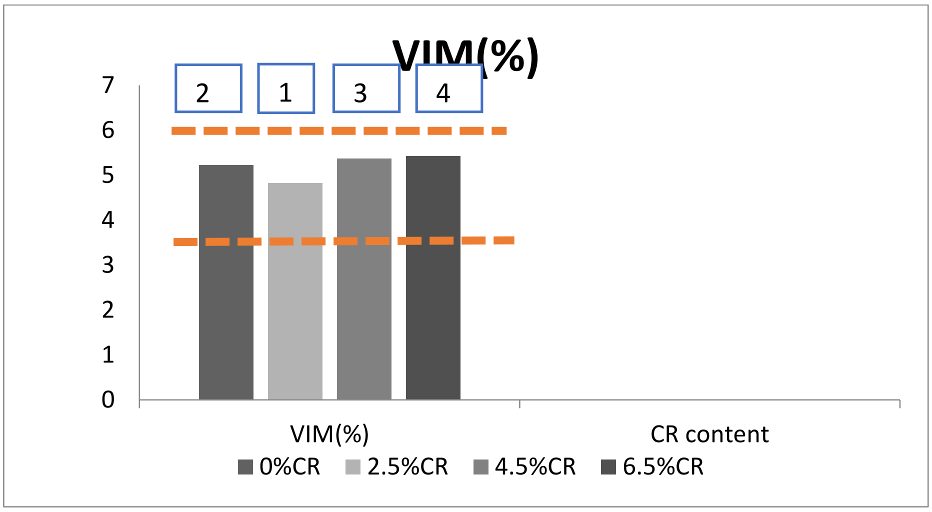

Figure .9 Comparison of cases VIM test for HMA with and without CR

5.4.4 Void in Mix (VIM)

The VIM test results analyzed in Figure 9 showed that HMA without crumb rubber,2.5%, 4.5%,6.5%, CR have maximum. The VIM has the values of 5.22, 4.83, 6.36, and 5.77 respectively. Therefore, it can be inferred that an increase in the amount of crumb rubber content can increase the VIM.

Al-Azri et al. (2006) concluded that The use of petroleum asphalt as a pavement mixture although it meets the requirements of the specification, often shows a decrease in service behavior due to rutting, fracture, and other forms of damage. Fractures from or on the sidewalk make water easy to enter so that it can damage the paving structure due to the movement of air and water on the sidewalk, causing oxidation and evaporation to occur in the binder. As a result, sidewalks have relatively low durability. There is strong evidence that asphalt oxidation happens in the whole depth of pavement, dramatically affecting pavement durability. Shu and Huang (2014) stated that an increased amount of crumb rubber in the mixture of asphalt concrete would reduce the strength of Marshall. Nevertheless, this was not always accompanied by enough flow; thus, as expressed by the Marshall Quotient parameter, it resulted in less versatility. Waste tires pose significant health and environmental concerns if not recycled and/or discarded properly. Over the years, recycling waste tires into civil engineering applications, especially into asphalt paving mixtures. Crumb rubber or waste rubber is a mixture of natural rubber synthetic rubber, black carbon, antioxidants, fillers and extender form of oils that are soluble in warm paving grade.

	Scores for quality of Marshall properties			
	%CR	2.5%CR	4.5%CR	6.5%CR
Marshall stability (kg)	1	2	4	3
Flow (mm)	4	2	1	3
Marshall Quotient (kg/mm)	3	1	4	2
VIM (%)	2	1	3	4
Σ score	10	6	12	12
Ranking of overall quality	2	1	4	3*

* Having total scores = 12 similar to 4.5% CR, but it selected as no.3 because of the more amount of CR used as more desirable for environmental concern.

Conclusion

Several measurable chemical properties are believed to be associated with the mechanical or organizational resistance of a pavement. From the result, the comparative outputs of the elastic and viscous behavior differed with the structure. The conclusion as follows: the best CRMA mixture for overall condition according to the criteria of the Marshall Test is the one with the CR content = 2.5%. This 2.5% CR will exhibit the best mixture for hot mix asphalt concrete against fatigue cracking and rutting.

REFERENCES

[1]-ASTM D5381-93:2009. Standard Guide for X-Ray Fluorescence (XRF Spectroscopy Of
" .'Pigments and Extenders. American Society for Testing and Materials

[2]-American Society for Testing and Materials (ASTM, 1992, Standard Test Method for Specific American Society for Testing and Materials. Standard Test Method For Theoretical Maximum Specific Gravity And Density Of Bituminous Paving Mixtures. Philadelphia .ASTM D 2041

[3]-American Society for Testing and Materials (ASTM), 1992, Standard Test Method for Resistance to Plastic Flow of Bituminous Mixtures Using Marshall Apparatus. Philadelphia, .ASTM D 1559 Gravity and Absorption of Fine Aggregate. Philadelphia, ASTMC 128
[4]-American Society for Testing and Materials (ASTM), 1995, Concrete and Concrete Aggregate C117-35t Direct Responsibility of Subcommittee C09.20 On Normal Weight Aggregates. Philadelphia, ASTMC 117.
[5]- Indonesian Standard. 2012. Tata Cara Pemilihan Campuran Untuk Beton Normal, Beton Berat Dan Beton Massa. Sni 7656:2012. Bahan Konstruksi Bangunan Dan Rekayasa Sipil 91-01 Japtan Kerja Raya (Jkr), 1988, Standard Specifications For Road Works.
[6]- Mahrez, A. 1999. Properties Of Rubberised Bitumen Binder And Its Effect On The Bituminous Mix [Ms Thesis]. *Faculty Of Engineering, University Of Malaya, Kuala Lumpur, Malaysia*.
[7]-Pasetto, M. & Baldo, N. 2012. Performance Comparative Analysis Of Stone Mastic Asphalts With Electric Arc Furnace Steel Slag: A Laboratory Evaluation. *Materials And Structures,* 45**,** 411-424.
[8]- Peralta, E. J. F. 2009. Study Of The Interaction Between Bitumen And Rubber.
[9]- Presti, D. L. 2013. Recycled Tyre Rubber Modified Bitumens For Road Asphalt Mixtures: A Literature Review. Construction And Building Materials, 49**,** 863-881.
[10]-Mashaan, N. S. & Karim, M. R. 2013. Investigating The Rheological Properties Of Crumb Rubber Modified Bitumen And Its Correlation With Temperature Susceptibility. *Materials Research,* 16**,** 116-127.

[11]- Shu, X. & Huang, B. 2014. Recycling Of Waste Tire Rubber In Asphalt And Portland Cement Concrete: An Overview. *Construction And Building Materials,* 67**,** 217-224.

[12]- Al-Azri, N., Jung, S., Lunsford, K., Ferry, A., Bullin, J., Davison, R. & Glover, C. 2006. Binder Oxidative Aging In Texas Pavements: Hardening Rates, Hardening Susceptibilities, And Impact Of Pavement Depth. *Transportation Research Record: Journal Of The Transportation Research Board***,** 12-20

Tensile Behavior of Polymer Modified Bitumen in Hot and Arid Regions

Mohamed Khalifa Ali Ahmed

Department of Civil Engineering, Tripoli University, Tripoli, Libya

Mo.ahmed@uot.edu.ly

Abstract

Hot and arid regions characterized by its high normal maximum temperature and low precipitation rate. North Africa and Middle East are a typical example of this climate.

The performance of Asphaltic Concrete Pavement in such region showed a unique phenomenon of distress and early hardening and deterioration. The main distress modes are premature surface cracking, Research devoted to this region showed that, the main fatal factor contributing to this problem was the increase of applied thermal and traffic tensile stress compared with the own bitumen tensile strength.

Tensile strength is probably one of the main properties which bitumen must possess to perform successfully in pavement structural composites. Bitumen forms thin films between the aggregate surfaces. The physical properties of thin films of most materials are different from those of materials in bulk. Because tensile strength is very important to ensure adequate performance, it is desirable to evaluate the tensile strength of bitumen thin films in the range of thickness expected to be encountered in bituminous composites.

All tests were carried out using a Howden Universal Testing Machine, with a load capacity of 50kN. The output of the machine is connected to an X -Y plotter, where y-axis represents the load in (kN) and the X-axis represents the displacement in (mm). The variables studied in this investigation were selected from the available information related to the general behavior of material in thin films. These variables were film thickness over a range from 30 to 200 microns, testing temperature used were (0, 20, and 60 °C) and two different types of binders one base bitumen of 100 penetration and one polymer modified binders. The polymer was Acrylic (ACR). ACR was incorporated into 100 penetration bitumen. All experiments were carried out at a constant rate of extension 100 mm/min.

Keywords: *Hot and arid regions, premature surface cracking, bitumen tensile strength, Howden Universal Testing Machine, polymer modified binders, and* Statistical analysis

1. Introduction

In recent years, there have been numerous reported complaints about the quality of bituminous pavements because of premature aging problems in different parts of the world[1,2,3, 4 and 5].

The problem comes from the fact that bitumen hardening increases the mix stiffness and lowers the cracking strain making the pavement surface vulnerable to cracking [6].

Most of the research (1,9) in this subject has concentrated on the hardening which takes place during the time of construction, see Figures 1 and 2. Those efforts resulted in a number of specifications and standard testing procedures like the Thin Film Oven Test (TFOT) which aims to control the quality of bitumen binders to be used in paving mixes. Aging of the binder in service, has not received the required attention yet.

In this study special consideration is given to the behavior of thin film of bitumen binders in hot arid climates. Binder normally coated the aggregate in asphaltic concrete mixes by a thin film of bitumen with a thickness range from 8 t0 14 micron the tensile strength of the binder decreases with the increase of the film thickness. Most of the tensile strength determined using bulk binder thickness which not simulated the real continuation of the tensile strength of the bitumen in thin films. In this study we will measure the bitumen Tensile strength in thin films ranges from 10 micron to 100 micron. Due to the fact that the rate of hardening in service depends, to a large extent, on the pavement temperature system we will determine the bitumen tensile strength at different temperatures. Hardening of the surface is generally greater due to the higher temperature and ultraviolet radiation [6,7, and 8].

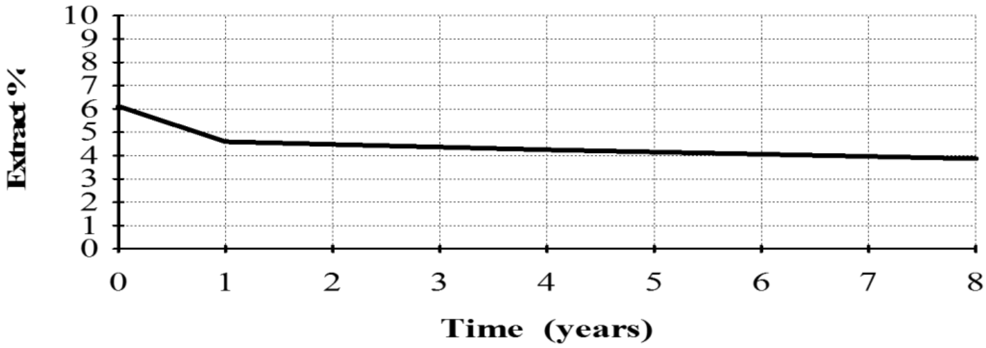

Figure1 Percentage of extract against age (9)

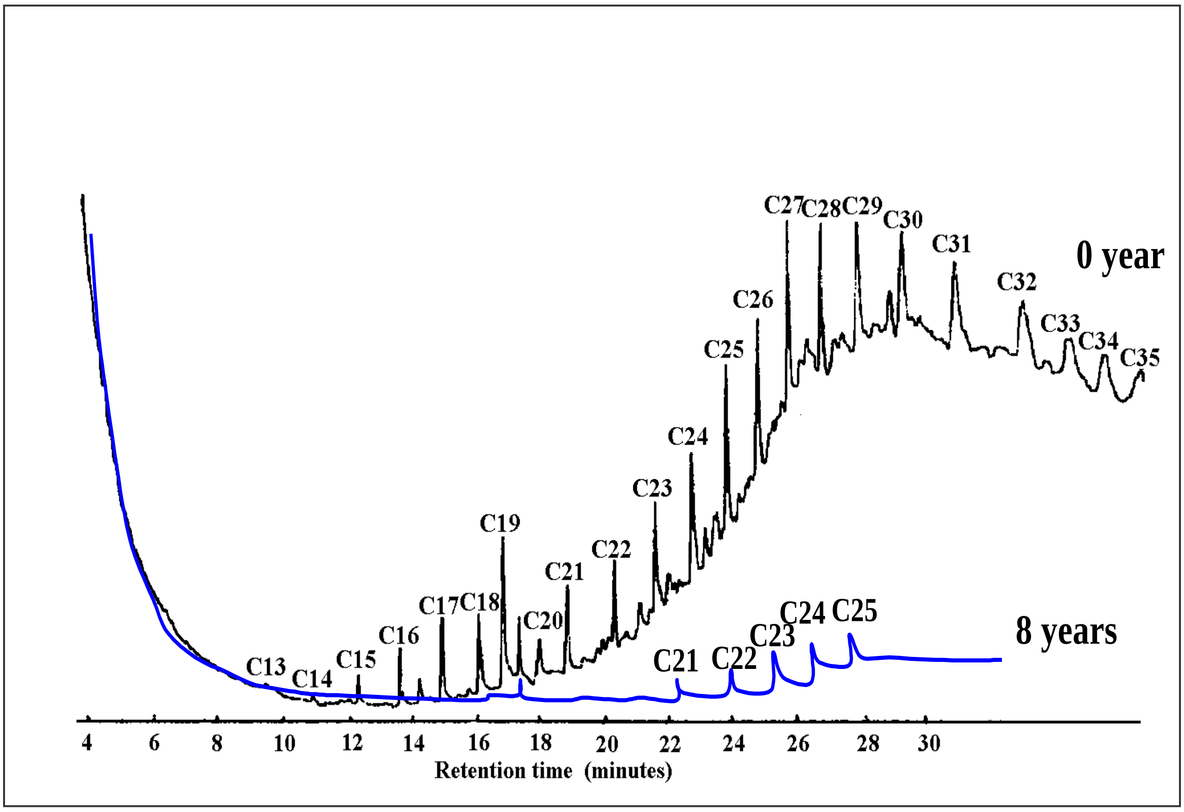

Figure 2 Chromatograms for the heptane fraction of 0 and 8 years **(9)**

2. Testing Procedure

2.1 General

Energy of adhesion and cohesion is an important characteristic of bituminous materials when used as binder on bitumen aggregate composites. Most of tests used to assess the properties of bituminous materials are designed to test bitumen in bulk and therefore do not simulate actual conditions in a bituminous composite subjected to complex stresses in the field. Tensile strength is probably one of the main properties which bitumen must possess to perform successfully in pavement structure [9].

Ali (10) reported that: cracking and subsequent failure of bituminous surfaces can often be attributed to excessive tensile stress induced in pavement by various cases. When the tensile stresses exceed the tensile strength of the bitumen present in thin films between the aggregates, the pavement will fail. Thus, an understanding of mechanism of failure and rheological behavior of bitumen in simple tension is required for the final selection of bitumen to be used in composite.

2.2 Devolving of Testing Procedure

The testing procedure developing during this investigation is divided in three stages as follows: Stage one: Preparation of thin films of bitumen, stage two: testing of the prepared thin films, and stage three: examination of the resulting fracture surfaces of thin films of bitumen by using the scanning Electron Microscope

2.2.1 Preparation of thin film of bitumen

Stainless-steel test blocks with a diameter equal to 25 mm were manufactured for this study to be used instead of aggregate for the tensile stress. The stainless-steel test blocks have the quality of ease of machining, ability to retain quality of surface finish, and have similar thermal coefficient to the mineral aggregates used in bituminous mixtures [11]. Figure 3 shows a photograph of the stain-less steel test blocks. The surface of test blocks which were to receive had been polished to get surface roughness such that maximum difference between the peaks and valleys were less than 0,038µm

2.2.2Testing Procedure

Figure 4 shows a schematic diagrammed of the testing machine. The machine named a Howden Universal Testing Machine with a load capacity of 50 kN. The output of the machine is connected to an X-Y plotter, where Y-axis represents the load in (kN) and X-axis represents the displacement in (mm).

2.2.3 Bituminous Binders

Two types of binders were used in this investigation, one is 100 penetration base bitumen another one is polymer modified bitumen named Acrylic (ACR), ACR were incorporated in 100 penetration bitumen. Table 1 represents the binder types, their designation, and properties.

Table 1 The properties of bituminous binders

Properties	Binder Type	
	Base Bitumen (BB100)	ACR modified Bitumen (ACR)
Penetration, 100g, 5 sec		
4 ºC	11	-
10 ºC	22	18
15 ºC	35	30
25 ºC	98	44
35 ºC	199	70
45 ºC	-	150
Softening Point, ºC	45	81
Specific Gravity @25 ºC	1.020	1.025
Penetration Index	-0.55	4.05
Stiffness Modulus Pa	2.5 x10^8 @-10 ºC, and 5x10^5@40 ºC	1.0 x10^9 @-10 ºC, and 2x10^6@40 ºC

2.2.4 Placing bitumen between test blocks

The test blocks were heated to 100 ºC and a thin layer of a measured quantity of liquid bitumen was placed on the surface of heated test block. The exact thickness of resultant film thickness was calculated by a weight difference technique. That is, by measuring the mass of test blocks before and after bitumen was placed to find the mass of bitumen and knowing the specific gravity of bitumen and they are of the test block surface the film thickness could be calculated.

Figure 3 Stainless Steel Test Blocks

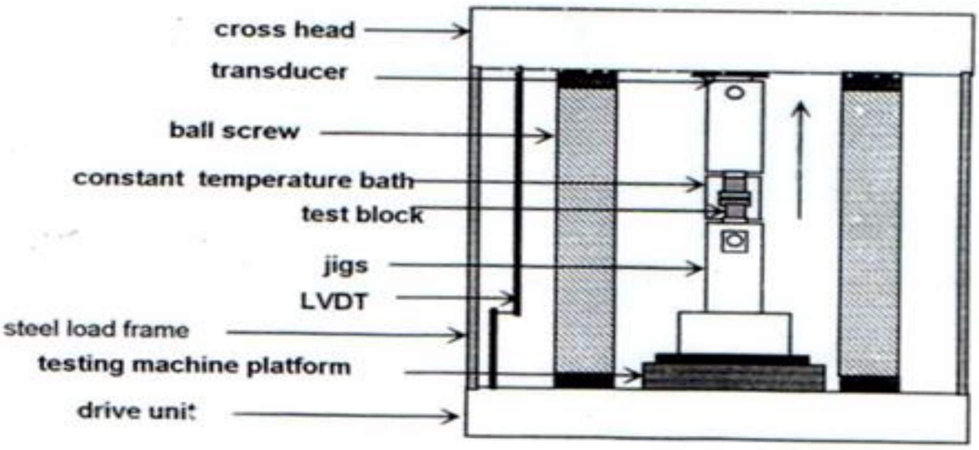

Figure 4 Schematic Diagram of the Testing Machine

2.2.5 Temperature Control

To control the temperature of the specimen during the test a small water bath was especially manufactured for this test and placed on the lower platform on the testing machine as shown in Figure 4.

2.2.6 Electronic Microscopy

A Camscan Series3 scanning electronic microscope was used foe examining the tested samples in this investigation. It can be used to generate images of the surface of an object or specimen at magnification in the range of 20X to 20000X and upwards. The specimen is bombarded by electrons in the microscope it must be conducted. An Emscope Sc500 gold coater was used to coat the surface of the sample to be examined. A 200 µm thick gold layer was spread on the fractured bitumen surface without any apparently altering the surface topography.

3. Discussion of Experimental Results

3.1 General

The variables studied in this investigation were selected from the available information related to the general behavior of materials in thin films [10]. These variables were film thickness over a range from 30 µm to 200 µm, testing temperature used were (0, 20 and 60 ºC) and two types of binders one base bitumen of 100 penetration and ACR polymer modified Bitumen, their characteristics as presented in Table 1.

3.2 Load Deformation and Tensile Strength Characteristics

The load deformation characteristics of visco-eleastic materials such as bitumen depends on the rate of loading and temperature (10,11, and 12). When this bitumen tested in thin films, the load deformation characteristics are also significantly influenced by the variation of testing temperature.

3.3 Regression Analysis

A correlation between the tensile strength, film thickness, and temperature can be numerically expressed by an equation of the following form:

: $Y = \frac{A}{X} + (\frac{Z}{B})^{n} + C$ ……………………………………………………………… (1)

Where:

Y = tensile Strength (MPa)

x = Film Thickness (µm)

Z = Testing Temperature (ºC)

A, B, C, and n = constants indicate the sensitivity of the binder to variation of bitumen film thickness and temperature.

Statistical analysis of the results allowed to obtain regression equation which gives numerical values between tensile strength, temperature, and bitumen film thickness. These equations are as follows:

For BB100 Bitumen: $S = \frac{115.72}{H} + (\frac{T}{20})^{0.85} + 2.65$……………………………………. (2)

For ACR Modified Bitumen: $S = \frac{140.25}{H} + (\frac{T}{18})^{0.63} + 3.00$………………… ………… (3)

Where

S = Tensile Strength in (MPa)

H = Film Thickness in (µm)

T = Temperature (ºC)

Comparison is made between the tensile strength values obtained in the laboratory design process with those predicted from the above numerical equations. The statistical data and the obtained Multiple coefficients of Determination (MCD) and Multiple Correlation coefficient (MCC) = $\sqrt{MCD}$ are presented in Table 2. The predicted values for MCD and MCC from the equation are reasonable.

Table 2 Tensile Strength curve regression analysis

Binder	A	B	C	n	Multiple coefficients of Determination (MCD)	Multiple Correlation coefficient (MCC) = $\sqrt{MCD}$
BB100	115.72	20	2.65	0.85	0.9450	0.9720
ACR	140.25	18	3.0	0.65	0.7462	0.8640

3.4 The effect of ACR Polymer

Figures 5 and 6 represents the relation between bitumen film thickness in (µm) and bitumen tensile strength in (MPa). The influence of ACR polymer on tensile strength of the binder at different testing temperature is illustrated in Figure 6. The addition of ACR polymer increases the tensile strength of the binder. The maximum tensile strength values increase by 20% at low temperature (0.0 ºC) and 4.62% at high temperature equal to 60 ºC, also the stiffness modulus values are significantly influenced by the addition of ACR polymer.

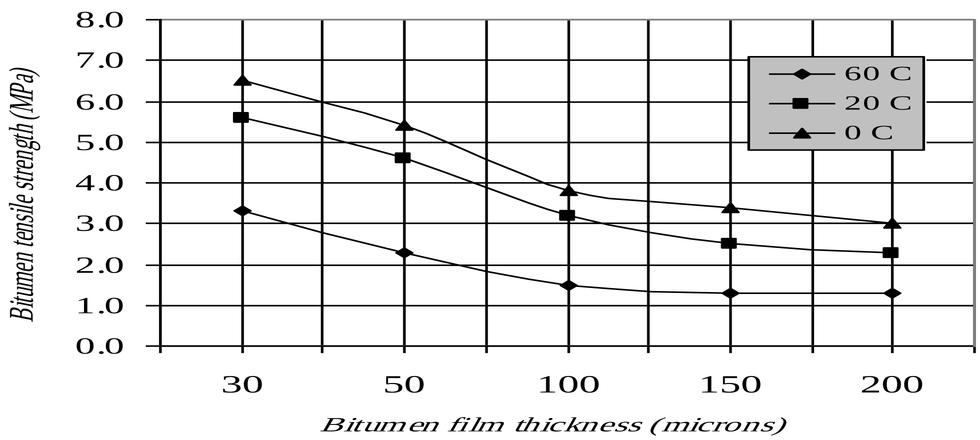

Figure 5 tensile strength of base bitumen BB100

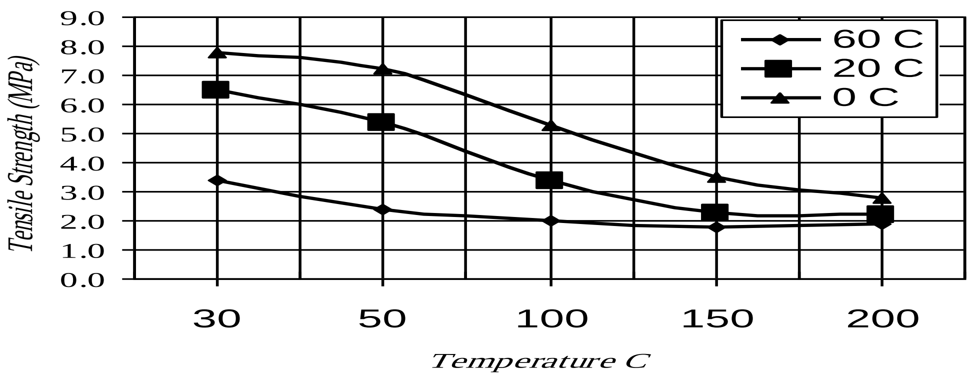

Figure 6 tensile strength of ACR polymer modified bitumen

3.5 Modes of failure

Three modes of failure were observed in the test specimen depending upon the film thickness, temperature, and type of binder. These three modes of failure are: Flow failure, normally related to high temperature, intermediate failure take place at temperature equal to 20 ºC and brittle failure at low temperature. Figures 7 and 8 show a photograph of these types of failure for BB100 and ACR polymer modified bitumen.

3.6 Fracture Surface Topography

A limited study to observe the surface of the fractured specimen was carried out using a Scanning Electronic Microscope (SEM). Immediately after failure the blocks were coated with 200 µm thin film of gold-palladium and placed in the SEM chamber. The test blocks were exactly the same size and geometry of the sample holders use in the SEM. This facilitated the rapid transferee of specimens from the vacuum coating unit to the SEM. Figure 7 shows random distribution of points, these points are the origin of the initiation of cracks which grow as the materials is stressed and reach a critical length at which failure occurs.

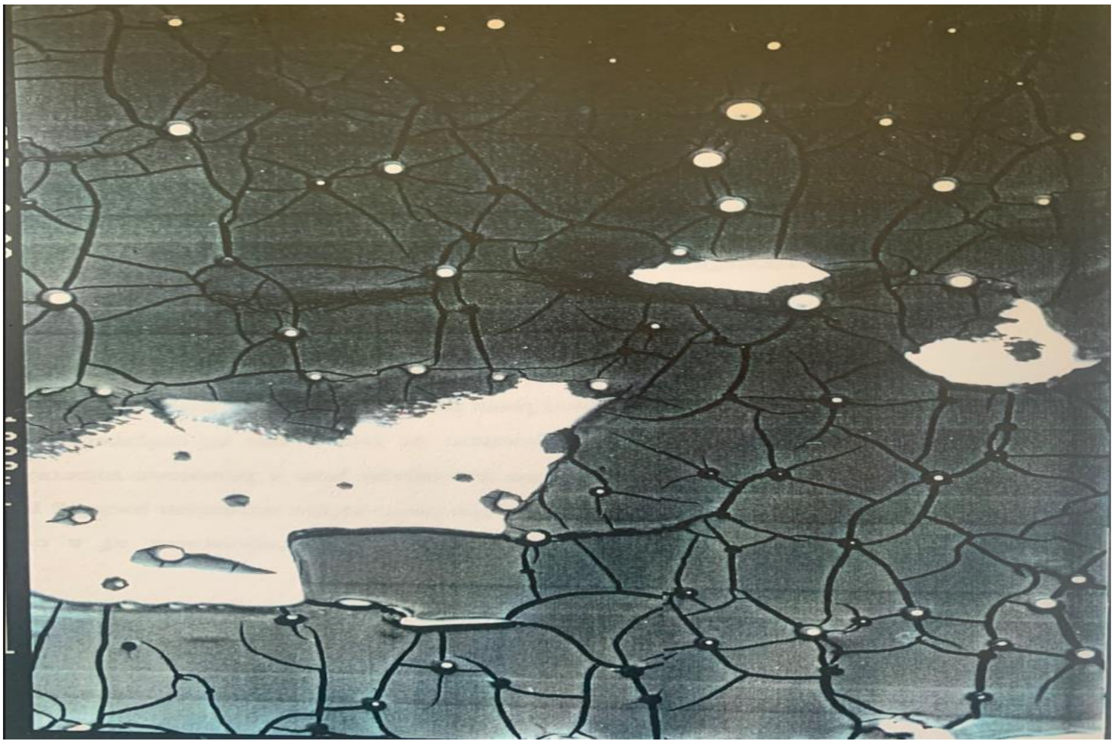

Figure 7 Scanning Electronic Micrograph for BB100 Bitumen

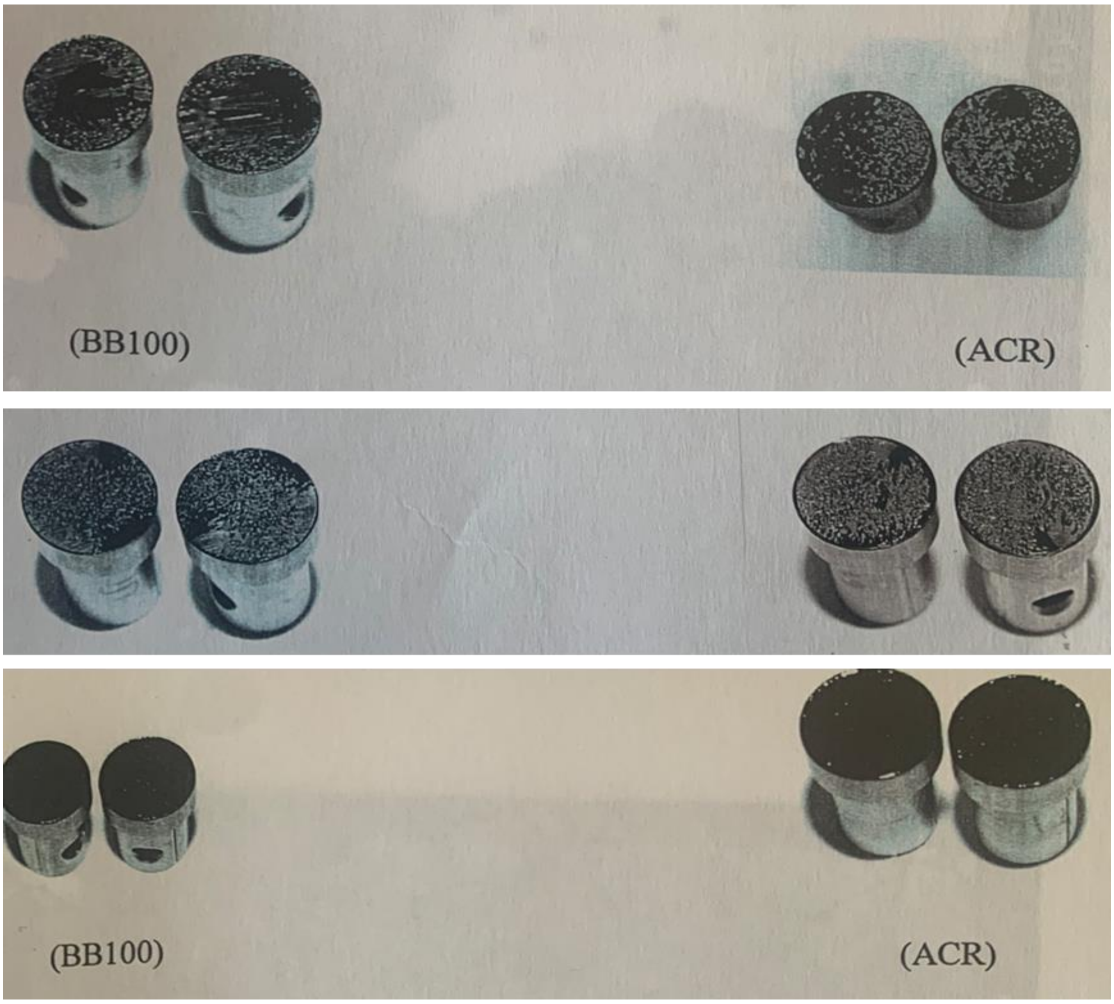

Figure 8 Failure Modes for BB100 and ACR modified bitumen

4. Conclusions and Recommendation

This experimental work has resulted in the following conclusions:

4.1 The tensile strength of bitumen thin films decreases as film thickness increases, and finally a approaches a constant value close to the cohesion value of bitumen in bulk. Bitumen films of the same thickness have higher tensile strength at lower temperature. As the temperature increases the tensile strength of bitumen in thin films decreases.

4.2 The addition of ACR polymer to base bitumen BB100 increases the tensile strength of the binder. This increase is more pronounced at low temperature

4.3 The mathematical models which were developed using regression analysis may be used to predict the tensile strength of a bitumen as a function of film thickness and temperature. For BB100 Bitumen: $S = \frac{115.72}{H} + (\frac{T}{20})^{o.85} + 2.65$ and

For ACR Modified Bitumen: $S = \frac{140.25}{H} + (\frac{T}{18})^{0.63} + 3.00$,

S = Tensile Strength in (MPa), H = Film Thickness in (μm), and T = Temperature (ºC)

4.4 Based on the results of thin film tests, The ACR polymer modified binder improved the performance of dense bituminous mixes in hot and arid regions. Considerable increase in tensile strength, and softening point is achieved by the addition of ACR polymer additive to base bitumen BB!00.

5. Recommendations

5.1 This laboratory investigation presented the influence of incorporating ACR polymer additive to predict the tensile strength of binders in thin films its recommended to use more polymer additives such as Styrene – Butadiene -styrene (SBS) polymers.

5.2 Since in this present work only Tensile strength of bitumen were tested. More research work is needed to use ACR modified binder in Dense Bituminous Mixes (DBM).

5.3 Field trials in hot and arid regions are recommended to be investigated using ACR polymer modified binder

6. References

[1] Omer M S, Gnabah T H and El-mudi M O (1994). “Mechanism of distress of asphalt Pavements in arid desert areas.” 2nd Maghrib Road Conference, 8-9 Nov., Biskara, Algeria.

[2] Mohamed, K A, Ahmed, and Jamal Shabani, " Semi – Flexible Pavement" Proceeding of the 9th National Conference for Construction and Structural Engineering, vol.2 pp 431 -437, University of Tripoli, Faculty of Engineering, Tripoli, Libya November 2022

[3] Richardson J T G (1994). “Bituminous Mixtures in Road Construction.” Edited by Hunter R N, Pub. Thomas Telford, London.

[4] Craus J, Ishai I and Sides A (1981). “Durability of bituminous paving mixtures as related to filler type and properties.” Proc. Assoc. of Asphalt Paving Technologists (AAPT), Vol. 50, pp. 291-318.

[5] Davis T C and Petersen J C (1967). “An inverse GLC (Gas Liquid Chromatography) study of asphalt used in Zaca Wigmore experimental road test.” Proc. Assoc. of Asphalt Paving Technologists (AAPT), Vol. 36, pp. 1-15.

[6] Dickinson E J (1980). “The hardening of Middle East petroleum asphalts in pavement surfacing.” Proc. Assoc. of Asphalt Paving Technologists (AAPT), Vol. 49, pp. 30-63.

[7] Kumar A and Goetz W H (1977). “Asphalt hardening as affected by film thickness, voids and permeability in asphaltic mixtures.” Proc. Assoc. of Asphalt Paving Technologists (AAPT), Vol. 46, pp. 571-605.

[8] Coons R F and Wright P H (1968). “An Investigation of the Hardening of Asphalt Recovered from Pavements of Various Ages.” Proc. Assoc. of Asphalt Paving Technologists (AAPT), Vol. 37, pp. 510-528.

[9] Ali, M. K., and Imbarek;, M. O., "Hardening and Aging of Bituminous Materials in Hot and Arid Regions", the 4Th European Symposium on the Performance and Durability of Bituminous Materials and Hydraulic Stabilized Composites", Nottingham, England, 11th/12th April 2002.

[10] Ali, M.K. “Tensile Behavior of Bitumen in Thin Films” Proceedings of Italian Infrastructure Conference, Parma, Italy, October, 2002

[11] Hend Ali Omar and et al "The Effect of Ageing on Chemical and Strength Characteristics of Nano clay – Modified Bitumen and Asphalt Mixtures", Applied Sciences Journal, Switzerland, July, 2021

[12] Mohamed K.A. Ahmed and Khalid Musa " Performance Tests on Styrene – Butadiene – Styrene (SBS) Polymer modified on Asphaltic Concrete Mixtures", The 4th International Conference on Welding and Failure Analysis of Engineering Materials, November 19-22, 2018, Aswan, Egypt

Evaluation of Compressive Strength of Concrete using Wood ash and Metakaolin as partial replacement for Cement

A.M.Akash[1] , A.A.Alhaddad[2] and H.M.Alamin[3]

[1]Professor at Civil Engineering Department, Wadi Alshatti University, Libya, confcivil3@gmail.com

[2] Assistant lecturer at Civil Engineering Department, Wadi Alajal Higher Institute of Science and Technology, Altaher772011@gmail.com.

[3] Assistant Lecturer at Civil Engineering Department, Sebha University, hamzasellam80@gmail.com

Abstract

Minimizing of energy consuming associated with cement industrialization operation could be a great opportunity to decrease CO_2 emission. Therefore, utilization such of agricultural waste in construction material has shown a good engineering method to reduce emission of CO_2. It considers another solution instead of disposal agricultural waste to landfill. Wood ash (WA) is one of agricultural waste and pozzolanic materials have shown a significant advantage when it used as constituent material in during the production of structural grade concrete. The aim of this study is to investigate the effect of Metakaolin (MK) on compressive strength developments of concrete containing WA. To attain the objectives, a normal strength concrete is designed as control mix. Total 5 batches of concrete mix were formulated: which includes of cement proportion in comparison to control mixture. Water-to-binder ratio of 0.45 and 0.50 were used in this study. Wood ash (WA) was replacement by 20% or 30% to cement and Metakaolin (MK) was constant at 10%. It was observed that wood ash decrease workability and water demand. Increased 30% WA showed reduction in strength. However, the presences of Metakaolin enhance properties of WA blended cement concrete in term of compressive strength. Wood ash 20% replacement in binary mixture shows slightly reduction in comparison to net OPC but, achieved target strength of 40Mpa. For ternary mix with 20% WA shows slightly improved strength than net OPC at 28 days. All binary and ternary mix by 20% WA achieved target strength of 40 MPa.

Keywords: Wood ash, Metakaolin, Compressive strength, CO_2 emission

1- Introduction

Utilization of concrete since a long time became the most extensive all over the world. It used as construction material which drives to environmental concern in term of operation of raw material and emission of CO_2. Portland cements are the more common hydraulic cements and the most important in construction. On the other hand, the development of technology and countries led to require more and more tons of concrete to be used in their construction industry. The production of cement manufacture emits roughly one ton of CO_2 for each ton of cement produced, therefore, it makes up 7% of all CO_2 release to the atmosphere [1]. To solve this issue is to reduce cement production with interaction waste material. Utilization of waste materials has become efficient sources to replace as partial cement in concrete, for the time being utilization of such wood ash and Metakaolin and other pozzolanic is a promising material and favorite research in cement and concrete field. In this regard, few researches have been published utilization of wood ash in presence of Metakaolin as blend to cement concrete.

1.1 Wood ash

Wood ash as by-product is generated during the combustion of wood products of energy production at pulp, paper mills, sawmills and wood product industrial facilities. Wood ash is classified under combustion temperature approximately more than 850^0C into two major forms bottom ash and fly ash. Bottom ash collected from the bottom of the burner whereas fly ash accumulates in the smoke stack filter. Both of them have different physical and chemical characteristics [2]

1.2 Metakaolin

MK is pozzolanic material used as an admixture to increase the strength and durability of structural concrete as well as to reduce the shrinkage and creep [3]

2 .Research Methodology

The experimental programme was planned to study properties of the materials used such as the maxing procedure and the test methods followed in conducting different experimental investigation for this research. The compressive strength characteristic of blended cement concrete includes Metakaolin (MK) and wood ash (WA) is the main parts of this study to identify the optimum mix proportion and present the mixing as well as test procedures for the blended cement concrete specimens with WA and MK.

To achieve the main goals of this study, a normal strength concrete of grade 40 with the specified characteristic strength of 40 MPa at 28 days is formulated as the main control mix. A total of 18 mixtures were prepared; which include of cement combination comprising Ordinary Portland Cement (OPC) Class CEM 1 42.5N with various percentage replacement of Wood Ash (WA) at 20% and 30% by weight. A third component is MK, which is further, used to replace to cement at constant percentage of 10% by weight, Chemical and Physical Characteristics of OPC, MK and Ternary Wood Ash as shown in Table 1.Coarse and fine aggregate are different weight at different water to cement ratio. Water to cement ratio are different at 0.35, 0.45 and 0.50. Superplasticizer dosage is utilized with varying percentages to achieve targeted slump of (50- 90 mm). Compressive strength for 3,7 and 28 days age cubes.

2.1 Cementations Material

2.1.1 Ordinary Portland Cement

OPC type 1 class 42.5N as classified according to the ASTM C 150 is used [4].

2.1.2 Wood Ash

Raw wood ash (WA) use for this study was collected from Excel Potry (M) Sdn Bhd, Pusat Industri Seramik, Chemor Perak, Ipoh, Malaysia after burn at temperature approximately 800 ^{0} C.

2.1.3 Metakolin

MK powder is used in this study supplied by local industry.

2.1.4 Superplasticizer

Superplasticizer a Master GLENIUM ACE 8109 as was used in this study to improve the workability of blended concrete.

2.1.5 Aggregate

Fine aggregate used is natural sand and the coarse is crushed aggregate, the aggregates are conducted according to BS 812 part (103) [5]. All aggregate were air dried in the laboratory prior to use in concrete.

Table 1. Chemical and Physical Characteristics of OPC, MK and Ternary Wood Ash

Property	OPC[a]	WA[b]	MK[c]
CaO%	56	29.53	0.08
SiO_2 %	20.5	28.11	50.08
F_2O_3 %	4	2.91	1.62
Al_2O_3 %	6.6	5.14	34.03
SO_3 %	2.28	0.97	2.8
Na_2O %	0.14	0.32	0.09
MgO %	3.9	5.14	3.9
K_2O %	0.69	9.64	2.79
Cl %	-	0.10	-
LOI %	1.63	1.87	0.08
SG	3.15	2.40	2.45
Specific surface (m^2/g)	0.778	0.538	1.6

2.2 Mix proportion

The concrete mix is conducted using (DoE) method. (DoE is British method used for the design of concrete, using cement and aggregate which conform to relevant British Standard)[1].The control mix design is based on characteristic strength of 40 MPa at 28 days with target slump of class S2 of (50-90mm) according to BS EN 12350-2 [6] water to cement binder is not fixed are 0.35, 0.45 and 0.50 and their corresponding of cement contents are 633Kg/m^3, 422 Kg/m^3 and 390 Kg/m^3 respectively. A total of 18 mixtures are prepared. Three of them are prepared as control mixtures with content of cement. The mixing phase is conducted according to BS EN2390-3 [7] at engineering material laboratory of concrete at University of Putra Malaysia. Electrical rotary drum mixture is used for this study**.** Concrete cubes of 150 mm × 150 mm × 150 mm are used. The mould is assembled before mixing and properly fixed also lubricant for easy removal of hardened concrete specimens. Concrete cubes are prepared in percentage replacement by weight of cement to WA and MK as showed in Table 2.

Table 2: Concrete Mix Proportion

Name	Cementation materials						Water	Aggregate	
	OPC		WA		MK			CA	FA
	%	Kg/m^3	%	Kg/m^3	%	Kg/m^3	Kg/m^3	Kg/m^3	Kg/m^3
W/C	0.35								
$M.C_1$	-	543	-	-	-	-	190	987	808
M_1	80	434.4	20	108.6	-	-	190	987	808
M_2	70	380.1	30	162.9	-	-	190	987	808
M_3	70	380.1	20	108.6	10	54.3	190	987	808
M_4	60	325.8	30	162.9	10	54.3	190	987	808

W/C	0.45								
$M.C_2$	-	422	-	-	-	-	190	987	808
M_5	80	337.6	20	84.4	-	-	190	987	808
M_6	70	295.4	30	126.6	-	-	190	987	808
M_7	70	295.4	20	84.4	10	42.2	190	987	808
M_8	60	253.2	30	126.6	10	42.2	190	987	808
W/C	0. 50								
$M.C_3$	-	390	-	-	-	-	190	987	808
M_9	80	312	20	78	-	-	190	987	808
M_{10}	70	273	30	117	-	-	190	987	808
M_{11}	70	273	20	78	10	39	190	987	808
M_{12}	60	234	30	117	10	39	190	987	808

2.3 Test on Fresh Concrete

Slump Test

The slump test is evaluating the matchmaking of fresh concrete. The test is conducted according to BS EN 12350-2:2002[6]

2.4 Test on Hardened Concrete

Compressive Strength Test

The compression test is conducted according to BS 1881-116:1983 [8]. These specimens are tested by compression testing machine after 3, 7 and 28 days. From every batch there were three specimens tested and the average strength is recorded.

3. Result and Discussion

Chemical property of wood ash is important criteria governing its appropriateness for utilize as Pozzolanic material in blended cement and concrete. ASTM C618, (1998) defines Pozzolanic as a siliceous and aluminums material which operates little or no cementitious characteristics. However, in finely it may react with Portlandite from hydration of cement. Therefore, the presence of significant quantity of silica, aluminum and iron oxide compounds in wood ash of finely divided powder is compulsory in order to qualify as Pozzolanic. From XRF analysis results that the total content of silicon dioxide (S_iO_2), aluminum oxide (Al_2O_3) and iron oxide (Fe_2O_3) was approximately 36.16% which was less then minimum of 50% specified in ASTM C 618, (1998) class- C. The main oxide phases of wood ash in decreasing in comparison of Metakaolin were the sum of S_iO_2, Fe_2O_3 and Al_2O_3 compounds was approximately 85.65% which is greater than the minimum of 70% specified in ASTM C 618, (1998). Thus, confirming that the Metakaolin was more reactive. Table 3 is shown the sum of main components of WA in comparison to other finding.

Table 3: Sum of Main Components of Wood Ash

Researches	Sum of Main Components	Percentage %
Current Research	(S_iO_2+ Al_2O_3+ Fe_2O_3)	36.16
Elinwa et al. 2005	(S_iO_2+ Al_2O_3+ Fe_2O_3)	85.65
Rajamma et al. 2009	(S_iO_2+ Al_2O_3+ Fe_2O_3)	52.9
Elinwa & Mahmood, 2002	(S_iO_2+ Al_2O_3+ Fe_2O_3)	73.55
Udoeyo & Dashibil, 2002	(S_iO_2+ Al_2O_3+ Fe_2O_3)	80.66
Elinwa & Ejeh, 2004	(S_iO_2+ Al_2O_3+ Fe_2O_3)	73.55
Abdullahi, 2006	(S_iO_2+ Al_2O_3+ Fe_2O_3)	62.14

Wood ash is reported to consist of a heterogeneous mixture of variable size particles which are generally angular in nature. These particles were unburned or partially burned. In terms of fineness, average amount of wood ash passing sieve (75um) and retained on sieve (45um) was 60%. The specific gravity of wood ash specimen was investigated to be 2.40.

Particular size distribution (PSD) is done to evaluate the distribution of particles and determinate the fineness of each material is used in this study. Material finesse include of distribution curve of particles over range of size, median size of particle and specific surface area. Table 4 is epitomizes the specific surface area (SSA) in (m^2/g) and median size in (um) of Ordinary Portland cement OPC, WA and MK.

Table 4: Specific Surface Area (SSA) and Median size of OPC, Wood ash and Metakaolin

Material	**OPC**	**WA**	**MK**
SSA (m^2/g)	0.778	0.538	1.6
Median size (um)	22.5	48.146	5.645

Comparison in distribution curve of particles over range of size material for ternary WA were shown in figure 1. Commonly, most of material shows to have wide distribution of particular and consider between (< 3μm) and oversized particular (> 100 μm). This is fact due to the material has subjected commination operation of crushing or grinding mechanism increase the finesses of material. Moreover, these materials also are desired to have good reactivity to hydration process and reversed in good fresh concrete workability and good in compressive strength development. Finesses material led to increase water demand due to higher surface area. Perceiving the particular size distribution is essential to come up with good understanding the reactivity of these material and packing effect that could occur as result of non-homogeneous behavior inside concrete matrix.

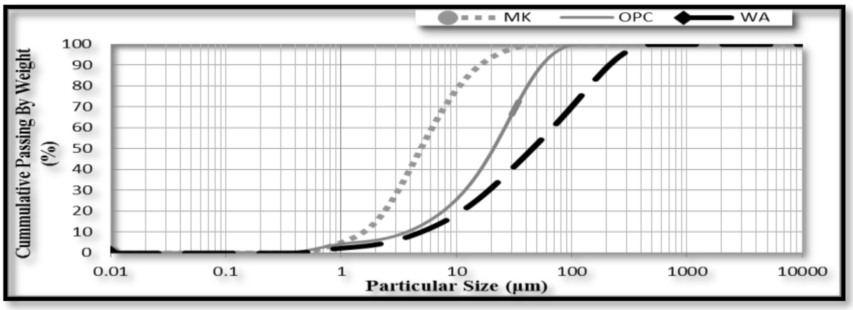

Figure 1: Particular Size Distribution for OPC, Wood Ash and Metakaolin

Also Figure 1 shows the results of sieve analysis of WA, OPC and MK. The result shows that wood ash include 48.146 um which is less than 75um (No.200 sieve) whereas OPC and MK slightly less than WA includes 22.520 um and 5.612 um respectively which is less than 25um (No.500 sieve). The corresponding surface area of WA investigates to be relatively is less than OPC and MK which includes 0.538, 0.778 and 1.6 m^2/g respectively. Thus, results demonstrate that wood ash particles are large in comparison to OPC and MK due to in generally is an angular in natural. On the other hand, SSA of WA relatively is less than OPC and MK the possible concluded that WA particles depend on wood type and temperature effect where carbon is less or large on surface area. Moreover, beside on distribution curve of particular over range of size material, specific surface area and porosity of WA shows significantly less than other finding whereby [9][10][11] in common concluded that wood ash consists of particles which are highly irregular in shape with a highly porous surface area. And also they concluded that although the biomass is burnt under sufficiently high temperature between 750°C to 1000 °C in the furnace, there is always some inefficiency on carbon conversion due to kinetic and mass transfer limitations. Their corresponding of results of specific surface area of WA is listed on table 5 in comparison to current research.

Table 5: Result of Specific Surface Area of Wood Ash Compare to Other Research

Researches	**Specific Surface Area m^2/g**
Current research	0.538
Nike et al. 2003	150
Rajamma et al. 2009	40.29 - 7.92

Based on the results shown in figure 2, Binary WA mix by 30% cement replacement indicates the reduction in strength in comparison to net OPC. The reduction value of 30% WA was 43% at 28 days curing time. The corresponding compressive strength obtained was 26 MPa, while control mix has compressive strength by 45.49 Mpa at same curing; when water to cement binder was 0.50. It is observing that at early ages, WA blended concrete shows lower strength than control. This reduction is due to the lower cement content of the binary WA concrete in comparison to control which generates less secondary calcium silicate hydrate (C-S-H) gel. Also, due to slow reactivity of pozzolanic which requires more curing time to react and improve compressive strength of binary mixture at later ages.

A common finding whereby wood ash decrease strength when increase WA content was reported by [12]. They also concluded that due to the mechanism that wood ash particles act more like filler material within the cement paste matrix than as binder cement. In addition, [13][14][15] in common concluded that wood ash as a partial cement replacement material in concrete at level of cement replacement by 30% WA it reduced the compressive strength of the concrete mix produced relative to control OPC concrete for all ages time. On the other hand, binary WA mix by 20% cement replacement demonstrates decline in compressive strength by 13% in comparison to net OPC value for 28 curing time. WA20% has compressive strength of 39.79 MPa when water to cement ratio is 0.50. Despite of the reduction of WA 20%, however, it achieves target design strength of 40MPa at 28 curing time. This achievement in the compressive strength of concrete with WA 20% content as early as 28 days was attributed to the micro filler effect of the super fine particles of wood ash which contributed to the denser packing of the concrete matrix. Hence, binary 20% WA observed to achieve target strength of 40 MPa and had a higher rate of compressive strength gain for concrete mix with wood ash content when binder to cement ratio is 0.50 and similar trend of strength was found when cement to water ratio were 0.35 and 0.45.

Figure 2: Compressive Strength Development of Binary Wood Ash

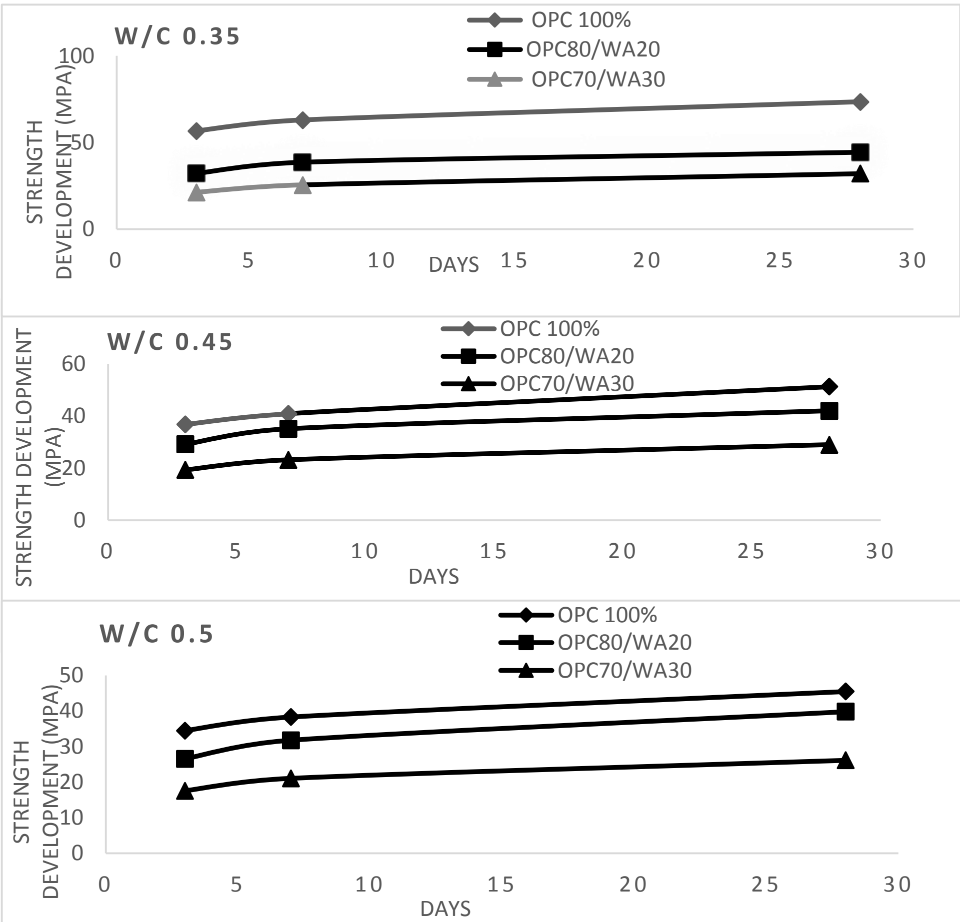

Ternary wood ash mix by 30% and 10% Metakaolin cement replacement shows the reduction in strength in comparison to net OPC. The reduction value was 22% at 28 days curing time. The corresponding compressive strength obtained was 35.40 MPa, while control mix has compressive strength by 45.49 MPa at same curing; when water to cement binder was 0.50. The increment in strength of ternary WA 30% in comparison to binary 30% WA was 36%. Thus, results demonstrate that Metakaolin increased the early strength of the concrete than early-age loss of strength due to the slow process of hydration when WA alone. A common finding whereby [16] endeavored to enhance compressive strength of wood ash concrete by the including trace amount of MK as an additive in the concrete mixes. Results indicated that the inclusion of Metakaolin though at small trace, contributed to enhance of an early rate of compressive strength gain of wood ash concrete.

Ternary WA mix by 20% WA cement replacement shows slightly enhancement in strength in comparison to net OPC. The compressive strength obtained was 46.73 MPa, while control mix has compressive strength by 45.49 MPa at same curing; when water to cement ratio was 0.50. This improvement is due to the silica provided by 20% WA and 10% MK was adequate to react with the calcium hydroxide Ca(OH)2 produced by the hydration of cement [17]. Hence, ternary 20% WA observed to achieve target strength of 40 MPa and significantly had a higher rate of compressive strength gain than net OPC and 30% ternary WA for all concrete mix when binder to cement ratio is 0.50 and similar trend of strength was found when cement to water ratio were 0.35 and 0.45as shown in figure 3.

Figure 3: Strength Development of Ternary WA blended Cement Concrete.

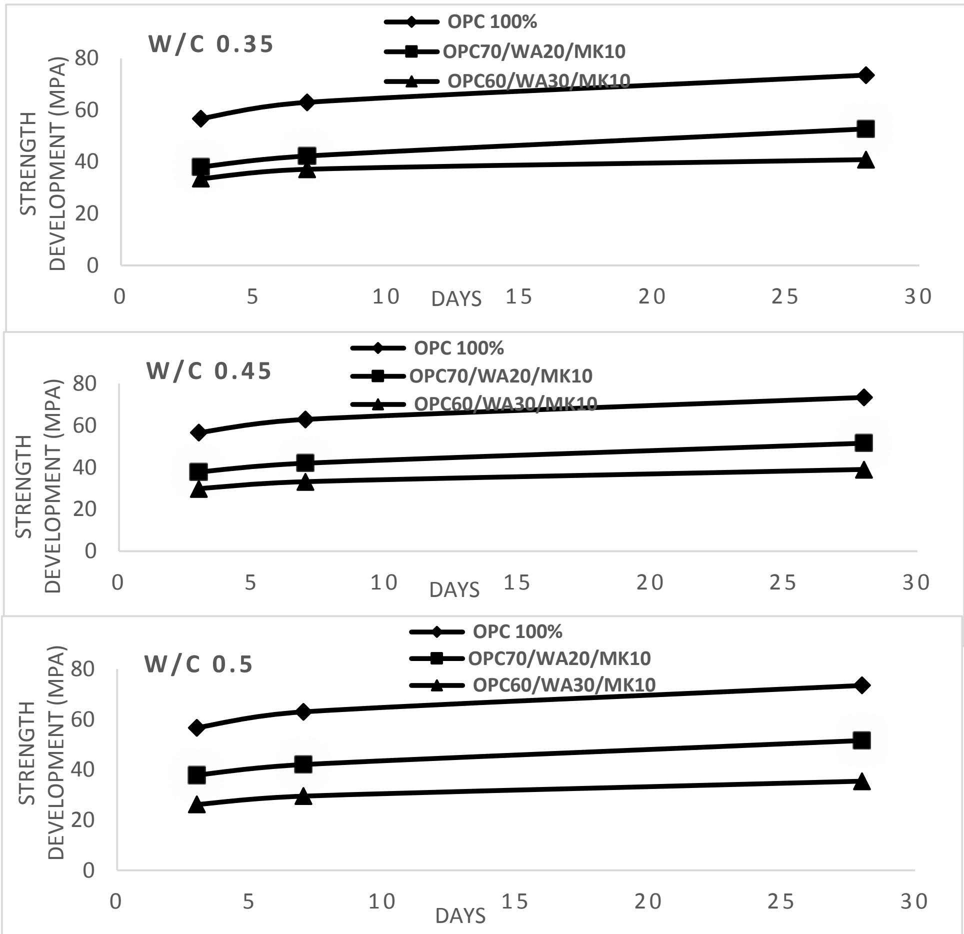

4 .Conclusion

As indicated to the results obtained throughout the laboratory investigation, the following conclusions can be derived:

1) Loss of ignition results of wood ash was found to be 1.87% which is less carbon compare to other research.

2) Particle size distribution of wood ash (WA) is basically coarser in comparison to ordinary Portland cement (OPC) but, specific surface area of wood ash is relatively less than OPC and MK and was found to be 0.538 m^2/g.

3) Wood ash has higher water demands to achieve a given level of mix workability as compared to equivalent neat OPC mixtures whereas SP dosage requirement increase to enhance favorable workability level.

4) In general, compressive strength development of binary WA 30% blended cement concrete demonstrated decline in comparison to the net OPC 100% was found to be 43% whereas binary 20% WA showed slight reduction in comparison to the blank OPC was found to be 13% where water to cement ratio was 0.50 at curing 28 days, however, it achieves target design strength of. Thus, wood ash content of about 20% can suitable to be used in structural application.

5) Compressive strength development of ternary WA 30% blended cement concrete demonstrated slightly reduction in comparison to the net OPC was found to be 22% where water to cement ratio was 0.50 at curing 28 days whereas ternary WA 20% reveal slight improvement than blank OPC. This improvement was due to Pozzolanic reactivity and filler impacts of superfine of Metakaolin which enhances the concrete at early age. Furthermore, the silica provided by 20% WA and 10% MK had good reaction with the calcium hydroxide produced by the hydration of cement. Thus, the optimum strength obtained by ternary WA 20% can suitable to be used in structural application as well.

5. Recommendation

Further investigation on this research can improve recent laboratory works in future study

1) Wood ash used in this study is a slightly pozzolanic in comparison to other research, therefore, it is of interest for future study to investigate WA has higher pozzolanic to evaluate the chemical and physical properties of wood ash.
2) Finding suitable mix proportion of the ternary blended concrete that could improve strength development in comparison to net OPC.

6. References

[1] Mehta, P. Kumar, and Paulo JM Monteiro. (*Concrete: microstructure, properties, and materials)*. McGraw-Hill Education, (2006).

[2] Siddique, Rafat. (Utilization of wood ash in concrete manufacturing). *Resources, conservation and Recycling* 67 (2012): 27-33.

[3] Srinivasu, K., M. L. N. K. Sai, and N. Venkata Sairam Kumar. (A review on use of metakaolin in cement mortar and concrete). *International journal of innovative research in science, engineering and technology* 3.7 (2014): 14697-14701.

[4] Standard, A. S. T. M. (C150: Standard Specification for Portland Cement) *Annual Book of ASTM Standards* (2009).

[5] No, Amendment.(Specification Methods for determination of particle size distribution). BS 812-103.1: (1985).

[6] En, B. S. "12350-2" (Testing fresh concrete. Slump-test). *British standards* (2009).

[7] Standard, British. "BS EN 12390-3: 2009 "Testing hardened concrete.(*Compressive strength of test specimens). London, UK: British Standard Institution* (2009).

[8] Standard, British. " Bs 1881-part-116-83 (Testing of determination of compressive strength of concrete cube*) London, UK: British Standard Institution* (1983).

[9] Naik, Tarun R., Rudolph N. Kraus, and Rafat Siddique. (Demonstration of manufacturing technology for concrete and CLSM utilizing wood ash from Wisconsin.). *UWM Centre for By product Utilization* 538 (2002): 124.

[10] Wang, Shuangzhen, Larry Baxter, and Fernando Fonseca. (Biomass fly ash in concrete: SEM, EDX and ESEM analysis). *Fuel* 87.3 (2008): 372-379.

[11] Rajamma, Rejini, et al. (Characterisation and use of biomass fly ash in cement-based materials). *Journal of hazardous materials* 172.2-3 (2009): 1049-1060.

[12] Udoeyo, Felix F., et al.(Potential of wood waste ash as an additive in concrete). *Journal of materials in civil engineering* 18.4 (2006): 605-611.
[13] Abdullahi, M. (Characteristics of wood ash/OPC concrete). *Leonardo Electronic Journal of Practices and Technologies* 8 (2006): 9-16.
[14] Elinwa, Augustine Uche, and Yakubu Abba Mahmood.(Ash from timber waste as cement replacement material). *Cement and Concrete Composites* 24.2 (2002): 219-222.
[15] Elinwa, A. U., and S. P. Ejeh.(Effects of the incorporation of sawdust waste incineration fly ash in cement pastes and mortars). *Journal of Asian Architecture and Building Engineering* 3.1 (2004): 1-7.
[16] Elinwa, Augustine U., Stephen P. Ejeh, and Ibanga O. Akpabio. (Using metakaolin to improve sawdust-ash concrete). *Concrete International* 27.11 (2005): 49-52.
[17] Cheah, Chee Ban, and Mahyuddin Ramli.(The implementation of wood waste ash as a partial cement replacement material in the production of structural grade concrete and mortar: An overview). *Resources, Conservation and Recycling* 55.7 (2011): 669-685.

Influence of Spatial-related Factors on Hydraulic Performance of Compacted Clay Liners (CCLs) in Municipal Solid Waste Landfills: Southern Region of Libya as an Example

[1]Abdulghader A. Hassan and [2]Mohammad T. Rayhani

1 Lecturer, Department of Civil Engineering- Wadi Alshatti University, Brak Alshatti, Libya.

2 Professor, Department of Civil and Environmental Engineering- Carleton University, Ottawa, Ontario, Canada.

Abstract

Landfills have long been used for final disposal of municipal solid waste. They show efficient performance in waste containment assuming proper design and construction procedure of their elements. Compacted clay liner (CCLs) is one element that is widely utilized as a hydraulic barrier in landfills. CCL isolates the contaminants from the surrounding environment and regulates the migration of chemical leachate to the substrata. Prior to waste placement in landfills, CCLs are often exposed to temperature fluctuations inherited from the phenomena of daily thermal cycles. After waste placement, waste biodegradation takes place and is often accompanied with the production of chemical leachate and the release of high temperatures. Daily thermal cycles and the combined thermo-chemical exposures can both affect the hydraulic performance of the CCLs in the landfills in the short and the long term. In the region of southern Libya, the effects of daily thermal cycles and the combined thermo-chemical exposures can be multiple times higher than what can be experienced in temperate regions. The experimental results summarized in this paper showed that hydraulic conductivity of CCLs with low plasticity indices can be 8 times higher than the initial after exposure to 30 daily thermal cycles, while the CCLs with plasticity indices ranging from 25% to 37% showed minimal change in their hydraulic performance under the effects of thermal cycle effects. The exposure to chemical leachate was preferable by reducing the hydraulic conductivity by an order of magnitude. The rate of reduction due to leachate exposure, however, was less at higher internal landfill temperature.

Keywords: Compacted Clay Liner; Hydraulic conductivity; Temperature; Leachate; Landfill

1. Introduction

Compacted Clay Liners (CCLs) are hydraulic barriers featured with low permeability for applications where control upon flow of fluids is desired. Municipal solid waste landfills is one example where CCLs are used to minimize the migration of liquid contaminants to the surrounding such that a chemical pollution of soil and underground water is mitigated. Therefore, the functional integrity of landfills depends substantially on the hydraulic performance of the CCL barrier systems. The later, however, is prone to performance alteration due to exposure to environmental factors and/or functional conditions.

Prior to waste placement in landfills, CCL might be exposed to daily thermal cycles induced by solar radiation. The impact of solar radiation is multiple times higher when overlaying the CCL with geomembrane layer such as in the composite barrier systems. [12] recorded temperature readings underneath the geomembrane as high as 60°C. Therefore, CCLs in both barrier systems may experience desiccation cracking, volume shrinkage, and subsequently changes in hydraulic performance. High-temperature exposure leads to desiccation due to water evaporation, thus, generating voids within the soil matrix and increasing soil suction ([8], [11]). As a result, a reduction in the soil matrix volume, known as shrinkage, occurs. This shrinkage could induce volumetric change and crack formation in the soil matrix that may lead to a considerable increase in permeability of the CCL (e.g., [7], [9]).

After waste placement in landfills, chances of exposure to climatic factors are less; however, CCLs may still be exposed to elevated temperatures and chemical leachate from within the landfill. Landfill leachate is generated from the expulsion of waste moisture, percolation of surface water into the landfill, and decomposition of organic waste. On the other hand, biodegradation of the organic waste is often accompanied with significant heat release. Temperatures of 60 °C and 70 °C were recorded in landfills in Germany [3] and Japan [14] 10 years and 6 years post-closure respectively. Previous case studies in North America have also shown temperatures higher than 55 °C at the bottom of the landfill close to the liner (e.g., [5], [10], and [13]). These temperature conditions may affect the hydraulic conductivity of the CCLs by decreasing the leachate viscosity and inducing micro-cracks.

Landfill leachate exposure may also cause changes in the soils' chemical composition ([1], [2], [4]), mineral composition, and physical properties (i.e. Atterberg limits) of clay liners ([6], [4]).

Following these changes, the hydraulic performance of the treated clay might change. Cation Exchange Capacity (CEC), thickness of the double layer, and mineral composition were the parameters used to assess the effect of landfill leachate on the hydraulic performance of clay barriers.

This study is devoted to evaluating the effects of daily thermal cycles and thermo-chemical exposures on the hydraulic performance of CCLs simulating field conditions of landfills before and after waste placement respectively.

2. Soil and leachate properties

2.1 Soil properties

Two native clayey soils and two clayey soil mixtures were used in this study for constructing CCLs samples. The native soils are marine clay know as Leda clay, and a clay till known as Halton till. The two mixtures, on the other hand, were achieved by mixing Leda clay with 5% sodium bentonite and Halton till with 10 % sodium bentonite to attain variety in the plasticity index of the soil specimens. The basic geotechnical properties of the four clayey soils including particle size distribution, Atterberg limits, metric suction potential and the optimum water content were determined and presented in Table 1.

A chemical analysis was performed on the extracted pore waters obtained by squeezing the soil samples under high pressure. Cation concentrations including potassium, calcium, and magnesium ions were determined in the pore water (mg/l), while sodium concentration was measured based on acid extractable sodium ions (mg/kg). Cation exchange capacities (CEC) were determined and the results presented in Table 1.

Table 1. Physical and chemical properties of the test soils.

Characteristics (%)	Halton till	Leda clay	Halton + Bent.	Leda + Bent.
Soil classification	CL	CH	CL	CH
Liquid limit	23.5	50.8	43.5	60.0
Plasticity index	9.5	23.3	25	37.2
qd (Max.), kg/m3	1700	1410	1560	1270
Gravimetric water content	13.5	30	17	34.5
Shrinkage limit	16.0	22.5	18.1	24.4
Shrinkage index	7.5	28.3	25.4	35.6

Clay content	24	71	34.0	76
Activity	0.4	0.33	0.83	0.5
Sodium (mg/kg)	160.0	1700	-	-
Potassium (mg/l)	6.0	15.0	-	-
Calcium (mg/l)	721.0	83.0	-	-
Magnesium (mg/l)	25.0	40.0	-	-
(CEC)a meq/100 g	67.0	18.0	-	-

2.2 Soil Leachate properties

The chemical composition of the synthetic leachate used in this study is summarized in Table 2. This synthetic leachate was made based on the chemical analysis of a leachate sample extracted from the Keele Valley Landfill in Ontario, Canada.

Table 2. Composition of synthetic leachate and trace metal solution.

Leachate component	(mg/l)	Leachate component	(mg/l)
Acetic acid (ml/l)	7	NaNO3	50
Propionic acid (ml/l)	5	K2CO3	324
Butyric acid (ml/l)	1	KHCO3	312
NaHCO3	3012	K2HPO4	30
CaCl2	2882	Trace metal solution⁄ (ml/l)	1
MgCl2.6H2O	3114	Surfactant, Igepal CA720 (ml/l)	5
MgSO4.7H2O	319	pH (adjusted by adding either NaOH or H2SO4) (–)	6
NH4HCO3	2439	Eh (adjusted by adding 3% w/v Na2S_9H2O) (mV)	-120
CO(NH2)2	695		

3. Experimental program

3.1 Experimental cells and specimen preparation

Cylindrical Plexiglas cells were used to prepare compacted soil specimens with dimensions of 140 mm in diameter and 150 mm in height simulating a typical CCL profile in landfills. Prior to soil compaction, rubber membranes were stretched inside the cells to eliminate the effect of side-wall leakage during saturation and leachate permeation (Fig. 1). Bulk samples of Halton till and Leda clays were oven-dried at 105 °C for 24 h and pulverized to pass through a No. 4 sieve. Leda clay + 5% bentonite and Halton clay + 10% bentonite mixtures were obtained by adding 5% and 10% sodium bentonite to Leda and Halton clay powders respectively. All four soil types were then hydrated up to 2% above their optimum moisture contents. A water sprinkler and a mechanical mixer were used for mixing and hydration of the soils to achieve uniform mixtures and eliminate water heterogeneity. The hydrated soils were then allowed to cure in airtight plastic bags for at least 48 h to ensure uniform moisture distribution. The hydrated soils were then compacted into the test cells in three layers to obtain at least 95% of their maximum dry densities. At each compaction layer a sample of soil was obtained to measure the moisture content of the soil throughout the cell. Non-woven geotextile fabrics were placed on the top and bottom of the soil specimens for uniform permeant distribution. The specimens were eventually sealed using upper and lower aluminium lids (Fig. 1).

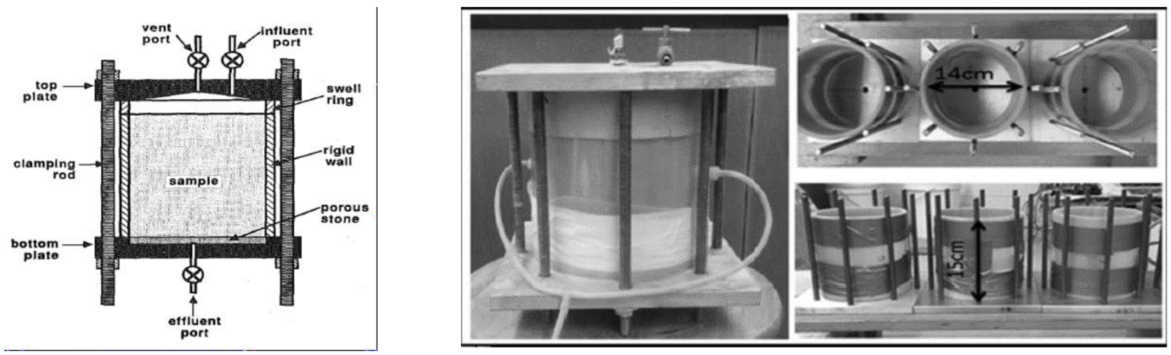

Fig. 1. Rigid-wall permeameter cross section and dimensions of test cells.

The upper lids were manufactured with influent and venting ports, whereas the lower lids featured effluent ports in order to enable the permeant to move throughout the soil columns. Upon saturation, the falling head method was adopted to conduct saturated hydraulic conductivity tests using a rigid-wall permeameter based on the ASTM standard (ASTM D5856, 2007). Saturated hydraulic conductivity tests were performed on the test samples initially and after exposure daily thermal cycles as well as after exposure to combined thermos-chemical effect. Each exposure condition had dedicated set of soil samples.

3.2 Application of exposure conditions

CCL forms the foundation of the landfills and often is constructed over a wide area of the landfill, relatively, wider than the area that will initially receive the waste. Thus, its lift exposed to weather conditions for a good time before being covered with waste. In the composite linear system, CCLs are covered with a layer of geomembrane during this time. In both cases, however, CCLs will be exposed to heat-cool cycles inherited from the successive sunlight and nighttime. Heating period is longer and more intense during summer time, particularly in areas with desert climate such as the southern part of Libya. In this experiment, the heat waves were imposed onto the CCLs samples to study the change in their hydraulic performance. A heating blanket has been used to generate the temperature on top of the test samples. The blanket was connected to a temperature controller to apply 55 °C (± 1 °C) on the soil surface for 8 h simulating the daylight period. The heater was then shutdown for 16 h to simulate overnight cooling. The test samples were removed from the heat-cool system for volume measurements and saturated hydraulic conductivity testing after different exposure periods (15, 30, 45, and 60 days). The experiment considered both scenarios namely CCL with geomembrane cover and CCL without geomembrane cover as shown in Fig. 2a&b.

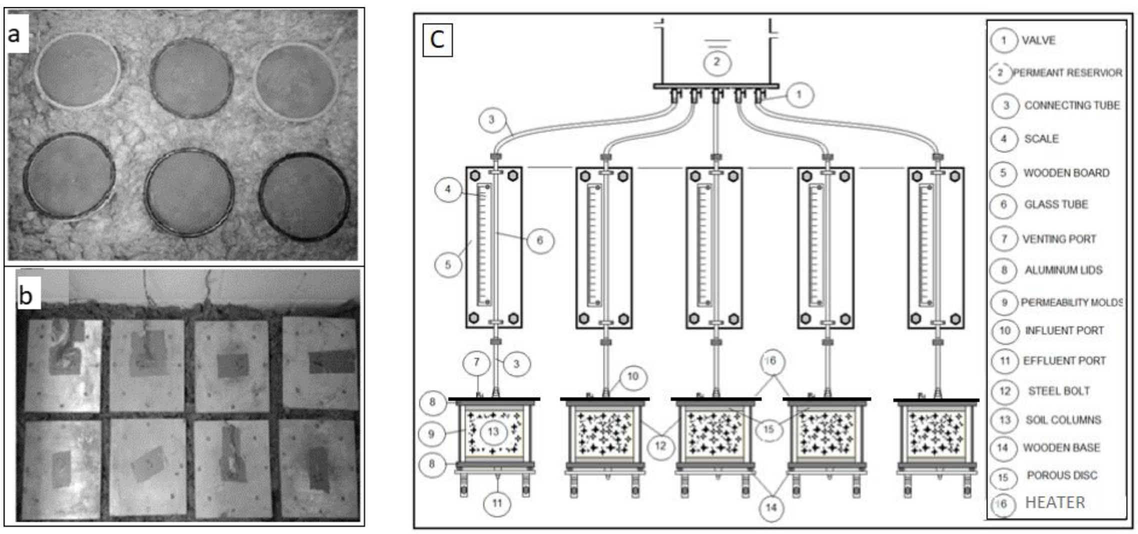

Fig. 2. a) Thermal cycles on CCL samples without simulated geomembrane. b) Thermal cycles on CCL samples with simulated geomembrane, c) Thermo-chemical exposure and hydraulic conductivity measurement setup.

After waste placement in landfill, CCL will be entering another stage of exposure resulted from waste biodegradation and moisture migration into and from within the landfill. This combination of thermo-chemical exposure has been simulated by simultaneously exposing the CCLs samples to chemical leachate and temperature in the lab as illustrated in Fig. 2c.

4. Results and discussion

4.1 Effect of daily thermal cycles on CCLs hydraulic conductivity

Heat-cool cycles have induced volumetric shrinkage to all test samples causing reduction in samples' heights and diameters and forming cracks. The volumetric shrinkage and crack dimensions was directly proportional to the number of thermal cycles and plasticity index, where increasing plasticity index and number of thermal cycles have increased the percentage of the volumetric shrinkage. For high plasticity soil (PI =37.2), volumetric shrinkage recorded 19.5% and 23.8% after 15 and 30 thermal cycles respectively. The medium plasticity soil recorded 14.1% and 19% volumetric shrinkage after 15 and 30 thermal cycles respectively. The low plastic soil recorded 7.4% and 13.6% volumetric shrinkage after 15 and 30 thermal cycles respectively. The soil with higher plasticity index contains higher optimum moisture content and a thicker double layer around the particles. Therefore, higher plasticity soil will lose greater amount of water upon dehydration, thus, showing higher volumetric shrinkage. Nevertheless, the soil with higher plasticity index experienced less change in their saturated hydraulic conductivity after exposure to heat-cool cycles. The initial saturated hydraulic conductivity as well as the saturated hydraulic conductivity after exposure to 15 and 30 daily thermal cycles are presented in Fig. 3. The saturated hydraulic conductivity after daily thermal exposure was generally higher than the initial value for all test samples. The change in hydraulic conductivity due to thermal exposure is expressed by the normalized hydraulic conductivity (Kr), where the measured hydraulic conductivities at set intervals of thermal exposure were normalized by their initial values (Fig. 4). The hydraulic conductivity value for Halton clay (PI = 9.5%) increased from 8.3 x10^{-10} m/sec to 4.7 x10^{-09} m/s after exposure to 15 daily thermal cycles. The normalized hydraulic conductivity (kr) was 5.8 representing more than half an order of magnitude increase in the hydraulic conductivity at the end of 15 thermal cycles for this soil. Further increase in hydraulic conductivity was recorded after 30 daily thermal cycles reaching approximately one order of magnitude with a kr value of 8.

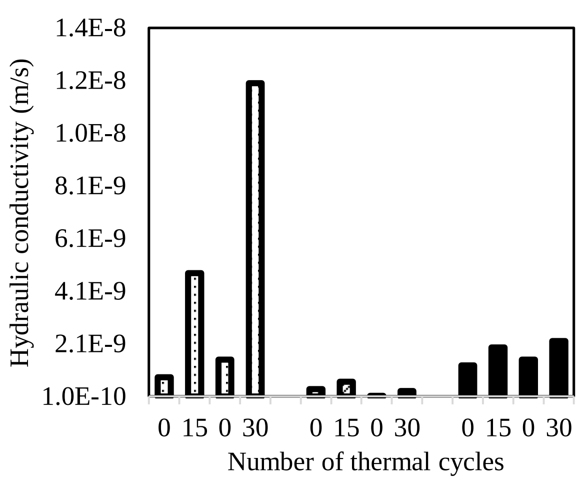

Fig. 3. Changes in hydraulic conductivity under thermal cycles

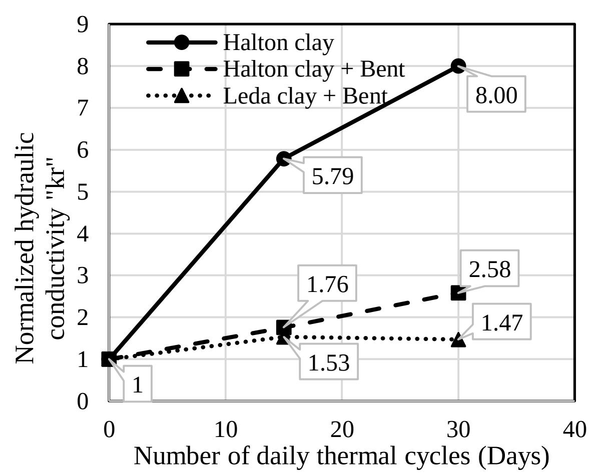

Fig. 4. Normalized hydraulic conductivity (kr)

However, such deterioration in hydraulic performance was not observed in medium and high plasticity soils even after exposure to 30 thermal cycles. Leda clay + bentonite and Halton clay + bentonite maintained almost constant hydraulic performance even though they underwent greater volume deformations. Their normalized hydraulic conductivity values after exposure to 30 thermal cycles were 2.58 and 1.47 for medium and high plasticity soils respectively (Fig. 3b). Their steady hydraulic performance against thermal cycles could be related to their self-healing that is often manifested in clays with higher plasticity indices. Such clay soils contain expandable interlayers that have the ability to absorb large quantities of water, increase their volume, and seal most of the cracks and fissures upon wetting. Clays with medium or high plasticity may not be always available for landfill liner and clays with low plasticity could be prevalent at the area of construction. The question in this case: Can low plasticity clays be used for landfill liners and ensuring better performance against thermal cycles? The answer is "yes" and the evidences are presented in Fig 5. The use of geomembrane layer on top of the CCL samples have shown to provide good protection against desiccation and deterioration of hydraulic conductivity. After 30 thermal cycles, Halton clay (low plasticity clay) experienced about one order of magnitude increase in its hydraulic conductivity when geomembrane was not used. However, when geomembrane overlaid the CCL, Halton clay showed significantly lower variation in hydraulic conductivity and maintained constant hydraulic performance even after exposure to 60 thermal cycles. Similar behaviour was recorded for the CCL made of Leda clay + Bentonite.

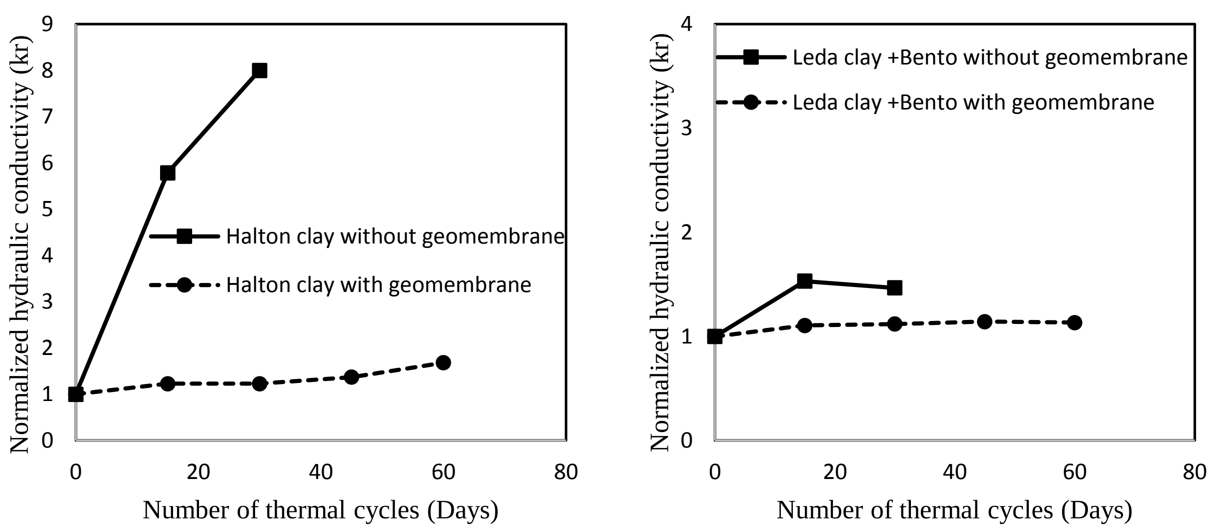

Fig. 5. Reduction of thermal cycles effects on CCLs by geomembrane installation.

When geomembrane installed on top of CCL, daily thermal cycles are found not to have any significant impact on the hydraulic performance of the CCL. These results underscore the importance of geomembrane installation in providing protection and sealing from weathering effects on CCLs. Geomembrane seemed to guarantee a lower moisture loss from the underline CCL. The atmosphere applies suction force in order to reach humidity equilibrium with the soil matrix. However, when a geomembrane overlays the CCL, there would not be an immediate exposure to the atmosphere, thereby diminishing the role of suction, preventing water movement out of the soil, and minimizing the risk of volume shrinkage and crack generation.

4.2 Change in hydraulic conductivity of CCLs due to thermo-chemical exposure

After waste placement in landfills, biodegradation of organic waste components would produce gases, liquid (landfill leachate), and heat (landfill temperature). CCLs as a part of the barrier system at the bottom of the landfill might be exposed to the combined effects of landfill leachate and elevated temperature, both of which could impact the hydraulic performance of the CCLs. Elevated temperature has been shown to increase CCLs hydraulic conductivities. In contrast, the landfill leachate has led to decreases in the CCLs hydraulic conductivities. However, the effects of simultaneous leachate and temperature exposure, which is more relevant to the actual field conditions, are not well understood. The combined effects of landfill leachate and temperature were investigated using 12 soil specimens exposed to three different temperature conditions (22 °C, 40 °C, 55 °C) while permeated with leachate. This combined thermo-chemical exposure was maintained for up to 75 days, with hydraulic conductivity readings recorded every 15 days for all specimens. Normalized hydraulic conductivity for each specimen was obtained by dividing the hydraulic conductivity reading at every set interval and certain exposure condition by the initial hydraulic conductivity of the specimen (Fig. 6). All trend lines in Fig 6 show a decrease in hydraulic conductivity over time due to exposure to the combined thermo-chemical effects. However, the hydraulic conductivity reduction exhibits an inverse relationship with temperature.

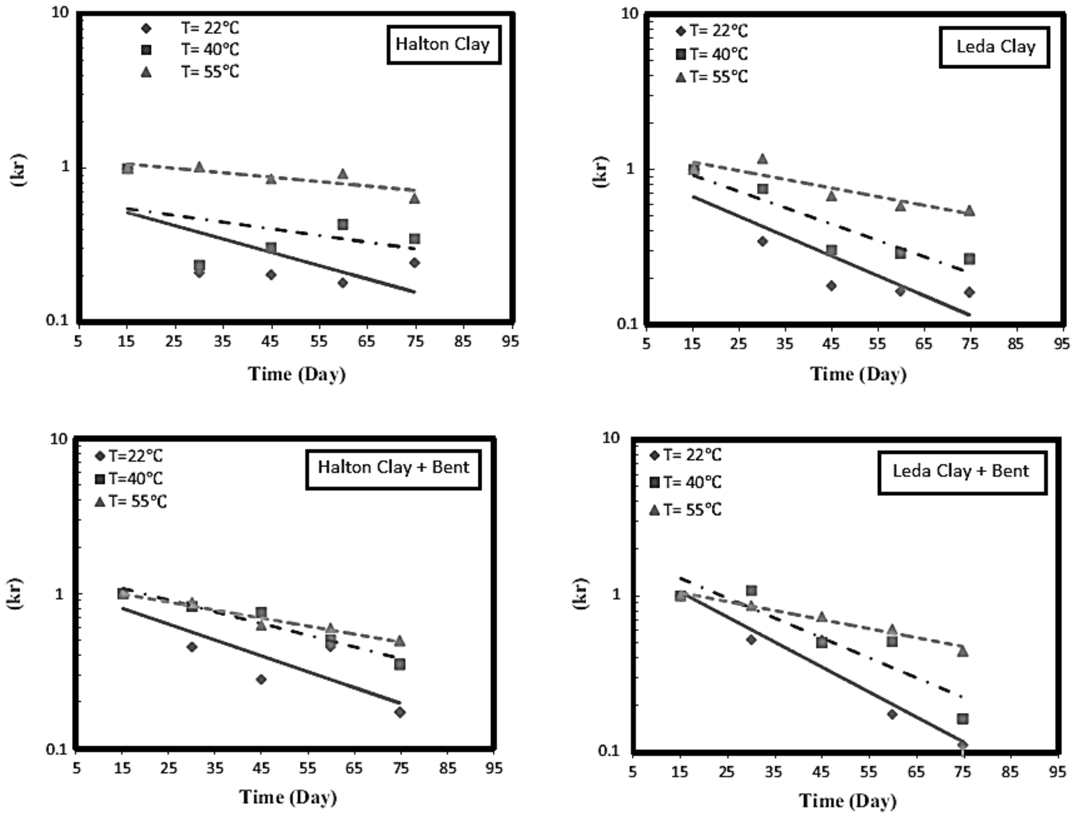

Fig. 6. Effect of thermo-chemical exposure on hydraulic performance of CCLs.

For all soil specimens, the rate of reduction in hydraulic conductivity decreases as the temperature increases from 22 °C toward 55 °C. The highest reductions in hydraulic conductivity occurred at lower exposure temperature (room temperature), while the lowest hydraulic conductivity reductions corresponded to the higher exposure temperature (55 °C). In other words, as the temperature increases, the final hydraulic conductivity of the soil specimens increases. This behaviour can be attributed to the decrease in permeant viscosity as the temperature increases, which leads to higher hydraulic conductivity at higher temperature. In addition, a visual inspection after test termination showed a decrease in biofilm generation as the exposure temperature increased (Fig. 7). Intense biofilm generation due to bacterial growth was observed on the surface and within the soil specimens exposed to leachate permeation at room temperature. However, the tendency for biofilm formation decreased as the temperature increased toward 55 °C. Thus, lower biological clogging may occur at higher temperature, which, along with decreased viscosity, could lead to higher hydraulic conductivity at higher temperature when combined thermo-chemical conditions are applied.

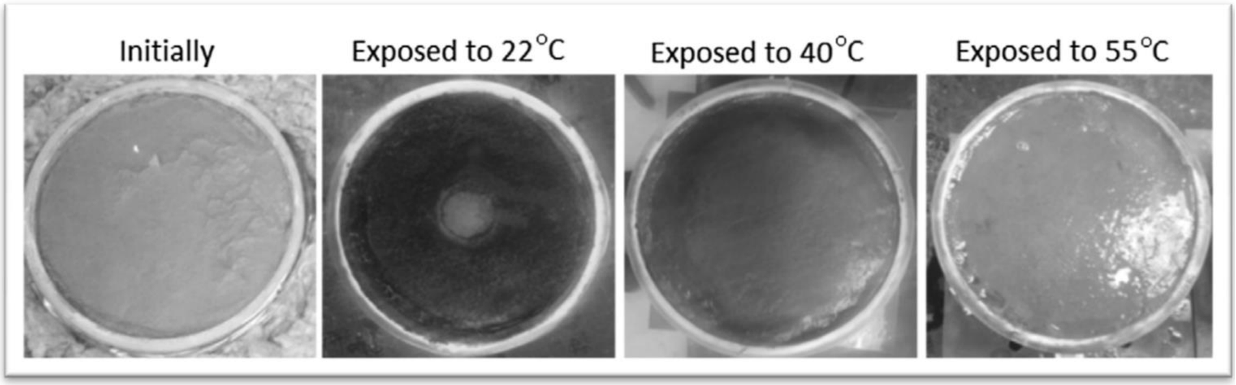

Fig. 7. Effect of temperature on biofilm formation during leachate permeation.

5. Conclusions

Compacted Clay Liners (CCLs) with plasticity indices ranging from 25% to 37% showed reliable hydraulic performance and withstood the thermal cycle effects. Hydraulic performance of low plasticity CCLs can be improved against thermal cycles by overlaying the CCLs with a layer of geomembrane right after construction to minimize the moisture loss and crack formation. The thermo-chemical exposure led to reduction in hydraulic conductivity of the CCL samples that sometimes reached an order of magnitude. The decrease in the CCLs hydraulic conductivities was attributed to chemical precipitation and clogging of pore voids within the soils. The rate of reduction in hydraulic conductivity due to leachate permeation was smaller at temperatures higher than room temperature. Thus, better CCL hydraulic performance would be expected at lower landfill temperature due to the higher clogging potential.

6. References

[1] Aldaeef, A. A., & Rayhani, M. T. (2014). Hydraulic performance of Compacted Clay Liners (CCLs) under combined temperature and leachate exposures. Waste management, 34(12), 2548-2560.

[2] Allen, W.M., (2005). The Relationship Between Plasticity Ratio and Hydraulic Conductivity Bentonite Clay During Exposure to Synthetic Landfill Leachate. M.Sc. thesis, University of south Florida.

[3] Collins, H., (1993). Impact of the temperature inside the landfill on the behaviour of barrier systems. In: Proceedings of the 4th International Landfill Symposium, Sardinia ’93, vol. 1, pp. 417–432.

[4] Frempong, E., (2006). Compatibility of Tropical Clayey Soil Liners with Industrial and Domestic Leachates, PhD, Thesis. University of Western Ontario, ON, Canada.

[5] Hanson, J.L., Yes_iller, N., Oettle, N.K., (2010). Spatial and temporal temperature distributions in municipal solid waste landfills. J. Environ. Eng. 136 (8), 1095– 1102.

[6] Joseph, J.B., Styles, J.R., Yuen, S.T.S., Cressey, G., (2001). Variations in clay mineral performance in the presence of leachates. In: Proceeding of the Eighth International Landfill Symposium, Sardinia, Italy, 10p.

[7] Omidi, G.H., Thomas, J.C., Brown, K.W., (1996). Effect of desiccation cracking on the hydraulic conductivity of compacted clay liner. Water Air Soil Poll. 89, 91-103.

[8] Peron, H., Hueckel, T., Laloui, L., Hu, L.B., (2009). Fundamentals of desiccation cracking of fine grained soils: experimental characterisation and mechanisms identification. Can. Geotech. J. 46, 1177-1201.

[9] Rayhani, M.H.T., Yanful, E.K., Fakher, A., (2007). Desiccation-induced cracking and its effect on the hydraulic conductivity of clayey soils from Iran. Can. Geotech. J. 44, 276-283.

[10] Rowe, R.K., Yu, Y., (2010). Factors affecting the clogging of leachate collection systems in MSW landfills. In: Proc. of 6th International Congress on Environmental Geotechnics, Tata McGraw Hill Education, New Delphi, India, November 2010, pp. 3–23.

[11] Tang, C.S., Shi, B., Liu, C., Gao, L., Inyang, H.I., (2011). Experimental investigation of the desiccation cracking behaviour of soil layers during drying. J. Mater. Civ. Eng. 23, 873e878.

[12] Thiel, R., Giroud, J.P., Erickson, R., Criley, K., Bryk, J., (2006). Laboratory measurements of GCL shrinkage under cyclic changes in temperature and hydration conditions, geosynthetics. In: Proceedings of 8th International Conference on Geosynthetics (8ICG), Millpress Science Publishers, Yokohama, Japan 1-4, pp. 157-162.

[13] Yesiller N., Hanson, J.L., Yoshida, H., (2011). Landfill temperatures under variable decomposition conditions. In: Proceedings of the Geo-Frontiers 2011 Conference, Dallas, TX, USA, 13 March 2011, pp. 1055–1065. Reston, VA: ASCE, American Society for Civil Engineers, Dallas, TX.

[14] Yoshida, H., Hozumi, H., Tanaka, N., (1996). Theoretical study on temperature distribution in a sanitary landfill. In: Proc. 2nd Int. Congress on Environ. Geotech., vol. 1, Osaka, pp. 323–328.

Methods of Thermal Analysis of Massive Concrete Structure under hot climate action: Kufra City

Aeid. A. Abdulrazeg*, Mahmoud A. T. Khatab, Mustafa. A. Aljarrah
Department of Civil Engineering, Omar Al Mukhtar University, El-Beida, Libya
*Corresponding author email: aeid.abdulrazeg@omu.edu.ly

Abstract: The surrounding environment of massive concrete structure such as dams and retaining wall structures play a significant role in the temperature distribution and stress fields variation within the structure. High temperatures are generated in concrete due to the hydration process and the effect of surrounding environment. All these factors induce thermal tensile stresses. These stresses must be controlled to eliminate the creation of cracks in mass concrete structures. The thermal analysis has to be performed accurately to avoid this problem. Therefore, in this study, a two dimensional (2D) mathematical model based on finite element method is developed with the aim of improving predictions of the temperature profile of large concrete elements during the hydration process at early ages and during its lifetime under hot climate. The factors considered in this study are the thermal adiabatic rise of temperature with age and the change of air temperature. The study suggested deferent techniques to control the temperature in the massive concrete structure during the construction. The suggested techniques should be helpful to control the thermal tensile stresses.

Keywords: FEM, Mass concrete, Thermal stress, Numerical method

1 Introduction

The temperature control of massive concrete structures plays an important role in their design and construction. It is of great importance to the thermal control to properly determine the lowest quasi-stationary temperature which serves as the base point of the controlling temperature variation range. Simulation of the heat exchanges between the concrete and surrounding environment will finally lead to realistic temperature distribution profile. This will be helpful in determining the accurate structural response where the thermal loads are the predominant loads in these types of dams (roller compacted concrete dams).

Noorzaei et al. developed a three-dimensional finite element code for coupled thermal and structural analysis of concrete dams. The actual climatic conditions and thermal properties of the materials were considered in the analysis. The structural stress analysis was performed using the elasto-plastic stress analysis. The studies concluded that, the elasto-plastic analysis can redistribute the state of stresses and produce a more realistic profile of stresses in the dam. But the time dependent deformations such as; creep and shrinkage have not been considered by the authors [1]. Temperature and stress fields of the Mianhuatan RCC gravity dam in China was simulated by Zhang and Zhu [2]. In the presented study several factors of RCC affecting temperature distribution and stress field were taken into account in the numerical simulation such as placing process, creep, heat of hydration, and effects caused by surrounding temperature. The main annual air temperature and mean annual river water temperature are used to predict the temperature and stress fields for long-term operation period [2]. Xie et al. and Zhang et al. used a three-dimensional finite element relocating mesh method to simulate construction process and compute temperature field. In their work, many factors have also been considered, such as thermal adiabatic rise of temperature with age, the process of placement by layer, creep, work suspension in summer and the change of air temperature. However, the studies were limited for thermal analysis only. In addition, further studied to select the proper relocating age of concrete is essential [3], [4]. Penghui et al. determined creep values for thermal analysis of Dahuashui RCC arch dam, applied time and stress dependent coefficient, in a multi-term expression, whereby certain constants were apparently derived through experimental study to an accuracy of six decimal places. In the presented work, the variation of the RCC mechanical properties with time was not been considered and fixed values were used during the analysis [5].

2 Numerical Modelling

The Fourier equation governed the thermal generation and temperature distribution, is expressed by the following formula [6]:

$$\frac{\partial}{\partial x}\left(k_x \frac{\partial T}{\partial x}\right) + \frac{\partial}{\partial y}\left(k_y \frac{\partial T}{\partial y}\right) + \dot{Q} = \rho c \frac{\partial T}{\partial t} \tag{1}$$

where T is the concrete temperature, k_x and k_y are the concrete conductivity coefficients in x and y directions respectively, $\dot{Q}$ is the rate of heat of hydration introduced per volume, ρ is the material density, and c is the specific heat.

Two main types of boundary conditions are Drichlet and Cauchy boundary, which can be written respectively as :

$T=T_p$

$$k_x \frac{\partial T}{\partial x} l_x + k_y \frac{\partial T}{\partial y} l_y + q + h\left(T_s - T_f\right) = 0.0 \tag{2}$$

where T_p is the known values of the nodal points of the temperatures on the boundaries; q is flowing heat from surface; h is the film coefficient; T_s is unknown temperatures at the boundary nodal points; T_f is the ambient temperature; l_x and l_y are the direction cosines of the normal to the surface under consideration .

3 Computation of Thermal Field

The Numerical solution scheme used in this study is based on the Taylor–Galerkin approach. Upon applying this approach, the following system of differential equations is obtained [7]

$$[K_t]^{(e)} \{T\}^{(e)} - [C]^e \left\{\frac{\partial T}{\partial t}\right\}^{(e)} = \{F\}^{(e)} \tag{3}$$

where, $[C]^e$ is the capacitance matrix; $[K_t]$ is the heat stiffness matrix; $\{F\}$ is the total load heat vector due to hydration and convection actions.

The finite difference approximation was used to solve Eq. (1) in the time domain numerically

$$\left([C] + \theta\Delta t[K_t]\right)\{T\}_b = \left([C] + \theta\Delta t[K_t]\right)\{T\}_a + \Delta t\left((1-\theta)\{F_t\}_a + \theta\{F_t\}_b\right) \tag{4}$$

where $\{T\}_b$ and $\{F_t\}_b$ are {T} and {F_t} at time (b) and $\{T\}_a$ and $\{F_t\}_a$ are {T} and {F_t} at time (a), θ is a scalar ($0 \le \theta \le 1$) which is equal to 2/3 in the Galerkin method [1].

4 Initial Conditions

The temperature distributions in the foundation (rock ground) as well as the concrete placing temperature are the two initial conditions that need to be considered in the analysis.

4.1 Evaluation of the Foundation Temperature

The determination of the foundation initial temperature is usually performed by assigning the main annual air temperature as initial temperatures for the ground rock. Then, perform the thermal analysis of the block foundation for a period of two or three years prior to the dam construction time [8].

4.2 Concrete Placing Temperature

In thermal analysis of concrete, the placing temperature can be taken as the surroundings temperature unless there is any restriction taken in the design. These restrictions for example are to lower the placing temperature to a certain limit by apply some control techniques such as adding ice cubes or cooling the ingredients. Thus in this case, this limit will be used for this specified lift [9].

5 Heat Hydration

Isothermal or adiabatic hydration heat test is usually performed in laboratory, and then analytic models are used to describe the hydration heat development at various temperature regimes. The adiabatic model is the well-establish model used for the simulation of the heat of hydration in massive concrete structures. The adiabatic temperature rise of concrete based on the aforementioned model is given by [10]:

$$T_{adj} = T_{\max}(1 - e^{-\alpha t})$$

(5)

where;

$T_{\max}$ is the maximum temperature rise of concrete under an adiabatic condition and α is a parameter which represents the heat generation rate and t is the time (days). The cumulative heat generated due hydration up to time t is given by;

$$Q = c\rho T_{adj} \tag{6}$$

Substituting Eq. (5) in Eq. (6) and differentiating with respect to time *t*, the expression for the rate of heat of hydration $\dot{Q}$ can be expressed as:

$$\dot{Q} = c\,\rho\,\alpha\,T_{\max}\,e^{-\alpha t} \tag{7}$$

The values of $T_{\max}$ and α are usually determined from tests on concrete samples that will be used in the construction [6].

6 Problem Definition

The example presented in this study is to be constructed in south-east of Libya (Kufra City) (Fig. 1) in a hot dry climate area (maximum temperature rises above 41 ^{o}C). According to the proposed schedule, the concrete will be casted in August and this is to simulate the worst casting schedule where the temperature will reach its peak at this time of the year.

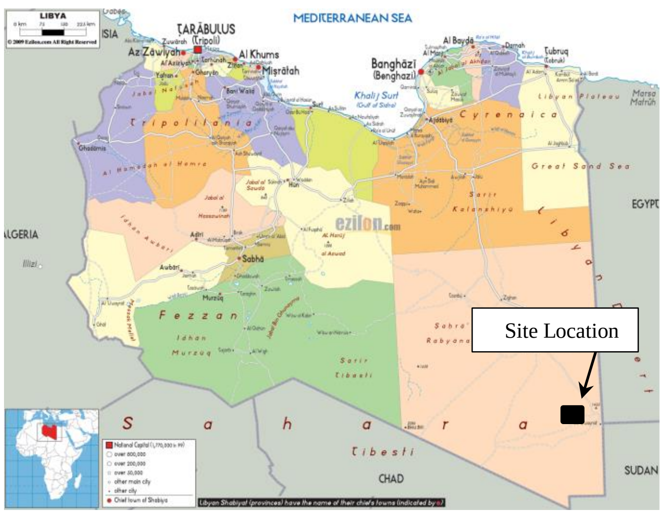

Figure 1: Vicinity Map and construction Site Location

6.1 Material Properties and Site Conditions

The material properties for the concrete and the rock foundation are tabulated in Table 1. These values were chosen based on values reported in the literature for concrete materials which is used in proposed example [11]. In addition, the average monthly air temperatures at the project site are plotted in Fig. 2.

Table 1: Thermal and Structural Properties of Trial Segment [8]

Material	unit	Symbol	Concrete	Rock
Heat conduction coefficient	W/m °C	K	2.8	2.7
Heat convection coefficient	W/m^2 °C	h	15.25	15.25
Specific heat	J/kg°C	c	1256	1256
Density	kg /m^3	ρ	2400	2710
Elasticity modulus	KN /m^2	E	2.25E+6	0.6E+6
Poisson ratio	-	ν	0.18	0.3

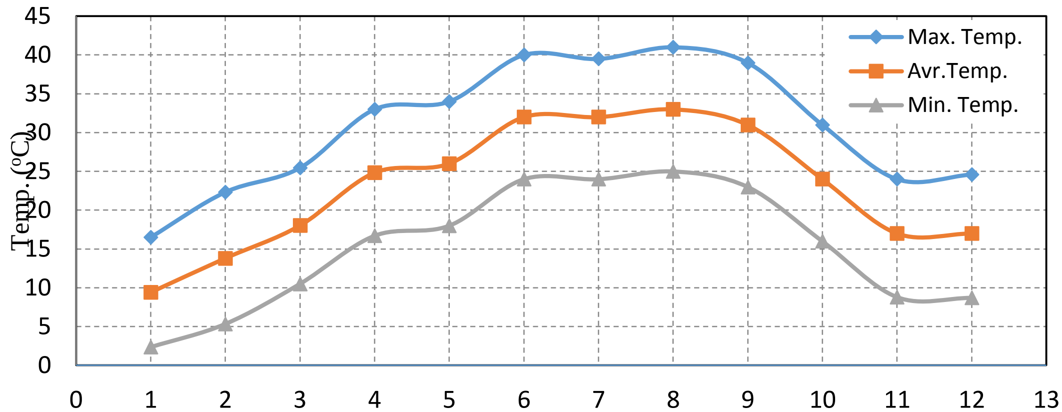

Figure 2: Monthly air Temperature at Kufra City

7 Finite Element Modeling

The geometrical details of the trial segment are shown in Fig 3. It is placed in 80 cm horizontal layers of concrete. The 2-D finite element model of the concrete block is shown in Fig.4. Eight noded isoparametric elements are used in the analysis.

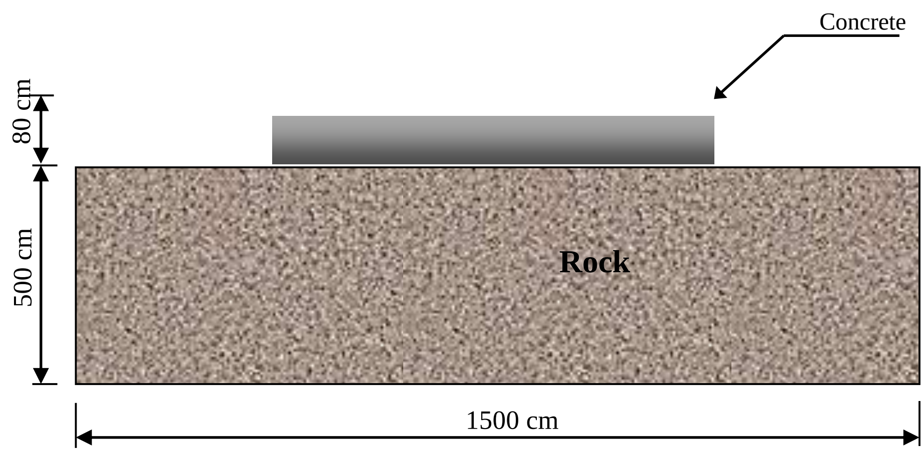

Figure 3: Typical Cross Section of Proposed Segment

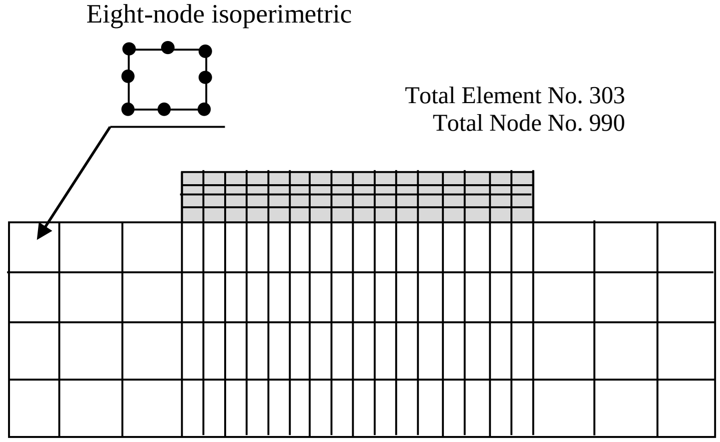

Figure 4: 2D Finite Element Mesh of Proposed Segment

8 Result and Discussion

In order to study the temperature variation with time, the temperature has been plotted for four different location along the Segment as shown in Fig. 5.

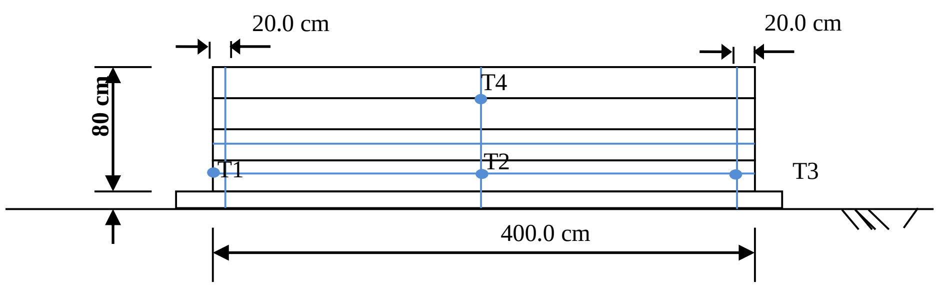

Figure 5: Location of Predicted Temperature

Fig. 6 shows the temperature at different location along the concrete block. The temperature increases due to the heat produced by hydration, then reaches a maximum point about 7 days after casting. Then the block starts to cool down due to the interaction with ambient temperature. It is obvious from this plot that, the higher temperature zone is at the center of the block (T_2) with maximum predicted temperature of 44 ^{0}C, which gradually reduced to reach approximately the air temperature at the boundaries (T_4).

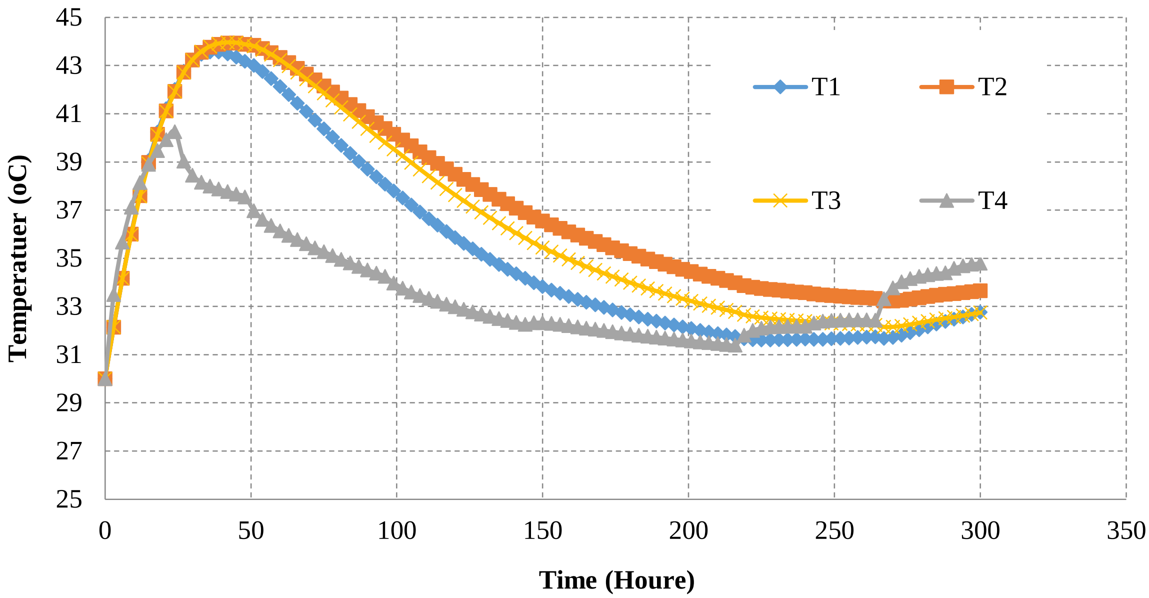

Figure 6: Temperature Variation at different location along the concrete block

In the present study alternative casting schedule has been examined to evaluate the influence of the ambient temperature in the overall thermal response of the structure. According to the proposed schedule, casting of the concrete will be started on January. Fig. 7 shows the temperature at different location along the concrete block. Similar to the pervious schedule, It is obvious from this plot that, the higher temperature zone is at the center of the block (T_2) with maximum predicted temperature of 38 ^{0}C, which gradually reduced to reach approximately the air temperature at the boundaries (T_4). However, point 1 and 4 (boundary) are greatly affected by the surroundings temperature.

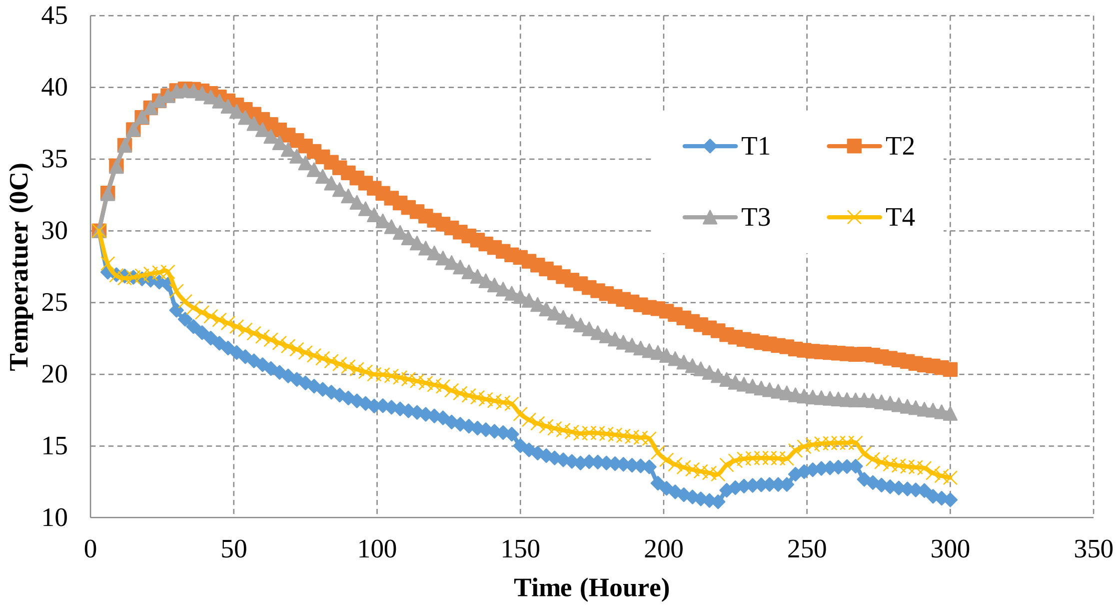

Figure 7: Temperature Variation at different location along the concrete block (January casting schedule)

9 Conclusions

In mass concrete works the temperature difference between the interior and surface of the concrete should not exceed 20 ºC [12]. This limitation is based on the allowable tensile strain capacity of the concrete at given age. Hence, the boundaries are possessing air temperature and the average annual temperature is 11 ^{0}C, so the temperature inside the concrete should not rise to more than 31 ºC. There are several techniques to control the temperature in RCC dam during the construction such as;

i. Cooling concrete with ice flicks.

ii. Reducing the cement content, just to support the required mechanical and elastic efforts. This technique decreases the hydration temperature [13].

iii. Stoppage between the lefts. Stoppage (delay) in casting schedule is essential for such hot- dry climate, the main reason is to cool the hydration heat and avoid the work in very hot weather.

References

[1] J. Noorzaei, K. H. Bayagoob, A. A. Abdulrazeg, M. S. Jaafar, T. A. Mohammed, Three Dimensional Nonlinear Temperature and Structural Analysis of Roller compacted Concrete Dam, CMES: Computer Modeling in Engineering & Sciences. 47(2009), pages 43-60.

[2] G. Zhang, B. Zhu, Thermal stress simulation and possible crack analysis of Mianhuntan RCC dam, in: Proceedings of the Fourth International Symposium on RCC Dams, Madrid, Spain, (2003), pages 603-609.

[3] H. Xie, Y. Chen, Influence of the different pipe cooling scheme on temperature distribution in RCC arch dams, Communications in numerical methods in engineering, (2005), 21: 769-778.

[4] X. Zhang, S. Li, Y. Chen, J. Chai, The development and verification of relocating mesh method for the computation of temperature field of RCC dam, Advances in Engineering Software, (2009),40: 1119-1123.

[5] L. Penghui, C. Hong, 3-D Simulating Analysis for thermal control during constructionperiod on Dahuashui RCC arch dam, In: 5th International Symposium on Roller Compacted Concrete Dam,Guiyang, China, (2007): 577-581.

[6] K. H. Bayagoob, J. Noorzaei, M. S. Jaafar, W. A. Thanoon, A. A. Abdulrazeg, Modelling heat exchange between RCC dam and reservoir, J. of Engineering and Computational Mechanics. 10 (2010), pages 33-42.

[7] A. A. Abdulrazeg, J. Noorzaei, M. S. Jaafar, P. Khanehzaei, T. A. Mohammed, Thermal and Structural Analysis of RCC Double- Curvature Arch Dam, Journal of Civil Engineering and Management, Vol.: 20, Issue: 03, (2014), pages 434 - 445.

[8]Ishikawa, M, Thermal stress analysis of a concrete dam. Computers & structures, pages 40(2), (1991).347-352.

[9]Luna, R., and Wu, Y.. Simulation of temperature and stress fields during RCC dam construction. Journal of Construction Engineering and Management, 126(5), (2000) , pages 381-388.

[10] Japan Society of Civil. Engineers. Standard specifications for design and construction of concrete structures, Part 2 (construction). Tokyo: JCI, (1986).

[11] Pazhouhab Consultant Engineers. (1999). Technical report of Zirdan roller compacted concrete dam,Irain.

[12] Neville, A.M**.,** “Properties of Concrete,” Third Edition, Longman Scientific and Technical, England, 1983.

[13] Hajilikhani, M. R. Modifying construction methods of Zirdan RCC dam . In: Proceedings of the Fourth International Symposium On roller compacted concrete dams, (2003): pages 273-276.

comparison between the materials used in thermal insulation and the possibility of choosing the best thermal insulation in desert areas

Salem. M. Alburki[a]*
[a]Chemical Engineering Department, Faculty of Engineering, El-Mergib University, Al-Khums,
*Corresponding Author: smalburki@Elmergib.edu.ly
Academic degree: assistant professor

Abstract : Construction and building in desert areas is considered a big challenge in turn due to the hot weather in these areas, when the average temperature in these areas reaches 45 degrees Celsius (°C) or a little more during the day, and decreases significantly at night. Comparison between materials used in thermal insulation and choosing the best and least expensive so that they are effective in isolating buildings from external heat in summer and keep buildings warm in winter. Fourier's law of thermal conductivity was relied on in this study to know the resistance of materials to heat, taking into account the type of material used and from The materials that were used in this study (polystyrene, fiberglass, and thermal wool)

*Keywords—**thermal insulation, thermal insulation materials, Fourier's law***

INTRODUCTION

The desert areas of our beloved country are characterized by a hot climate in summer and very cold in winter, and the average temperatures throughout the year in desert areas range from 40-50 degrees Celsius [2,1]. High temperatures to this extent may affect the building and construction operations in those areas. regions due to the exorbitant cost of cooling operations for homes and human dependence heavily on air conditioners in cooling operations in the summer and also the use of sources of heating in the winter, all of these devices used need a large amount of electrical energy as air conditioning consumes approximately 60% of household electrical energy, heat Which seeps into our homes and facilities through the walls in the summer, represents the bulk of the heat that needs to be removed by air-conditioning [3], and to support the idea of building and reconstructing desert areas and encouraging the reverse migration of these areas, we must think about building materials that are in line with the existing climate, and also use materials that resist the surrounding conditions From heat, humidity, winds and other environmental conditions in those areas. From here, the importance of studying thermal insulation emerges as one of the most important necessary elements in the architecture of the desert and hot areas. Thermal, which greatly reduces the costs of cooling and heating. In order to avoid these problems, the insulating materials used in thermal insulation have been studied and compared [4].

Heat insulating materials have been used for a long time in order to provide appropriate conditions for human life in housing and residence. Man has known from ancient times ways to limit the spread of heat, as he used rocks and stones as a barrier in front of fire to keep it hot for a long time, providing it with warmth after the fire is extinguished [5].

Thermal insulation materials appeared at the beginning of this century. Thermal insulation of the facilities began in an organized and studied manner for the purpose of reducing heat loss and gain, in addition to achieving thermal comfort for the person inside his house. Heat-insulating stone wools appeared in the field of industry and construction. With the beginning of the thirties of this century, glass wool appeared, and in the mid-forties, the manufacture of both types of polystyrene and polyurethane appeared. Urethane and in the fifties, foamed vinyl appeared [6].

2. Heat Insulation:

Thermal insulation is the use of materials that have properties that help limit the leakage and transfer of heat from outside the building to its interior in summer, and from inside to outside in winter.

1- The heat that penetrates walls, ceilings and floors.

2- The heat that penetrates windows, doors and other openings

3- The heat that is transmitted through the ventilation holes [7,6].

The heat that penetrates the walls and ceilings in the summer days is estimated at 60-70% of the heat to be displaced by air conditioning. As for the rest, it comes from windows and ventilation openings[3]. percentage of electrical energy consumed in the summer to cool the building is estimated at about 60% of the total electrical energy consumed. Hence the importance of thermal insulation to reduce the consumption of electrical energy used for air conditioning purposes; This is to reduce heat leakage through the walls and ceilings to achieve the appropriate functional goal for the dwelling and reduce the cost [4,3].

It expresses the time rate of the passage of thermal current in watts (W) through the structural elements inside and outside the building and the value of the thermal transfer coefficient is necessary to know the efficiency of the insulating materials and according to Fourier’s law of thermal conductivity, which directly affects the efficiency of the insulating materials so that the lower the value of the thermal coefficient, the greater the efficiency of the insulating material The mathematical relationship of Fourier's law illustrates this [8].

$$\frac{dQ}{dt} = K.A.\frac{dT}{dX} \ldots\ldots\ldots\ldots\ldots(1)$$ [8]

Where:

dQ/dt = time rate of heat flow (W)

A = Surface crossed by thermal current (m^2)

K = coefficient of thermal conductivity or thermal conductivity ($W/m.^{o}c$)

dT/dX = magnitude of the temperature gradient ($^{o}C/M$)

2.1 heat transfer methods

Heat is transmitted through materials and mediums through the three known means of transmission, which are conduction, convection, and radiation, which can be defined as follows:

1- Heat transfer by conduction

It is the transfer of heat through the hotter (higher temperature) solid body particles to its cooler (lower heat) particles in contact with the hot particles in it.

2- Heat transfer by convection

It is the transfer of heat in liquids as well as moving gases. It takes place as a result of the movement of the hot particles of the liquid or gas. This movement forms convection currents, which in turn work to balance the temperature of the liquid or gas. In a gas such as air, heat transfer is by convection in the air surrounding the heat source, so the air molecules in contact with the heat source rise up due to their expansion and light weight, and are replaced by molecules of cold air that is also being heated to rise to the top, transferring heat through its molecules.

3- Heat transfer by Radiation

and he. The conversion of thermal energy in a body into radiant thermal energy (energy radiating outwards) and transferring it to another body. It, in turn, converts it into thermal energy. Thermal rays are electromagnetic waves that are similar to light waves and differ from them in wavelength. They are called ultraviolet rays, and therefore they need a material medium to be transmitted through them. Thus, the transfer of thermal energy occurs radially in a in the void [8].

2.2 Thermal bridges:

They are the areas through which heat leaks from the outside to the inside and vice versa. For example, the heat that leaks from areas that are not thermally insulated, such as home building structures. There are also bridges consisting of the same building materials as in cement and pottery bricks [5].

3. benefits of thermal insulation

1- Rationalizing the consumption of electrical energy during cooling and heating operations, by a rate that may reach 30-40%.

2- Protecting the structural elements of the building and preserving the furniture from temperature changes

3- Raising the level of comfort and health safety for the building's residents

4-Reducing the costs of purchasing air-conditioning and heating equipment by reducing their capacity

5-Reducing environmental pollution, heat emissions and noise [7]

3.1 Guidelines for choosing the best thermal insulation materials

1- One requirement is that the insulating material have a low heat conductivity coefficient.

2- It must have a high level of resistance to permeability by water and water vapor.

3- Overall expense of utilizing the insulator to achieve the necessary thermal insulation.

4- To be extremely resilient to stressors brought on by significant temperature changes that cause ongoing, reciprocal expansion and contraction. which results in the thermal insulation material losing some significant mechanical properties.

5- It need to have strong mechanical qualities, such as a high coefficient of compressive resistance and a coefficient of fracture resistance.

6- It must be resistant to fire, chemical reactions, and alterations.

7- It should not cause health damage, and it should be resistant to bacteria and mold and not susceptible to the growth of insects.

8 - Operational life of the insulating material.

9- It should be easy to install and conform to standard specifications [9].

3.2 Thermal insulation materials

Their sources classify thermal insulation materials into the following four groups:

1- Insulating materials of animal origin: such as wool, animal hair and felt, and their use as insulating materials is limited.

2 Insulating materials of inanimate origin: such as glass wool, concrete and light concrete.

3- Industrial insulating materials: These include rubber and foamed plastics such as polystyrene and foamed polyurethane, as well as types of light concrete.

4-Insulating materials of plant origin: These include fibers or cellulosic materials such as reeds, cotton, etc [10].

Table (1): Thermal insulation materials[9.10]

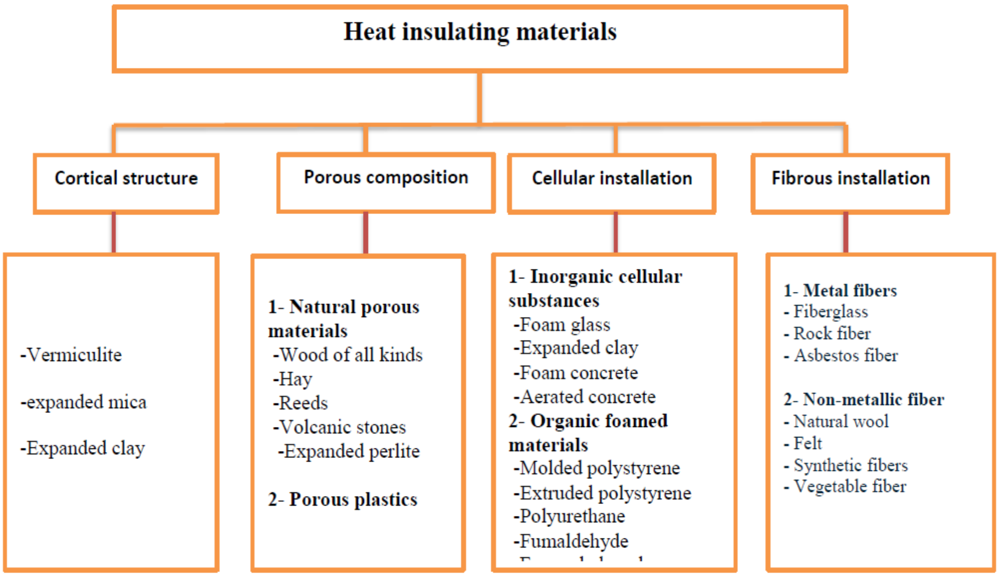

3.3 Types of insulating materials and their uses:

Insulating materials can exist in several forms as shown in the previous table, and we take some of them as examples used as follows:

1. Felt (fibers that are not metallic).

Long rolls of various thicknesses are available, and the majority of the felt is covered in paper or metal foil with a frame on both sides to hold the sides. The metal foil can be on one side of these rolls, and one of the sides can be coated with paper covered in asphalt or bitumen to act as a vapor barrier or moisture barrier, or a layer of perforated thin paper on the other side, which is currently of limited use. Felt is often made of organic materials that include glass fibers. Cellulose fibers can also be provided in the form of felt. The felt is placed on the inner wall of the building, and is often used to insulate ceilings and walls.

2. Light filler granules (natural porous materials). This insulating material consists of small granules, and when the granules are isolated, the suction equipment in the conveyors carrying this insulating material suctions the granules and directs them to the place to be isolated, where they are extruded.

3. Extruded foamy liquid (organic cellular materials).

This material is available in two types: one: inorganic fibers of the adhesive type, and the second: it is extruded, as it hardens shortly after extrusion, and the inorganic type is composed of mineral wool fibers. And it is installed by special machines designed for this purpose. As for the second type, it consists of two packages suitable for spraying (extrusion) purposes.

4. Solid boards or slats (inorganic foam materials).

It is widely used in buildings to insulate roofs and walls.

Insulating materials are made as follows:

1- Fiberglass:

The raw materials for fiberglass, which is also called glass wool or fiberglass, consist of sand, soda, and some other additives that are mixed and then melted in an oven at a temperature of (1400°C), after which they are transferred to the spinning apparatus to convert them by centrifugation into fine metal fibers. Then the fibers are treated with a resin binder, and fiberglass is produced with different thicknesses, densities, and shapes similar to rock wool as shown in the figure (1). Fiber glass is characterized by its great resistance to combustion and its ability to insulate sound, and it is recommended to use it in steel buildings. It is a material similar to rock wool, as it has a fair water and moisture absorption coefficient, and its pressure tolerance is very low.

figure 1: Fiberglass

2. Rock wool:

Rock wool is made from natural rocks, and it can also be made from iron, copper or lead slag instead of natural rocks as a raw material. The slag is melted using coal as fuel, and the rock wool is spun into fibers by pouring the molten material into a rotating vessel

figure 2: Rock wool

3 -polystyrene

It is a light and rigid cellular plastic material characterized by poor heat conduction and excellent insulation. Resistant to pressure, impermeable to water, recyclable. It is globally classified as one of the best types of thermal insulation see figure 3 . It is found in many forms and is used in many building applications. This material is made by heating polystyrene with steam inside molds to form solid white cubes. These cubes can be cut to obtain solid panels of different thicknesses.

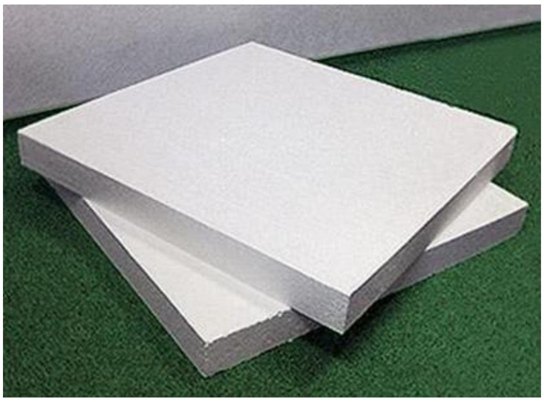

figure 3: polystyrene

4- Polyurethane

It is a sticky material characterized by having a very low thermal conductivity coefficient and little absorption of water or water vapor. It is also light in weight and resistant to compression. It comes in the form of ready-made panels. Polyurethane is commonly used as a thermal insulator, especially in ceiling insulation.

figure 4: Polyurethane

5- Perlite

They are glassy volcanic rocks that have a low thermal conductivity coefficient, are solid and do not burn, and perlite, which is known for its usefulness, is used in insulation and for inclined ceilings and wall insulation.

6- seaborks:

Insulating material	Fire resistant	pressure bearing strength kg/m^2	water vapor permeability (ASTM E 96)	Percentage of water absorption %(ASTM C272)	Thrmal conductivity at 24 c w/m.k	Usage:	Density Kg/m^3	Thermal properties change with time
Expanded polystyrene moulds	burns and smokes	528-80	5 -0.6	2.5	0.0374	walls	20 -13	Not affected
					0.0331	roofs	35 -32	
Extruded polystyrene sheets	burns and smokes	2000-240	1.4-0.4	0.3	0.0288	walls	28 -26	It is greatly affected by the use of freon gas in its manufacture
					0.0288	roofs	35 -32	
Polyurethane	burns and smokes	960-320	4 -2	5 -2	0.026	walls	28-26	It is greatly affected by the use of freon gas in its manufacture
					0.023	roofs	48 – 35	
light concrete	resists heat and melts at 1100 C	--	--	49.33--12.52 High absorbency can be treated	43.0 -0.065	Ceilings and walls	1040-240	Not affected
foam glass	resists heat and melts at 430 C	--	--	00	0.55	Ceilings and walls	140	Not affected
Fiber glass	fibers are fire retardant and the binders burn	few	Very high	Very high	0.051	Metal ceilings and walls	120 -17	Not affected
rock wool	fibers are fire retardant and the binders burn	few	Very high	Very high	0.051	Metal ceilings and walls	120 -29	Not affected
Perlite	resists heat and melts at 1300 C	Depends on the strength of the cement mixture	Very high	Very high	0.39 -0.16	walls	240 - 80	Not affected

It is a cellular and structural concrete material that is heat-insulating and fire-resistant. It is widely used to insulate external walls and roofs, and to insulate foam concrete [6, 10, 11]. In Table No (2), the different values of the thermal conductivity of some insulation materials, in which some other characteristics are also noted, which help in choosing the appropriate type of insulator>

Table2: General properties of thermal insulation materials

4. Systems used in thermal insulation

There are several systems used in insulation techniques for external walls, ceilings and floors

4.1 Wall insulation:

4.1.1 Building a wall of thermally insulated bricks: This method is one of the currently prevailing methods in the process of thermal insulation of walls, where a wall with a width of (20-25 cm) is built of thermally insulated blocks or bricks or lacquer, insulated cement and insulated red bricks , as there is an inside of this type The blocks or bricks consist of several strips of thermal insulation made of expanded polystyrene or rock wool and other thermal insulation materials see figure (5) , but this method or system does not completely isolate, as the heat is transmitted to the buildings through thermal bridges, which are represented in the cement mixture that is used In the construction process, which represents about (10%) of the wall in the template, in addition to the thermal bridges that connect the two ends of the blocks.

figure (5): Building a wall of thermally insulated brick

4.1.2 Building a wall of thermally insulated blocks next to the white blocks of aerated concrete: wall is built of thermally insulated blocks or blocks with a thickness of (20-25 cm) as shown in figure (6). In addition to white blocks of aerated concrete, however, this system does not completely isolate the heat, but it is better than the previous method in semi-insulation, as the bridges that transmit heat remain in this system, which work to connect it to the inside of the building represented by the cement mixtures used in construction.

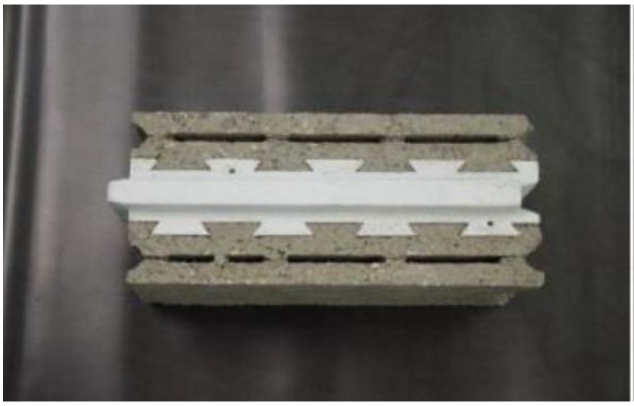

figure (6)

4.1.3 Building a wall between them thermal insulation panels:

In this method, the building is isolated from the outside, as some may wish to clad the building from the outside with marble, stone, granite, metal panels, and other types of materials that can be installed or installed, provided that this is done before installing these materials of stone, granite, and others see figure (7).

figure (7): Building a wall between them thermal insulation panels

Adding a thermal insulation material such as polystyrene panels or rock wool and other thermal insulation materials, this is the ideal method in the thermal insulation process, as the entire walls and concrete columns are covered, which does not allow the presence of bridges to transfer heat to the interior, and this method is considered suitable for buildings, whether they are existing or under construction[11,7,6]

4.1.4 External insulation system: Where thermal insulators are installed on the external walls of the building so that it is completely encapsulated

Then external finishes such as glass or STB materials are installed from the outside, and in this system all thermal bridges are overcome, and it is the only system that isolates columns and bridges and cancels their work as thermal bridges, but consideration must be taken to review the method of installing external ventilation materials for the building and the total cost of this system [11].

figure (8): External insulation system

4.2 Thermal insulation of the floors: The floors are isolated from moisture and salts, as well as they can be thermally isolated. The method of insulation, as well as the insulation materials for the floors, is very similar to the method of insulation for the ceilings. Soil temperatures at a depth of 3 meters may reach approximately (33 ^{O}C), and therefore the insulation of the floors is important The process of good floor insulation reduces the flow of heat from the floors in air-conditioned buildings, and the thermal insulation material for the floors must meet basic conditions, which are:

1- It should have high compressive strength

2-To be resistant to water and moisture absorption

3-It should have a low coefficient of thermal conductivity, that is, it must provide the minimum required level of thermal insulation [7].

4.3 Surface insulation:

Roofs can be insulated by applying one of the two systems:

4.3.1 The traditional roof system

The waterproofing layer is placed on top of the thermal insulating layer to protect the thermal insulator from water, especially the thermal insulation materials as shown in figure (9a).

In which the water absorption rate is relatively high, and in this system the waterproofing membrane (waterproofing) is exposed to continuous thermal stresses resulting from the large difference in temperatures between night and day and between the different seasons of the year, which leads to the expansion and contraction of this membrane, which leads to its loss. Its flexibility and to mechanical stresses during or after installation as a result of the presence of some air-conditioning devices, and others and maintenance work on the roof of the building, and thus the life span of the waterproofing is reduced and maintenance costs increase.

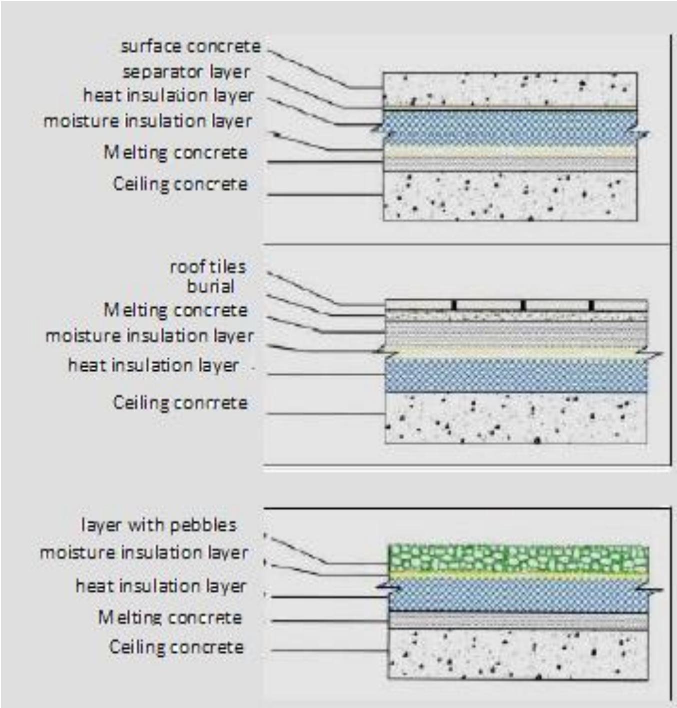

figure (9a): Roof insulation with the traditional system

4.3.2 Inverted surface system

In which the thermal insulation is above the waterproofing layer, and the thermal insulator protects the waterproofing from thermal stress and exposure to ultraviolet radiation, as well as mechanical stress during and after installation, and thus increases the life as shown in figure (9b).

Default for waterproofing membrane, thus maintenance costs are greatly reduced.

In order for the inverted roof system to be used, the thermal insulation material must have a high resistance to water and moisture absorption [11,12]

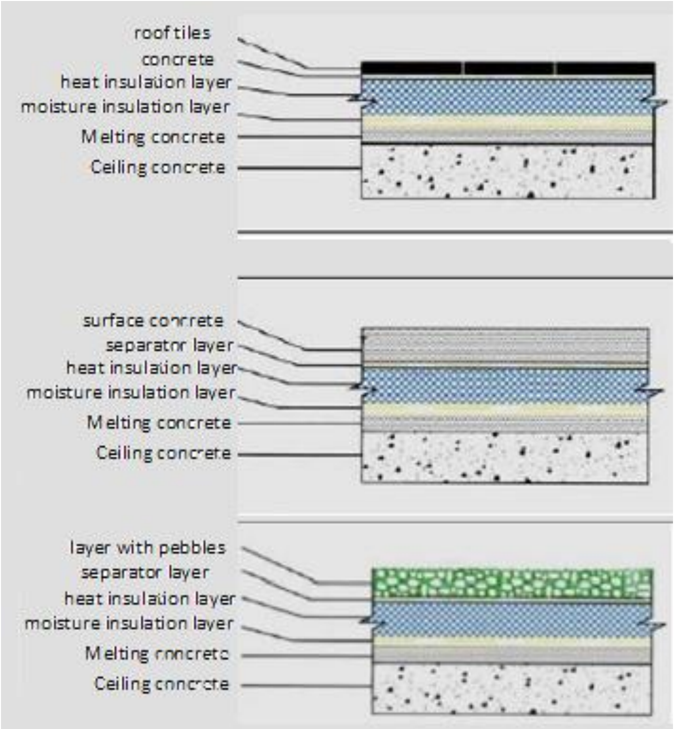

figure (9b): Roof insulation with Inverted surface system

5. Conclusion :

1. The application of thermal insulation systems in buildings reduces the consumption of electrical energy if applied on a sound scientific and technical basis.

2. Thermal insulation works to protect and protect the building from temperatures, weather changes, and weather fluctuations.

3. Choosing the correct heat insulating material gives an economic return.

4. The thermally insulated building saves the energy expended in heating or cooling.

5. Polystyrene is considered one of the best materials for insulation due to its ease of obtaining and its efficiency in thermal insulation

6. Providing thermal stability for the building significantly reduces the exorbitant maintenance expenses of the building.

7. Heat insulating materials bear the pressures they are exposed to during their operational life.

8. The quality of thermal insulation materials is achieved when they have a low thermal conductivity coefficient.

6. Recommendations:

* Work on manufacturing heat and moisture insulation materials locally with high quality so that they conform to the specifications and compete with the materials that are imported.

* Identifying the chemical composition of the thermal insulator to prevent skin allergy or the damage it may cause to humans.

* Insulating materials must be selected in construction operations by engineers specialized in thermal insulation systems

Giving courses and workshops on how to choose and install insulating materials that are in line with the nature of the building and the surrounding conditions.

* Planting trees and plants around buildings and creating green spaces helps reduce the rise in temperatures and climate fluctuations and provides a kind of environmental relief.

REFERENCE:

[1] Current ClimateClimatology", worldbank, Retrieved 28/11/2021. Edited - [1]

[2] Interesting Facts About Libya", worldatlas, Retrieved 8/12/2021. Edited

[3] J.Kadoori AlRobayie ,H.Hausner. Mechanical properties of SiC-TiC and SiC-TiB2 composites".Journal of research –Technical university of Berlin .March(1993), 18-21.

[4] د. جليل إبراهيم قدوري واخرون (العزل الحراري لمواد البناء) مجلة ديالى للعلوم الهندسية المجلد الثالث , العدد الأول. 2010, صفحات البحث 28 – 4 4

[5] معاوية ابراهيم عيد عساف (اثر العزل الحراري في المباني) المجلة العلمية للنشر العلمي ajsp 2022

[6] حسين محمد جمعة ، (عزل وحماية المنشآت الخرسانية ضد رطوبة التاكل والحرارة و الكيمياويات) ، دار الفكر المعاصر ، القاهرة، مصر. 2008 م

[7] سعيد علي خطاب ، (عزل وحماية المنشآت الخرسانية) دار الكتب العلمية للنشر والتوزيع ، القاهرة، مصر. 2005 م

[8] Bergman et al. "Fundamental of heat and mass transfer seventh edition". John Wiley & sons. ISBN 13 978-0470-50197-9. (2007).

[9] م. ناديا حماد ، (العزل الحرا ري للمباني) مجلة المهندس العربي/ سوريا العدد /153 حزيران 2007

[10] Chaykovskiy German.."Comparison of Thermal Insulation Materialsn for Building Envelopes of Multi-storey Buildings in Saint-Petersburg". Bachelor Thesis. Mikkely University of applied sciences. 13-16. (2010)

[11] د.محمد بن آل سعد حمود (خصائص و تطبيقات مواد العزل الحراري في المباني) .جامعة الملك فهد للبترول و المعادن الظهران.

[12] انتصار قدروري , فيصل كاضم (دراسة مقارنة لاستخدام الخرسانة الخفيفة الوزن بدلا من الطابوق التقليدي في بناء القواطع) جامعة بغداد .2010.

Finite Element Modeling to Study the Insolation Heat Gain Behavior for a Residential Building in Temperate Climate

Associate Professor :Mohamed Ali karim
Civil Engineering, Engineering Faculty, Elmergib University, AL-khoms, Libya
email: omgaon2x@yahoo.com

Abstract:

Nowadays, studying the possibility of getting the benefits as much as possible from available energy in our natural resources is one of the most important concerns of scientists and researchers, because this energy contributes well to reducing pollution that may result from using fossil fuels. In countries with a temperate and arid climate, such as the climate of the Libyan state, the energy consumption for cooling homes is large, so it is important to reduce this energy by following the appropriate method of insulation against the heat gained from insolation. This work presents a study on finite element modeling (FEA) of the temperature distribution in a one-story building and how this structure gains heat from its surroundings during a day of solarization. In this model the building envelop is thermally insulated and that the roof and the opining are not insulated, ANSYS 2020 R2 is used to model (thermal-structural analysis) a 3-D concrete building which is 3.20 m in floor height and has a footprint area of 40 m^2. Due to the large size of this model for such an analysis type, using the FEM is a bit challenging and may be a little complicated, but FEM is widely prevalent in most other fields because of the high effectiveness of this method on simulation. The results of the analysis showed how the heat gained from insolation is distributed, as well as how the building elements vary at different rates in the heat transfer through them to the building interior. Moreover, the results clearly showed that the insulation of the walls only of the building is not sufficient to avoid overheating of the building. This gives us a good enough idea of the priorities for implementing the insulation layers of the building in temperate and arid climates (the climate of the Libyan state), which will make the building more sufficient and more sustainable.

Keywords: Sustainability, Morphology, Radiation, Insulation, Ambient, Insolation

Introduction

One of the most important factors in promoting environmental sustainability is improving buildings' energy efficiency. In the fields of construction, civil engineering, and architecture, many ideas have been introduced in the field of energy and natural resources, which are related to the shape of the structures, the locations and distribution of elements necessary to provide ventilation and capture the sun's rays, such as the windows, building aspect ratio, directing of the block, the position of vertical cores, and the structural system . Often, these variables directly depend on the climatic zone in which the building will be built [1].

Generally, in a temperate and arid climate, such as the climate of the Libyan state [2], the energy consumed in cooling is the highest for HVAC systems (Heating, Ventilating, and Air Conditioning). Therefore, the design of residential buildings must take into account how to take advantage of the natural factors in which climate zone the house is located; where the characteristics of the building morphology can be manipulated to adapt to these features or to avoid their unwanted effects. The characteristics of the structural system and the proper building configuration contribute to reducing the energy consumed for cooling and heating by up to 30%, depending on the climatic zone [3]. Also, the implementation of the thermal insulation layers for the building has a great role in conditioning the houses, but the thermal insulation layers for the building envelope must be implemented in a successive manner by knowing the parts of the building that cause the temperature to rise inside the building.

Concrete, wooden, or steel buildings, as the air temperature is different between the exterior and interior, the heat transfers through the walls, ceilings, floors, and openings, part of the heat transferred is stored in the building components, and the rest goes to the rooms of the building. Thus, the heat transfer rate depends on the thermal resistance of the material components of the building. The common ways that a building gains heat are first by convection, which is heat transferred through walls, ceilings, floors, and openings (windows and doors) as a result of the temperature difference between the air inside the rooms and outside. Second by radiation which is heat transferred through the external walls of the building, roofing, and the openings exposed to the sunlight. Third by heat that is from internal sources, lighting of rooms, equipment, heat inside the rooms, and occupants of the rooms. Fourth, by heat that is from air leakage through the cracks in the openings [4].

In previous studies, Cheung et al. showed that a reduction in energy consumption for cooling load of 31.4% can be obtained as a result of modifying the building envelope to match the local climate [5]. Anderson & Silman [6] and Webster [7] identify how the structural engineer may work with an integrated design team of architects, civil engineers, builders, and owners to make the structure sustainable. The Structural Engineering Institute of the American Society of Civil Engineers published Sustainability Guidelines for the Structural Engineer [8], which emphasizes material selection and life cycle cost analysis as the basis for structural sustainability. Australia's guide to environmentally sustainable homes [9] and TecEco sustainable technologies [10] show that concrete in its basic form has relatively low embodied energy, but its high usage in construction results in higher total embodied energy than any other material. Jones et al. [11] developed a method for the optimum mix of energy conservation and solar energy. He emphasized that the designer's decision should always involve the "trade-off between the cost of the improvement versus the increased performance."

However, during this decade in the Libyan state, It has been noticed a lot of promotion by some companies and factories for materials and products that are used in the thermal insulation of homes. Citizens are also frequently asked about what materials are suitable for insulation as well as how to isolate buildings, especially after not obtaining good results in some cases in which the external thermal insulation layers were implemented for the homes of some citizens. It has been noticed that in most cases, insulating layers were implemented for the external walls, and the thermal insulation layers were neglected or not implemented for the roofs and the openings.

Therefore, this paper studies the rates of heat gain for the building from various external elements, such as walls, roofs, opening, which will give us an idea of which parts of the building should be given more thermal insulation as needed. Taking into account the summer climate of the Libyan state, the results of the analysis revealed how the heat generated by insolation is distributed to the surface of the structures, as well as how the rate of heat transfer from the building elements to the interior varies. In addition, the results showed that it is quite clear that the insulation only the walls of the building are simply insufficient to prevent the room from overheating. This provides us with a decent enough concept of how to implement insulation layers for buildings in a temperate and arid climate (such as that of Libya State), which increases the building's sustainability and self-sufficiency.

1. Problem Statement

In this study, the efficiency of the building envelope heat insulation was explored, and how the absence of thermal insulation of the roof and the openings might cause the temperature inside the building to increase. Note that using the thermal insulation just for the building external walls is the most common way these days in Libya State. Based on the results of this study, the answer to the following question can be found. Why is the building temperature still high in the summer even after thermally insulating the building envelop except for the roof and the openings?

2. Concepts and Methodology

The thermal energy that a room may absorb from both internal and external sources is known as heat gain. Heat is transferred to the interior from the exterior due to the temperature difference between the interior and the exterior. This gain happens as a result of air leakage and the building envelope's walls, ceiling, windows, and ventilation systems. However, this analysis is a bit complicated and there is no room here to do so, so this study focuses on modeling the heat gain from the building envelope.

2.1. Heat Transfer

Heat transfer is the flow of heat energy from a high-temperature body to a lower-temperature body, which is fundamental to the second law of thermodynamics. Calculating the resistance to heat transfer (R-value) of each material in the building assembly will yield the overall quantity of heat transported via the building's components. The three main methods of transferring heat are conduction, convection, and radiation (see Figure 1). The definition of conduction is the transmission of heat energy from a source of higher temperature to a source of lower temperature through physical contact. Conductive heat transfer is described as occurring in stationary materials (solid bodies and immobile fluids). Convection is a mix of conduction and fluid movement that transfers heat whenever a surface comes into contact with a fluid that has a temperature that is different from its own. Electromagnetic waves that are emitted from a hot body and travel to a cold body are what cause heat transfer by radiation.

Basically, this study shows that heat will transfer from the heated side of the material to the cooler side of the wall when one side is warmer than the other. The slope of the temperature gradient for a homogeneous wall is proportional to the thermal resistances (R-values) of the individual layers making up the composite wall, and the gradient is linear between the two surfaces. Resistance to heat flow, or R-value, is the reciprocal of thermal conductance, or U-value, which measures the rate at which heat flows through a material: $R = 1/U$. Substances with a strong resistance to heat flow can be used as insulation (high R-value and low U-value) [12].

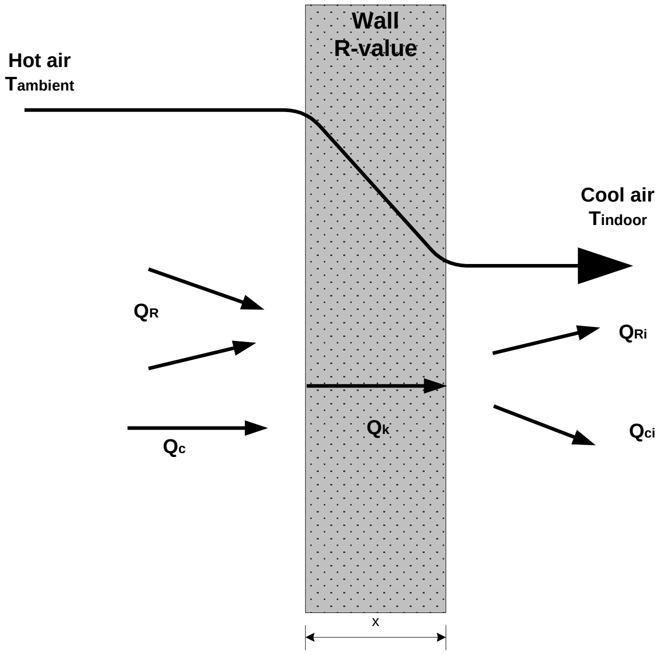

Figure 1. Heat exchange configurations

Nevertheless, this work is focused on heat gained by convection and radiation as boundary conditions, while conduction heat transfer depends on the properties of the materials used for the model envelope. The basic equations are as follows [8, 13]:

$$(\text{Conduction}) \quad Q_k = k\,A\,\frac{\partial T}{\partial x} \quad \ldots\ldots\ldots (1)$$

$$(\text{Convection}) \quad Q_c = h\,A(\Delta T) \ldots\ldots\ldots (2)$$

$$(\text{Radiation}) \quad Q_R = A\,\varepsilon\,\sigma\,\left(T_{\text{surface}}^4 - T_{\text{ambient}}^4\right) \ldots\ldots\ldots (3)$$

Q_k: the rate of heat flux by conduction (Watts)

k: the thermal conductivity (W/m k)

$\partial T/\partial x$: change of temperature with respect to x which is wall thickness (k/m)

Q_c: heat flux by convection (watt)

A: the surface area (m^2)

h: heat transfer coefficient difference ($w/m^2\ {}^oc$)

ΔT: difference in the surface temperature $T_{surface}$ & ambient temperature $T_{ambient}$

Q_R: heat flux by radiation (watt)

σ: Stefan-Boltzmann constant (5.6696E-8 $W/m^2.{}^0k^4$)

ε: Emissivity unit less

3. Building and Material

The building is a typical sized room in the geometry of a warm climate zone. The plan view and cross section are shown in figure 2. The walls of the building (thermally insulated walls) consist of concrete masonry with a thickness of 20 cm, the uninsulated roof consists of reinforced concrete of 15 cm in thickness, the uninsulated windows are made up of single-layer standard glass, and the uninsulated door is made up of oak wood. In table 1, the thermal properties of the material are presented. Figure 3 shows the temperature of July 21 [14], which is a typical summer design day for calculating cooling and heating load for a temperate climate zone, such as Libya state.

Table 1. Thermal properties of the material at ambient temperature 22^{o}c [15]

Material type	Density Kg/m^3	Thermal conductivity w/m ^{o}c	Specific Heat J/kg ^{o}c	Convection coefficient w/m^2 ^{o}c
Concrete slabs	2400	0.75	666	2.37
Concrete masonry	2000	0.7	836	2.74
Glass	2300	1.05	836	3.83
Wood oak	825	0.21	2385	1.55

4. Modeling

Using ANSYS 2020 R2 to run thermal finite element analysis, this FEA considers the thermal behaviors of both types of material: structural and non-structural, in the room's envelope. Moreover, the room is modeled in three dimensions as a scale model. Since the model consists of materials that differ in thermal properties, the element type is selected to be a solid element because all of the components of this structure are solid in reality except the inside air. It means there are fewer assumptions, which leads to more accuracy.

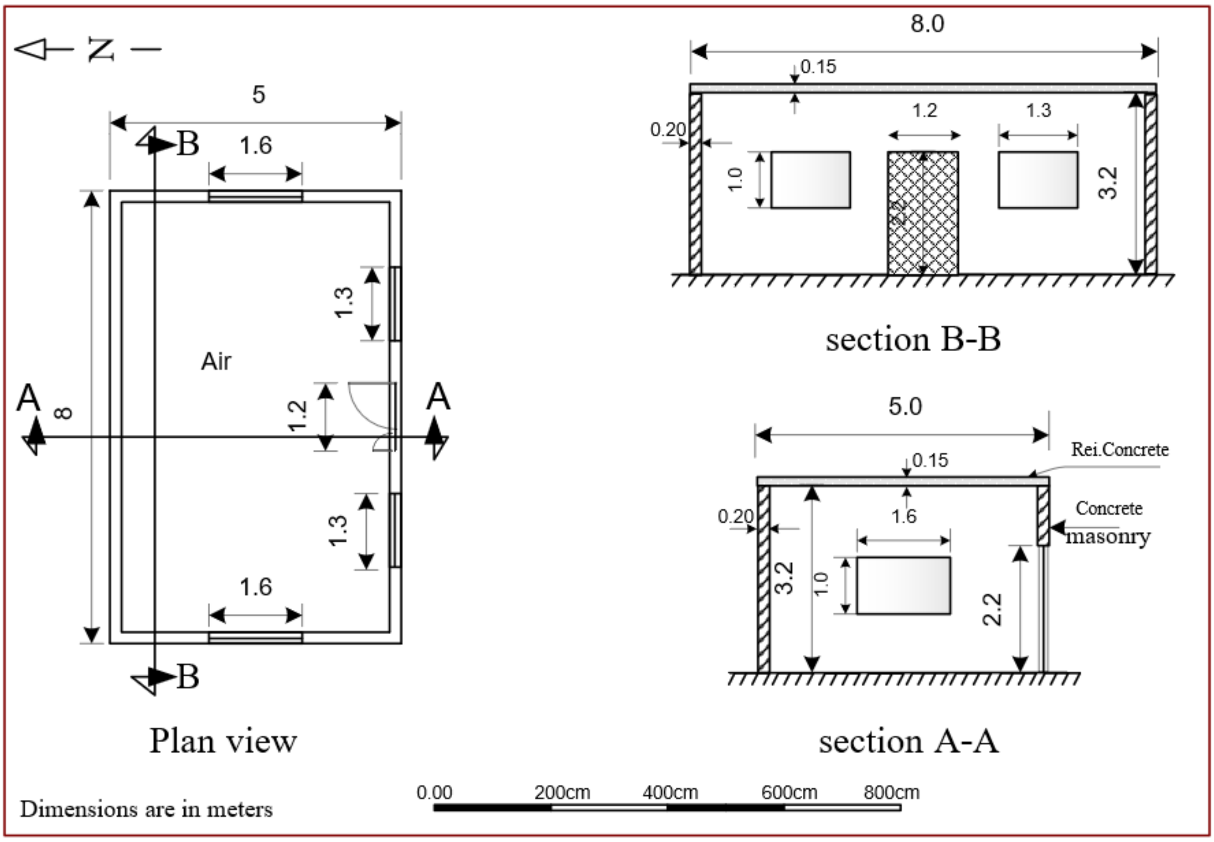

Figure 2. Room floor plan view & cross sections

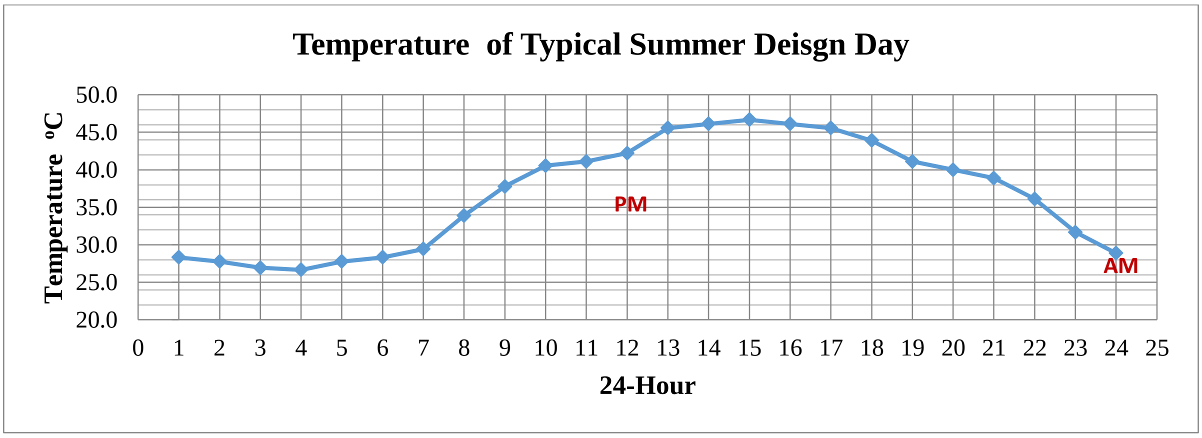

Figure 3. typical summer day design temperature of July 21.

4.1. Steady-State Analysis

At an initial room temperature of 20 °C. The steady-state thermal analysis is provided to study the static heat transfer between different building components due to the change in the surrounding temperature, which corresponds to the daylight hours. In other words, in the analysis settings, the number of steps is 24 steps. Each step has a different magnitude of the temperature, so here it does not matter the duration of loading. "Time is used for steady state multi-step and transient analysis" [3].

Thermal boundary conditions. Since the walls are thermally insulated, radiation boundary conditions are applied to all of the openings and the roof. while the convection boundary applied to all interior surfaces. Meshing size is controlled by a conversion study of maximum temperature as shown in figure 4.

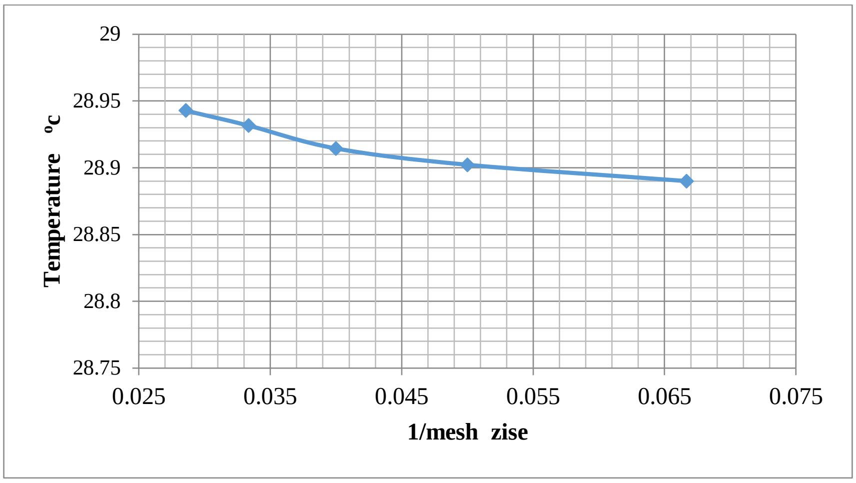

Figure 4. Conversion study of maximum temperature

5. Results

The results of the FEM analysis showed the behavior of the temperature distribution in the different parts of the room, where the highest temperatures are observed in the roof (45°c) and windows (40°c), and this behavior is expected because the roof and the openings are not thermally insulated, but it can also be seen that the walls gain heat even though they are thermally insulated (average of 31 °c) See figure 5.

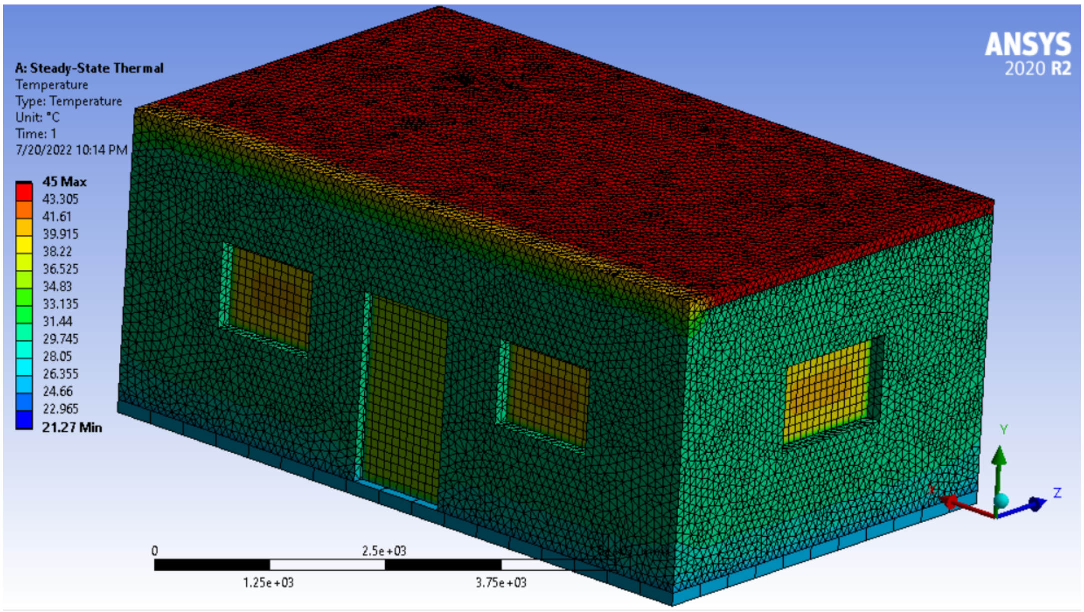

Figure 5. Temperature distribution on the room envelop

As the heat resulting from room insolation was transferred through the ceiling and the openings at different rates according to the thermal conductivity characteristic of each material. Also, this heat will be distributed through the air molecules inside the room due to the characteristic of convection heat transfer (see figure 6). This leads to a gradual rise in the room temperature during the day, as the room temperature increased from 20 °C to 45 °C near the ceiling and also led to the walls gaining heat from 20 °C to 31 °C, as well as 40 at the openings. This causes the room temperature to rise by 70%.. Figure 7 shows the total heat flux emitted by unit area from the parts of the building that are not thermally insulated; and since the walls are thermally insulated for the external fabric, they act as a retainer for the heat gained from the roof and windows through their inner surface and through their mass connected to heat sources.

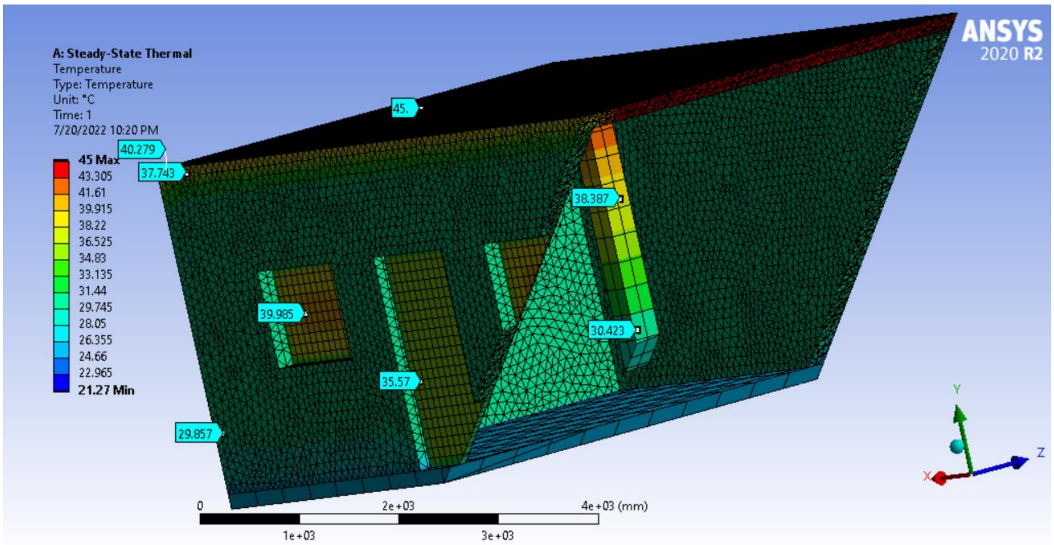

Figure 6. Section shows the distribution on envelop and inside the room

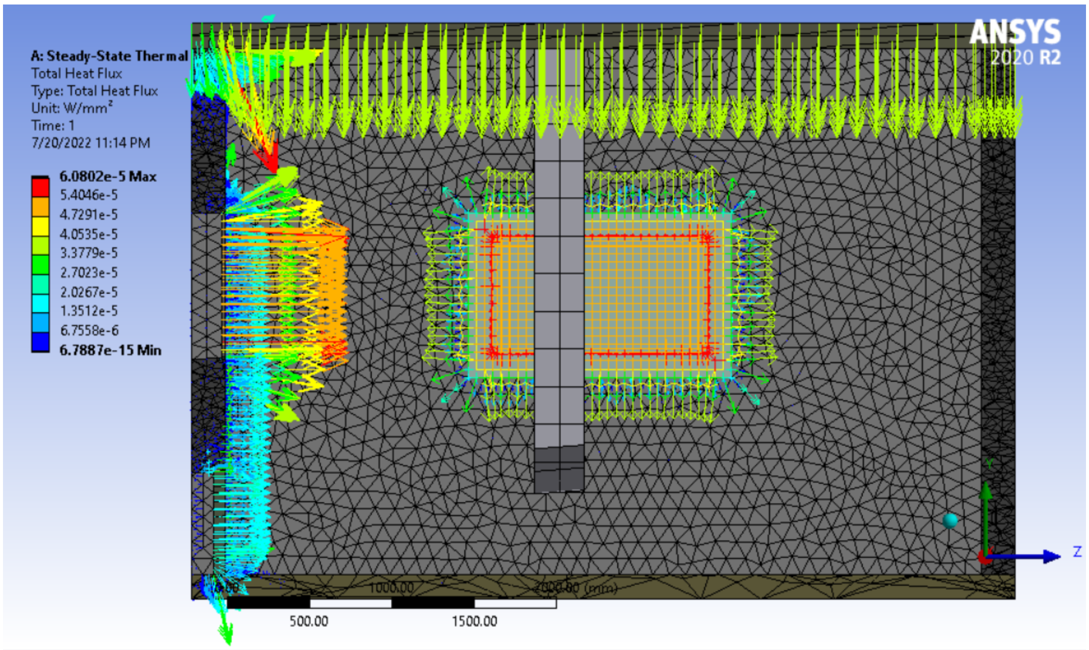

Figure 7. Section shows heat flux from elements that are not thermally insulated

6. Conclusions

In the context of improving the construction system of the building to improve energy efficiency, this research considered the method of reducing the energy consumption needed to cool residential buildings, as it is most often insulating the building envelope without insulating the roof and the openings. This technique of thermal insulation of buildings is a commercial process is somehow not subject to a precise scientific methodology that takes into account the local climatic conditions and the materials used in addition to the method of implementation. Where neglecting the thermal insulation of the roof of the building and the openings leads to a rise in the building temperature by approximately 70%

The results of the thermal study showed that the desired result would not be obtained from insulating the building envelope only and neglecting the roof and openings. Moreover, in the presence of the external insulation layer, and due to the thermal mass property of building materials, will cause the building's temperature to rise even at night. Therefore, in order to avoid a high temperature inside the building as a result of the high summer temperature, this study recommends that thermal insulation work be done for the entire building envelope (walls and roof). Also recommends the use of glass for windows which has higher thermal insulation properties. Correspondingly, this study recommends focusing on the proper selection of insulation method and materials (it is known that the best insulator is the dead air). Finally, this study recommends that even in the case of a multi-story building, the thermal insulation of the upper floor surface must be implemented because due to the thermal mass characteristic of the building materials, the temperature accumulates in the elements and over time affects the lower floors gradually.

REFERENCES

[1] Yeang K., (The Green Skyscraper), Prestel, Munich,1999.

[2] Kottek, M., Grieser, J., Beck, C., et al. (World map of the Koppen-Geiger climate classification updated), Meteorologische Zeitschrift. , (2006), 15:259-263.

[3] Krem, Mohamed, Hoque,S., and Arwade,S. (Structural configuration and building energy Performance), ASCE (2013).

[4] Johan H. Lienhard IV, and Johan H. Lienhard (A Heat Transfer Textbook), Third Edition, Phlogiston Press Cambridge, Massachusetts, USA, (2008).

[5] Cheung, C., Fuller, R., and Luther, M. (Energy-efficient envelope design for high-rise apartments), Energy and Buildings, (2004), 37: 37–48.

[6] Anderson, J.E., Silman R. (The role of the structural engineer in green building), The Structural Engineer, ,(2009), 87:28-31.

[7] Webster, M.D. (Relevance of structural engineers to sustainable design of buildings), Structural Engineering International, (2004), 14:181-185.

[8] Kestner, D., Goupil, J., and Lorenz, E. (Sustainability Guidelines for the Structural Engineer), American Society of Civil Engineers, Reston, Virginia, (2010).

[9] Technical Manual Design for lifestyle and the future. Australia's guide to environmentally sustainable homes. < http://www.yourhome.gov.au>, 2010.

[10] Technical Manual. Embodied Energy. < http://www.yourhome.gov.au/technical/ fs52.html >, 2010.

[11] Jones, W., Balcomb, J., Kosiewicz, C., et al. (Passive solar design Handbook). Volume3: Passive solar design analysis. Prepared for U.S. department of energy, Washington, D.C., 1982.

[12] CIBSE. Environmental design- guide A. London, 2006.

[13] A Guide to Heating & Cooling Load Estimation. < http://www.scribd.com/doc/ 38684860/4/ part-4-heat-gain-through-lighting-fixtures>, 2010.

[14]U.S. Department of energy, Energy plus. <http://www.energy.gov/index.htm>.2022.

[15] The U.S. Department of Energy Building (Energy Codes Program. International Energy Conservation Code 2009). International code council, INC.(2010).